P-04-294

Revised September 2006

Oskarshamn site investigation

Compilation of petrophysical data from rock samples and in situ gamma-ray spectrometry measurements

Stage 2 – 2004 (including 2002)

Håkan Mattsson, Hans Thunehed, Carl-Axel Triumf
GeoVista AB

November 2004

Svensk Kärnbränslehantering AB
Swedish Nuclear Fuel
and Waste Management Co
Box 5864
SE-102 40 Stockholm Sweden
Tel 08-459 84 00
+46 8 459 84 00
Fax 08-661 57 19
+46 8 661 57 19

ISSN 1651-4416
SKB P-04-294

Revised September 2006

Oskarshamn site investigation

Compilation of petrophysical data from rock samples and in situ gamma-ray spectrometry measurements

Stage 2 – 2004 (including 2002)

Håkan Mattsson, Hans Thunehed, Carl-Axel Triumf
GeoVista AB

November 2004

Keywords: Magnetic susceptibility, Remanent magnetization, Anisotropy of magnetic susceptibility, Density, Porosity, Electric resistivity, Induced polarization, Gamma-ray spectrometry, Geophysical anomaly, Potassium, Thorium, Uranium.

Reading instruction

For revision no. 1 of this report a change in some of the ID-codes has been performed. In the earlier report ID-codes in the interval PSM 006055–PSM006095 have been changed to the corresponding ID-codes in the interval PSM007836–PSM007876.

Abstract

This report presents a compilation and interpretation of all petrophysical surface data collected during 2002–2004 in connection to the site investigation in Oskarshamn. The work also comprises evaluation of results from gamma ray spectrometry measurements and in situ magnetic susceptibility measurements.

The purpose of petrophysical measurements is to gain knowledge of the physical properties of different rock types. This information is used to increase the understanding of geophysical measurements and to support the geological mapping. Data analyses were made with respect to rock type characteristics and the geographical distributions of the measured properties.

The petrophysical rock type classification as indicated from silicate density data generally conforms well to the classification from the geological bedrock mapping. The span in wet density of the most abundant rock type Ävrö granite is 2,659–2,746 kg/m^3 and the spatial variation in density shows that the Ävrö granite rocks in the Lilla Laxemar area have slightly higher densities than those located further west, closer to Mederhult. The magnetic properties of the main rock types are primarily governed by magnetite. The highest susceptibilities (and densities) are found in the diorite to gabbro rocks, and it is very likely that these rocks constitute the main sources of a majority of the large positive magnetic anomalies recorded in the helicopter borne survey. Frequency diagrams of the magnetic susceptibility deduced from outcrops of the most common rock types found in the Laxemar area often show bi- or tri-modal distributions. When comparing the distribution of the low-end peaks, i.e. very low magnetic susceptibilities, with identified lineaments and direct observations in outcrops of earlier tectonic activities, a correlation becomes obvious. Studies of the frequency diagrams also show that discrimination is impossible of the two most common rock types of the area, the Ävrö granite and quartz monzodiorite, based on magnetic susceptibility only.

The magnetic anisotropy data indicate a dominating regional rock fabric of west to west-northwest striking planes of foliation and a northwest oriented maximum strain. A fabric orientation with south to southwest striking foliation planes, possibly indicating secondary deformation, is also deduced from the AMS data.

The range of porosities between 0.1% and 1.0% is fairly normal for crystalline rocks of Proterozoic age. The highest median porosity is found for Ävrö granite (0.63%). The electric resistivity on rock samples from the central part of the investigated area (Ävrö granite), seem to show slightly lower resistivity and higher porosity than for the rest of the samples.

A comparison of gamma-ray spectrometry data from the two most common rock types in the Laxemar area, the quartz monzodiorite and the Ävrö granite shows that the latter has a higher content of potassium and thorium. The data also indicate that the composition of the Ävrö granite is rather inhomogeneous. The gamma ray spectrometry on ground thus supports the data from the helicopter borne gamma ray spectrometry. In the Laxemar area, southeast of Mederhult, the ternary map of the gamma spectrometry data shows that the Ävrö granite appears to have higher content of thorium as compared to areas further south. This observation is supported by results from the geological mapping where the silica content appears to decrease further south.

The highest content of thorium is found in the fine-grained granite. The uranium and potassium contents of this rock type are also quite high. The lowest contents of potassium, uranium and thorium are found in mafic rock types such as diorite to gabbro.

The investigations of petrophysical parameters carried out within this activity indicate that the geophysical anomaly maps and petrophysical parameters may add useful information for the characterization of the bedrock in terms of tectonics and for distinguishing between different rock types. Furthermore, the geophysical data may reflect a compositional variation within rock types which together with chemical and mineralogical information may lead to further subdivision of rock types in different compositional varieties.

Sammanfattning

Föreliggande rapport utgör en sammanställning och tolkning av alla petrofysiska data på bergartsprover som insamlats på markytan under 2002–2004 i samband med SKB:s platsundersökning i Oskarshamn. I rapporten behandlas även resultaten av gammaspektrometermätningar samt data från mätningar av magnetisk susceptibilitet direkt på berghällar.

Bestämning av bergarters fysikaliska egenskaper är viktig för att bättre förstå orsaken till anomalier i flyg- och markgeofysiska data. Petrofysiska parametrar (halten K, U och Th, samt silikatdensitet) används även som stöd vid bergartsklassificering i samband med berggrundsgeologisk kartering. Analyserna av data är dels gjorda med avseende på egenskaper för respektive bergartstyp, och dels med avseende på den geografiska fördelningen av olika parametrar.

Den petrofysiska bergartsklassificeringen överensstämmer väl med den klassificering som gjorts i samband med den berggrundsgeologiska karteringen. Huvudbergarten i området (Ävrögranit) varierar i densitet från 2 659 kg/m^3 till 2 746 kg/m^3. Den geografiska fördelningen visar att Ävrögraniten runt Lilla Laxemar-området har något högre densitet än Ävrögranit längre västerut, närmare Mederhult. Bergarterna i området är generellt sett högmagnetiska och magnetit är det mineral som primärt styr de magnetiska egenskaperna. Högst magnetisering (även högst densitet) har bergarten diorit till gabbro, och undersökningen visar att den bergarten orsakar de allra flesta magnetiska anomalier med hög amplitud som syns i data från helikoptermätningarna. Frekvensdiagram över den magnetiska susceptibiliteten från mätningar på hällar i samband med berggrundskarteringen visar att bergarterna i Laxemarområdet i regel har bi- eller tri-modala fördelningar. Jämförelser av de lägsta susceptibilitetsvärdena i respektive bergartsgrupp mot tidigare identifierade lineament och observationer av tektonisk påverkan i hällar, indikerar hög korrelation mellan deformationszoner och dessa lägsta susceptibiliteter. Vidare visar frekvensdiagrammen att det i princip är omöjligt att enbart utifrån magnetisk susceptibilitet skilja de två vanligaste bergartstyperna i Laxemarområdet, Ävrögranit från kvartsmonzodiorit.

Magnetiska anisotropidata indikerar ett regionalt strukturmönster i bergrunden som domineras av västligt till västnordvästligt strykande foliationsplan, samt en ca nordvästligt strykande, moderat stupande, maximal mineraldeformation (strain). Det finns dessutom ett antal strukturer som stryker i sydvästlig riktning, och dessa kan möjligen kopplas till en sekundär deformation.

Uppmätt porositet varierar generellt mellan 0,1% och 1,0%, vilket är normalt för Proterozoisk kristallin berggrund. Ävrögranit har den högsta medianporositeten (0,63%). I de centrala delarna av undersökningsområdet uppvisar berggrunden (som där främst består av Ävrögranit) något lägre resistivitet och högre porositet än för omkringliggande områden.

En jämförelse av gammaspektrometerdata mellan de två vanligast förekommande bergarterna kvartsmonzodiorit och Ävrögranit, visar att Ävrögraniten i medeltal har något högre halter av kalium och torium, men också att den är inhomogent sammansatt och uppvisar relativt stor spridning i kalium- och toriumhalter mellan olika områden. Markspektrometrin stöder resultaten från den helikopterburna spektrometrin. I

Laxemaområdet, sydost om Mederhult, visar mark- och helikopterdata att toriuminnehållet är relativt högt gentemot omgivningen. I detta område påträffas också en högre andel berggrund med granitisk sammansättning jämfört med området längre söderut där också förhållandet mellan kalium och torium förändras. Observationen stöds också av kiselhalter i prov som tagits i bägge områdena.

Det högsta toriuminnehållet påträffas i finkornig granit, i vilken också uran- och kaliuminnehållet är ganska högt. Det lägsta innehållet av kalium, uran och torium registreras i mafiska bergarter som diorit och gabbro.

Sammanfattningsvis visar denna undersökning att petrofysiska data i kombination med geofysiska anomalikartor, bidrar med viktig information för att bättre karakterisera berggrunden och tektoniken i platsundersökningsområdet. Geofysiska data visar vidare att det finns variationer i mineralsammansättning inom vissa bergartstyper, som tillsammans med mineralogisk och geokemisk information gör det möjligt att finindela dessa bergarter ytterligare.

Contents

1 Introduction

This document reports the compilation and interpretation of petrophysical data gained during 2002 to 2004 in connection to the site investigation in the Oskarshamn area. The work performed 2004 was carried out in accordance with activity plan AP PS 400-04-002. In Table 1-1 controlling documents for performing this activity are listed. Both activity plans and method descriptions are SKB's internal controlling documents. Information on the sampling and compilation of the data collected in 2002 is presented in the reports P-03-019 and P-03-097 /1, 2/.

Table 1-1. Controlling documents for the performance of the activity.

Activity plan	Number	Version
Geofysiska undersökningar med tyngdkraftsmätning, magnetometri och petrofysik inom delområde Simpevarp, Laxemar och del av regionala området (lokala modellområdet)	AP PS 400-04-002	1.0
Geologiska undersökningar för val av prioriterad plats på fastlandsdelen och modellversion 1.1	AP PS 400-02-015	1.0
Method descriptions	**Number**	**Version**
Berggrundskartering	SKB MD 132.001	1.0
Mätning av bergarters petrofysiska egenskaper	SKB MD 230.001	1.0
Bestämning av densiteten och porositeten hos det intakta berget	SKB MD 160.002	1.0

The data from rock samples are based on measurements on 294 bedrock samples collected by GeoVista AB at 66 sampling locations and on 72 rock objects. The geographical distribution of the sampling locations is shown in Figure 1-1. The sample measurements were performed at the laboratory of the Division of Applied Geophysics (Luleå University of Technology) and include the following methods: magnetic susceptibility, remanent magnetization, anisotropy of magnetic susceptibility (AMS), density, porosity, electric resistivity and induced polarization (IP).

Results of in situ gamma-ray spectrometry measurements at 171 locations are also presented in this report. The geographical distribution of the measuring locations is shown in Figure 1-1. The data were gained during the field control activities during the investigation of the selection of a preferred site /3/ and in connection to the collection of rock samples for petrophysical measurements in 2002 and in 2004.

Data from in situ magnetic susceptibility measurements carried out during the geological mapping in 2004 /4/ are also included in the report.

All data has been delivered to the SICADA database. Field note numbers are listed in Table 1-2.

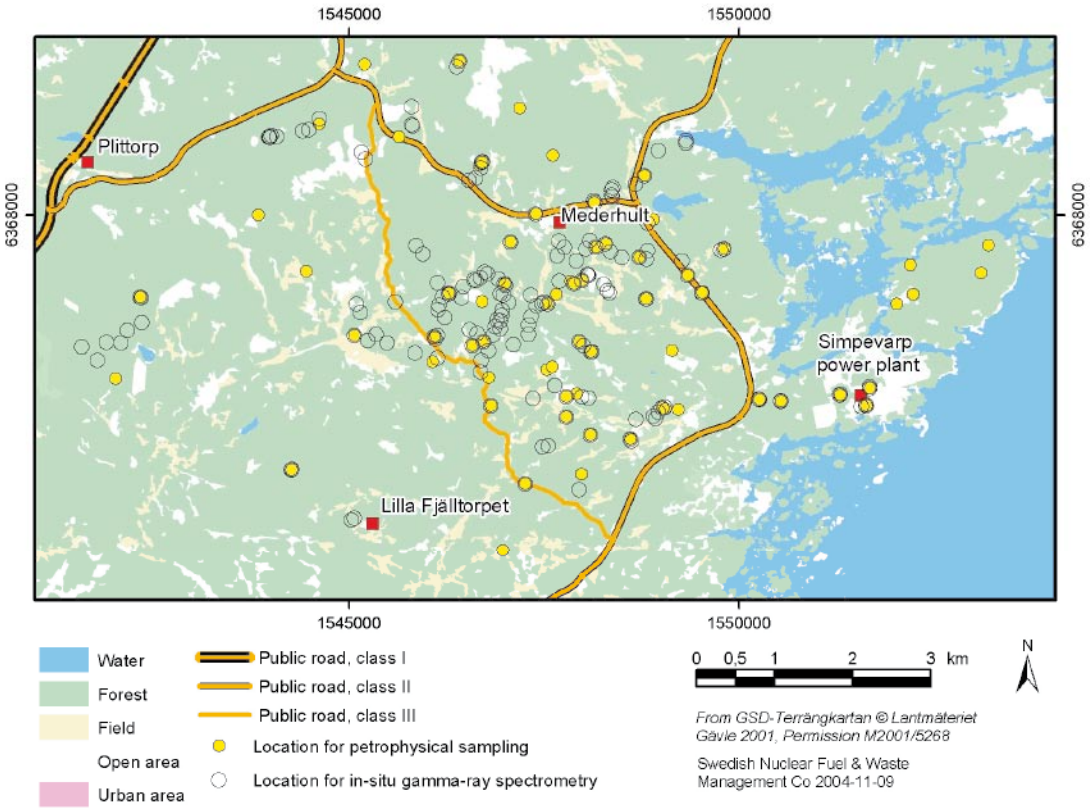

Figure 1-1. *Distribution of locations for petrophysical sampling and in situ gamma-ray spectrometry measurements in the area of Oskarshamn site investigation.*

Table 1-2. Data references.

Subactivity	Database	Identity number
Mätning av spektrometri i spridda punkter	SICADA	Field note 380
Mätning av porositet, densitet, resistivitet, IP, AMS och remanens	SICADA	Field note 537

2 Objective and scope

The main purpose of petrophysical measurements is to gain knowledge of the physical properties of different rock types. These data are mainly used as supportive information for the interpretation of ground, borehole and airborne geophysical data. The petrophysical data help to correctly identify and interpret anomalies observed in geophysical data caused by e.g. deformation zones, dykes and different rock types.

One of the most important aims of this compilation and evaluation is thus to create a database of physical characteristics of the main rock types occurring in the area of the Oskarshamn site investigation. Some of the petrophysical data can be used as tools for a better understanding of the geological evolution of the area and hence to aid in the mapping of the bedrock geology.

In some figures, contour maps based on interpolation methods of petrophysical parameters are presented. In some cases, the interpolation of petrophysical data is questionable, but it is performed in this report in order to better visualize the spatial variations in the data. Detailed variations in these contour maps should be ignored.

3 Methods and data processing

The collection of core samples is described in SKB P-03-19 /1/.

3.1 Density and magnetic properties

Different rock types vary in composition and this leads to variations in their petrophysical properties. The rock density (mass divided by volume) and magnetic properties (susceptibility and remanence) are therefore often used as tools and supportive information when classifying rocks. These properties also constitute input parameters when modelling gravity and ground magnetic data and they are important for the interpretation of airborne magnetic data.

In order to get a better picture of these data and to increase the possibility to compare different data sets and data from different rock types, a few sub-parameters are often calculated from the density, the magnetic susceptibility and the magnetic remanence. Two such sub-parameters are the silicate density and the Q-value (Königsberger ratio). The silicate density /5/ provides an estimation of the rock composition and is calculated by correcting the measured total density for the content of ferromagnetic minerals (e.g. magnetite and pyrrhotite) by use of the magnetic susceptibility. The Q-value /6/ is the quotient between the remanent and induced magnetizations:

$$Q = \frac{M_R}{M_I} = \frac{M_R}{KH} = \frac{M_R \mu_0}{KB}$$

where

M_R = Remanent magnetization intensity (A/m)

M_I = Induced magnetization intensity (A/m)

K = Magnetic susceptibility (dimensionless SI)

H = Magnetic field strength (A/M)

B = Magnetic flux density (T)

μ_0 = Magnetic permeability in vacuum ($4\pi 10^{-7}$ Vs/Am)

The Q-value thus indicates the contribution of the remanent magnetization to the measured total magnetic flux density and is therefore an important parameter when interpreting and modelling ground and airborne magnetic data. The Q-value is also grain size dependent and indicates what ferromagnetic minerals are present in the rock.

In this investigation so called density-susceptibility rock classification diagrams are used (see for example Figure 4-1). The Y-axis in these diagrams display the magnetic susceptibility on the left hand side and the estimated magnetite content to the right (from /7/). It has been shown that in rocks in which the magnetic susceptibility is primarily governed by magnetite, there is a fairly good correlation between the magnetic susceptibility and the magnetite content /7/. However, the scatter is fairly high so predictions of the volume-percentage of magnetite in rocks based on the magnetic susceptibility should be used with caution. The silicate density curves are based on equations from /5/ and the average densities of each rock type originate from /8/. The

diagram should be read in the way that if a rock samples plots on, or close to, a "rock type curve" it is indicated that the rock should be classified according to the composition of this rock type. Since there is often a partial overlap of the density distributions of different rock types, there is always a certain degree of uncertainty in the classification. A sample plotting in the middle between, for example, the granite and granodiorite curves should thus be classified as granite to granodiorite.

It must be noted that the rock types used in the rock classification diagram do not conform perfectly to the geology of the area of the Oskarshamn site. There is for example no corresponding rock type curve for quartz monzodiorite, which occurs frequently in the area. This is caused by the lack of high quality average density data for these rock types. We therefore suggest that the rock classification diagrams should be used as indicators of the compositional variation between different rock types (or groups of rocks), and that these diagrams will be used to help identifying possible faulty rock classifications during the bedrock mapping and that silicate density maps are used to spot spatial variations in rock composition.

3.2 In situ measurements of magnetic susceptibility

As part of the bedrock mapping /4/ in situ measurements of the magnetic susceptibilities have been carried out at 1,565 individual localities. At these localities in total 12,827 single measurements have been carried out, which gives 8 measurements as an average per single locality (Figure 3-1).

It is important to study the spatial variations of the magnetic susceptibility over an area where measurements of the magnetic field have been carried out. Such a study improves the knowledge and understanding of the sources behind the variations in the magnetic field.

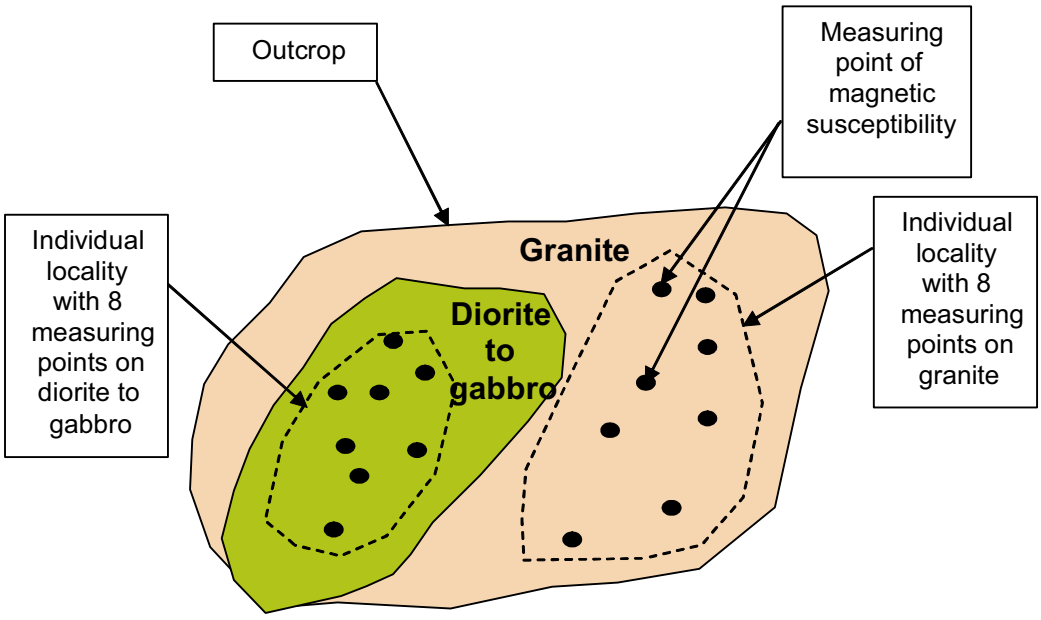

Figure 3-1. *Drawing showing one outcrop with two individual localities where measurements of the magnetic susceptibilities have been carried out. One locality represents eight measurements of the magnetic susceptibility in the granite and the other eight measurements in the diorite to gabbro rock.*

The processing of the magnetic susceptibility measurements included calculation of the geometric mean for each rock type at one location. All measurements of the magnetic susceptibility have been grouped with the rock type as the divider according to the rock descriptive nomenclature presented by SKB, see Table 3-1.

Table 3-1. Rock types used for the grouping of magnetic susceptibility data from measurements on outcrops.

Code	Rock type	Number of measured localities
501030	Fine-grained dioritoid (Metavolcanite, volcanite)	41
501033	Diorite to gabbro	153
501036	Quartz monzodiorite	269
501044	Ävrö granite	839
501058	Granite, medium- to coarse-grained	97
501061	Pegmatite	6
505102	Fine-grained diorite to gabbro	24
511058	Fine-grained granite	136

3.3 Anisotropy of magnetic susceptibility (AMS)

The magnetic anisotropy of rock forming minerals basically originates from two sources, the grain shape and the crystallographic structure. Magnetite is ferrimagnetic and carries strong shape anisotropy, whereas pyrrhotite and hematite are governed by crystalline anisotropy due to their antiferromagnetic origin. Paramagnetic minerals (e.g. biotite, hornblende) and diamagnetic minerals (e.g. quartz, feldspars) are also carriers of magnetocrystalline anisotropy. The orientation of the anisotropy of magnetic susceptibility coincides with the crystallographic axes for most rock forming minerals, so it is therefore possible to directly transfer “magnetic directions” to “tectonic directions” (foliation and lineation) measured in the field. Since magnetite carries a very high magnetic susceptibility in comparison to most other rock forming minerals, only a small portion present in a rock tends to dominate the magnetic properties, including the anisotropy. However, for example for “non-magnetic” granites the magnetic anisotropy is mainly governed by biotite and other paramagnetic minerals.

The AMS measurements were performed on four specimens per rock object (site), which produced four data readings per object. The four measurements allow a calculation of mean directions of the principal AMS axes (site mean directions) and corresponding “site mean values” of the degree of anisotropy (P), degree of lineation (L), degree of foliation (F) and ellipsoid shape (T). When calculating the site mean values of the anisotropy parameters, the orientation of the principal anisotropy directions of each specimen is taken into account. Vector addition is applied to the three susceptibility axes of the four specimens from the site, which results in a “site mean ellipsoid”. The site mean values of the anisotropy parameters thus give information of the site as a whole and are not just “simple” average values. According to statistical demands at least six measurements (specimens) are required for estimating uncertainty regions of the calculated mean directions. No such calculations were therefore performed. Instead, the data quality of each site was evaluated by visual inspection and site mean directions based on scattered specimen directions were rejected (about 10% of the data were rejected). A more complete description of AMS can be found in, for example, /2 and 9/.

3.4 Electric resistivity and induced polarization

The electric resistivity and induced polarization was measured with the samples soaked in both tap water and in salt water (2.5% NaCl by weight). Measurements were made on one drill core for each rock type at a sampling location.

3.4.1 Electric resistivity

The contrast in resistivity (ρ) between silicate minerals and more conducting media like water or sulphides/graphite is extremely high. The bulk resistivity of a rock is therefore more or less independent of the type of silicate minerals that it contains. Electric conduction will be almost purely electrolytic if the rock is not mineralized. Archie's law /10/ is frequently used to calculate the conductivity (1/ρ) of sedimentary rocks.

$$\sigma = \alpha \cdot \sigma_w \cdot \phi^m \cdot s^n$$

where

σ = bulk conductivity (=1/ρ, S/m)

σ_w = pore water conductivity (S/m)

ϕ = volume fraction of pore space

s = fraction of pore space that is water saturated

a, m, n = dimensionless numbers, m ≈ 1.5 to 2.2

Archie's law has proved to work well for rocks with a porosity of a few percent or more. Old crystalline rocks usually have a porosity of 0.1 to 2% and sometimes even less. With such low porosity the interaction between the electrolyte and the solid minerals becomes relevant. Some solids, especially clay minerals, have a capacity to adsorb ions and retain them in an exchangeable state /11/. This property makes clays electrically conductive but the same property can be found for most minerals to some degree. This effect, called surface conductivity, can be accounted for by the parameter *a* in Archie's law. The relative effect of surface conductivity will be greatly reduced if the pore water is saline. The amount of surface conductivity is dependent upon the grain size and texture of the rock. Fine grained and/or mica-rich, foliated rocks are expected to have a large relative portion of thin membrane pore spaces that contribute to surface conductivity.

The electric resistivity is in reality not a simple scalar. Most rocks show electric anisotropy and the resistivity is thus a tensor. On a micro-scale the anisotropy is caused by a preferred direction of pore spaces and micro fractures.

3.4.2 Induced polarization

The induced polarization (IP) effect can be caused by different mechanisms of which two are the most important. When the electric current passes through an interface between electronic and electrolytic conduction there is an accumulation of charges at the interface due to the kinetics of the electrochemical processes involved. Such situations will occur at the surface of sulphide, oxide or graphite grains in a rock matrix with water filled pores. The second mechanism is related to electric conduction through thin membrane pore spaces. In this case an accumulation of charges will occur at the beginning and end of the membrane. The membrane polarization is thus closely related to the surface conduction effect mentioned above for electric resistivity. Fine grained and/or mica rich, foliated rocks are therefore expected to show membrane polarization. Also, membrane polarization is greatly reduced in saline water.

3.4.3 Data processing

A correction for drift caused by drying of the sample during measurements is done automatically by the instrumentation software by comparing the harmonics of low frequency measurements with the base frequency result of the next higher frequency.

The resistivity data were compared with the measured porosity in order to make a fit in accordance to Archie's law. It should however be noted that the porosity measurements in this study were performed on all samples of a rock type from a site assembled together, whereas the electric properties were measured on one sample only. This will introduce some uncertainty in the fit to Archie's law.

The pore space geometry was analyzed by calculating apparent values for the power m in Archie's law for salt water measurements. Such calculations rely upon reasonable estimates of the contribution of surface conductivity. Since the relative effect of surface conductivity is small in saline water the estimates of apparent m-values can be justified. Based on these apparent m-values, apparent a-values for fresh-water measurements were calculated. These apparent a-values will give an idea about the relative contribution of surface conductivity in fresh water environments.

3.5 In situ gamma-ray spectrometry

There is no formal SKB method description for measuring gamma ray spectrometry on outcrops. As a consequence the measurements were carried out according to the instructions in Appendices 1 and 2 in /2/; these two documents are judged to provide an adequate method description.

Airborne gamma ray spectrometry is a remote sensing geophysical technique which provides information about the distribution of potassium (K), uranium (U) and thorium (Th) that is directly interpretable in terms of surface geology /22/. In order to be able to express in geological terms the outcome of an airborne gamma ray survey, it is essential to understand the sources behind the different distribution patterns recognized. This understanding is normally achieved gradually. The geological mappings of key outcrops within the boundaries of different types of anomaly complexes, together with measurements with hand-held gamma ray spectrometers at these key localities, are two of the most important activities.

In this report, data from gamma ray spectrometry on outcrops measured between 2002 and 2004 are covered. In total 171 individual localities were covered with measurements. Furthermore gamma ray spectrometry was carried out in 26 individual localities within a special study of fine-grained granite dykes /12/. The meaning of an individual locality is explained in Figure 3-2. Normally between one to three points were measured depending on the area available for measurements at every individual locality.

Two different instruments were used for the measurements: Exploranium GR130 BGO (version 4.15 G serial# 1099) and Exploranium GR320 (Envispec serial# EXP06 2012/1803, sensor mod GPS-21 serial# 1803). The sampling time used was 300 s (Exploranium GR130) and 240 s (Exploranium GR320).

For every locality the average concentrations of potassium, uranium and thorium were calculated together with the standard deviations. Such data were delivered to SKB. To describe the content of potassium, uranium and thorium in each rock type the averages from each single locality were used for a new averaging process, which resulted in an average for a specific rock type and a corresponding standard deviation.

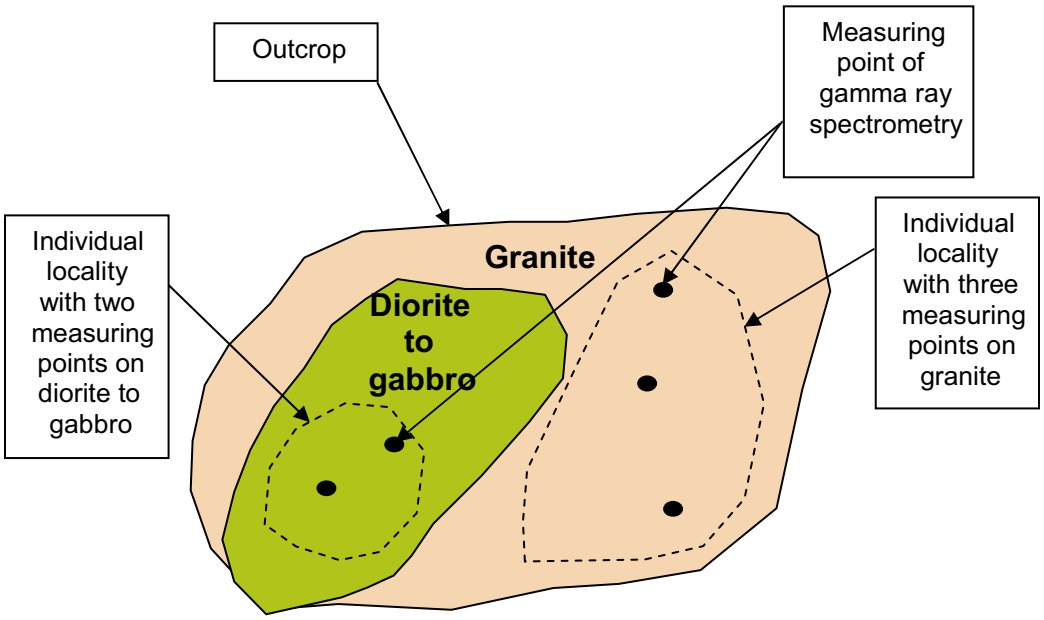

Figure 3-2. *Sketch showing one outcrop with two individual localities where measurements with gamma ray spectrometry have been carried out. In this case one of the localities is represented by three measurements on the granite and the other by two measurements on the diorite to gabbro rock.*

4 Results

The sampling covers 6 different groups of rock types (Table 4-1). The classification of the rock type at each object was done in accordance to the rock descriptive nomenclature presented by SKB, and with information from the feasibility study /13/ and from the detailed bedrock mapping in 2004 /4/.

Table 4-1. Rock types sampled for petrophysical measurements.

Rock type	Number of rock objects
Ävrö granite	32
Fine-grained dioritoid (Metavolcanite, volcanite)	5
Quartz monzodiorite	15
Fine-grained granite	7 (5 dykes)
Granite, medium to coarse grained	8
Diorite to gabbro	5

4.1 Density and magnetic properties

The rock type classification diagram in Figure 4-1 shows the distribution of the magnetic susceptibility versus density for each rock type. This “geophysical” rock classification correlates very well with the “geological” classification for a majority of the samples. Both types of granites (fine-grained and medium to coarse grained) fall at, or close to, the granite classification curve. The Ävrö granite samples range in the classification diagram from granite to granodiorite-tonalite composition. The quartz monzodiorite and the fine-grained dioritoid both classify as rock types with a composition mainly corresponding to tonalite (or quartz diorite). These two rock types can not be separated from each other on basis of their susceptibility-density properties. One of the quartz monzodiorite data points (PSM003764) plot on the diorite classification curve, which indicates that this rock has a more mafic composition than the other samples of this rock type. The data from one sample location of the fine-grained dioritoid rock type (PSM002091) deviates significantly from the rest of the samples, with a high density and a low magnetic susceptibility. A visual inspection of the drill cores shows that the rock at this site has a relatively higher content of dark minerals than the rocks at the other four locations, which could indicate a more mafic composition resulting in a higher density. This site location should be re-examined by a geologist. All five diorite to gabbro rock samples fall close to the gabbro classification curve, though there is a fairly large scatter in the magnetic susceptibility.

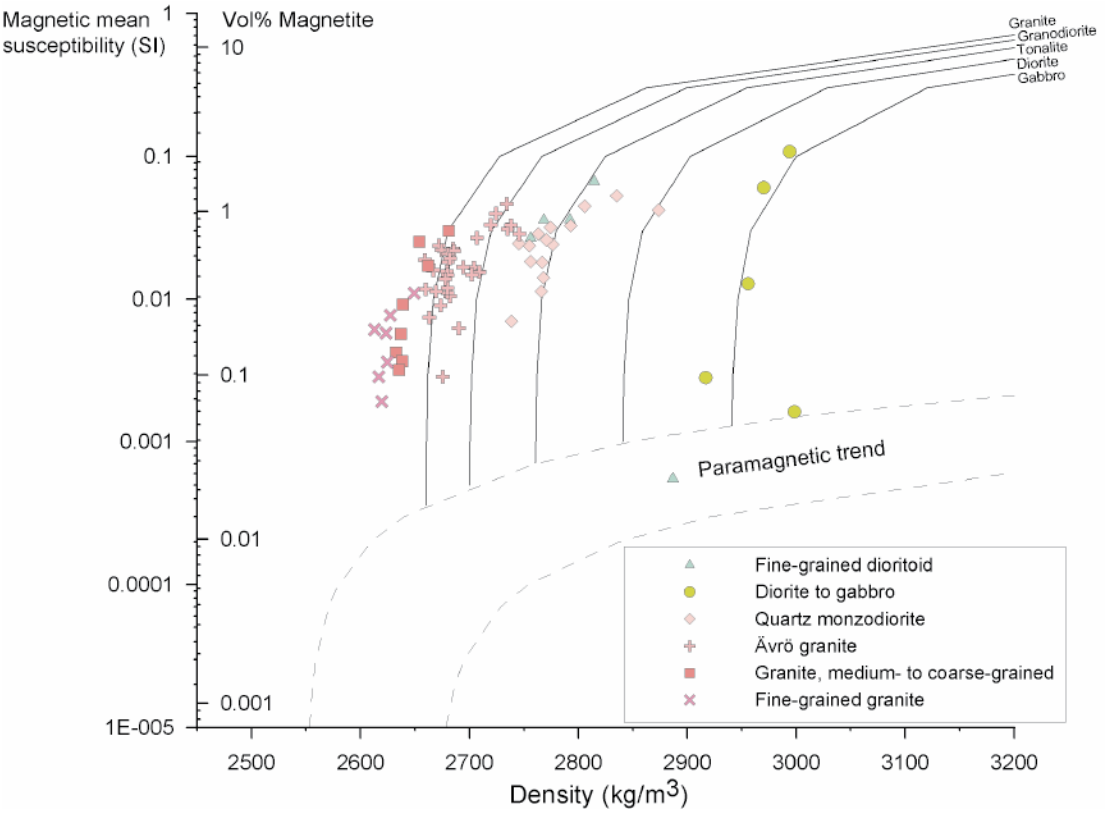

Figure 4-1. *Density-susceptibility rock classification diagram. See the text for explanation.*

The density distribution of the rocks shows four main intervals (Figure 4-2). Fine-, medium- and coarse-grained granite rocks fall in the range of c 2,600–2,650 kg/m^3, Ävrö granite ranges at 2,650–2,730 kg/m^3 and quartz monzodiorite and fine-grained dioritoid rocks mainly fall in the range c 2,750–2,850 kg/m^3. In the fourth interval the rock type diorite to gabbro is found, and it plots in the range of 2,920–3,000 kg/m^3.

The spatial distribution of calculated silicate densities (fine-grained granite dykes excluded), and the corresponding rock classification, is shown in Figure 4-3. The data is plotted with the existing bedrock map /13/ as background and the rock type legend from the feasibility study is therefore used. There is a fair agreement between the geological map and the silicate density rock classification. A majority of the rocks classify as rocks with a composition corresponding to granite to granodiorite. Within the quartz monzodiorite and the fine-grained dioritoid in the Simpevarp peninsula (both termed granodiorite to quartz monzodiorite in the geological map) the silicate density mainly indicates rock types with a composition corresponding to tonalite rock. Along the northern boundary of the indicated quartz monzodiorite rock body there are several locations with high density rocks corresponding to diorite or gabbro mineral composition. At one sample location within

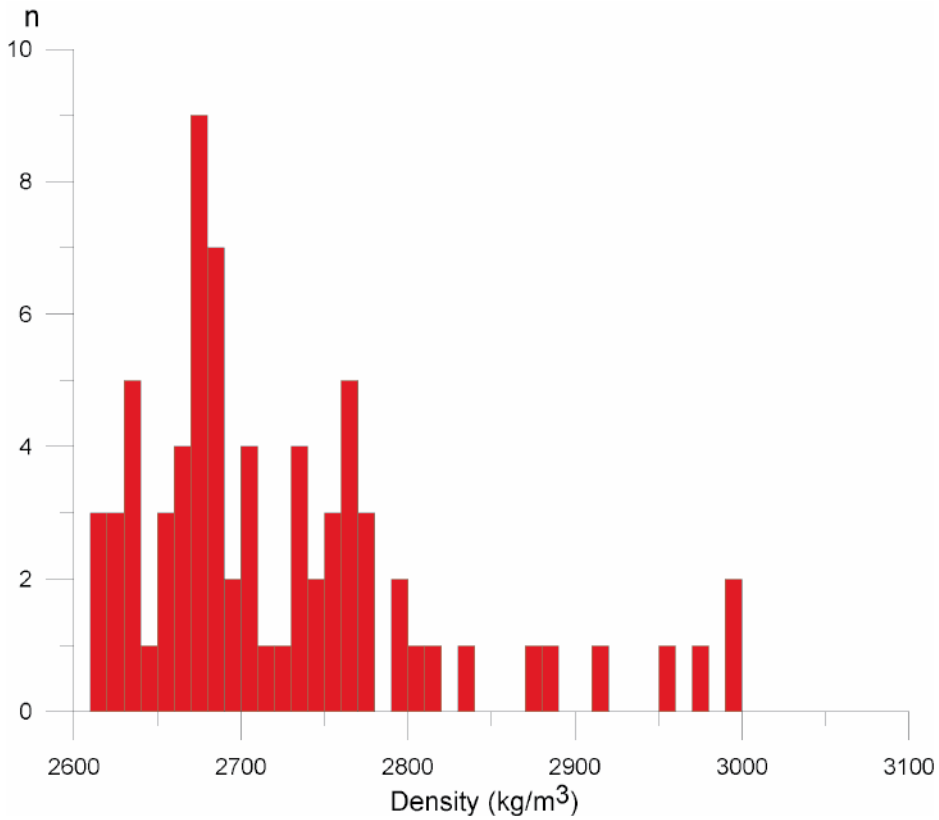

Figure 4-2. *Histogram of the wet density of all rock objects (n = number of measurements).*

the so-called Ävrö granite, close to the northern boundary of the quartz monzodiorite, the silicate density corresponds to that of tonalite rock, and vice versa there are two locations within the north western part of the quartz monzodiorite that classify as granodiorite rock.

A contour plot in Figure 4-4 shows the spatial variations in wet density of the main rock types. Fine-grained granite dykes and diorite-gabbro rocks are excluded to avoid unbalanced anomaly distributions. The contour lines have been interpolated by taking the mean value of values within a search radius of 600 metres. The relatively few data points make this kind of processing sensitive to anomalous data points and detailed anomalies must be ignored. The data indicates a rather homogenous pattern of low densities in the northernmost part of the investigated area, followed by a trend of slightly increasing density moving southward. The quartz monzodiorite rocks and the fine-grained dioritoid rocks in the Simpevarp peninsula come out as fairly well defined high density anomalies. Ävrö granite rocks in the Lilla Laxemar area have higher densities than those located further northwest, closer to Mederhult.

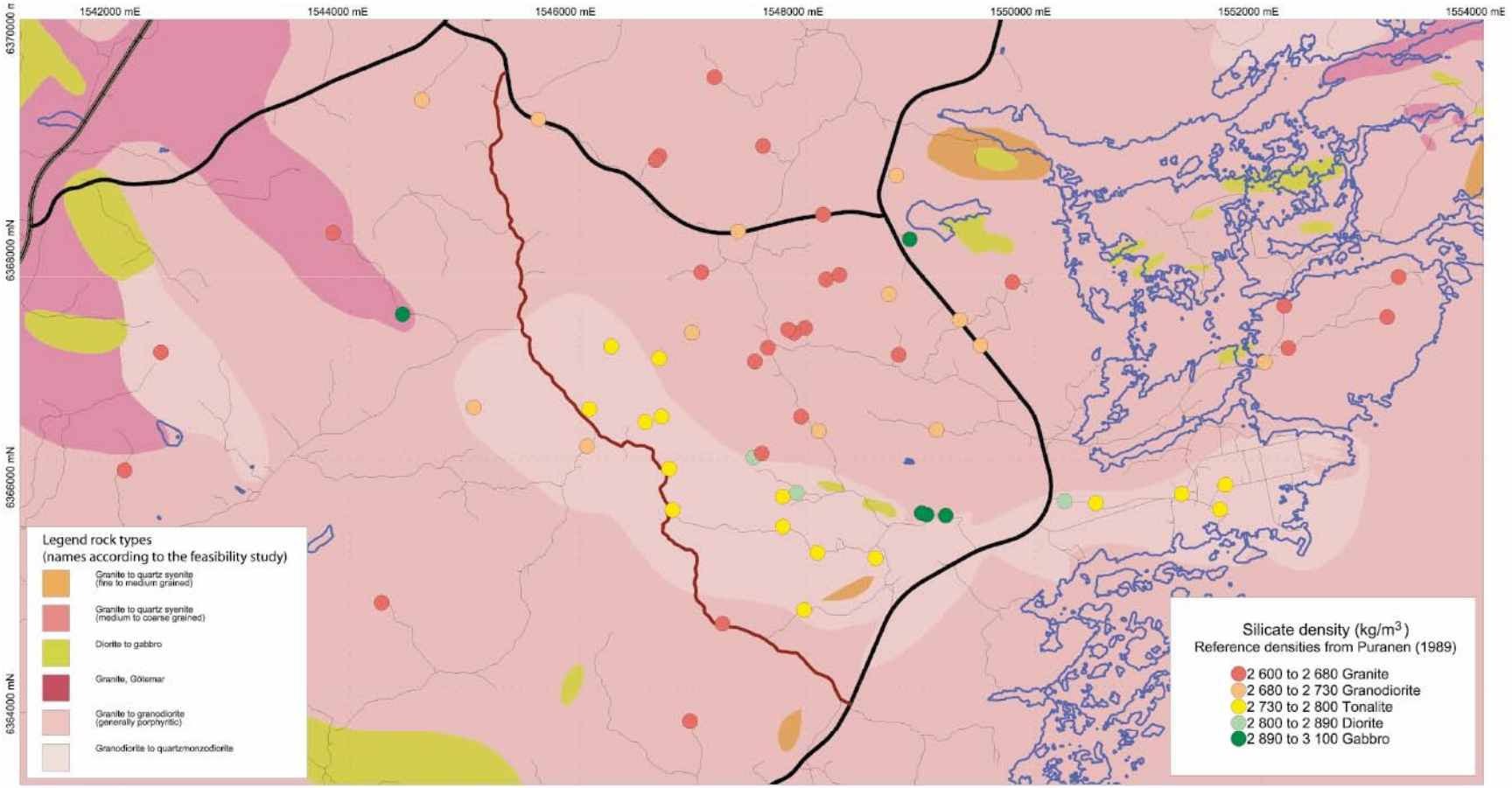

Figure 4-3. *Silicate density and corresponding rock classification for the main rock types in the area of Oskarshamn site investigation. The data is plotted with the existing bedrock map (slightly simplified) as background and the rock type legend from the feasibility study /13/. See the text for explanation. From GSD-terrängkartan ©Lantmäteriet Gävle 2001, permission M2001/5268 Swedish Nuclear Fuel & Waste Management Co 2004-11-09.*

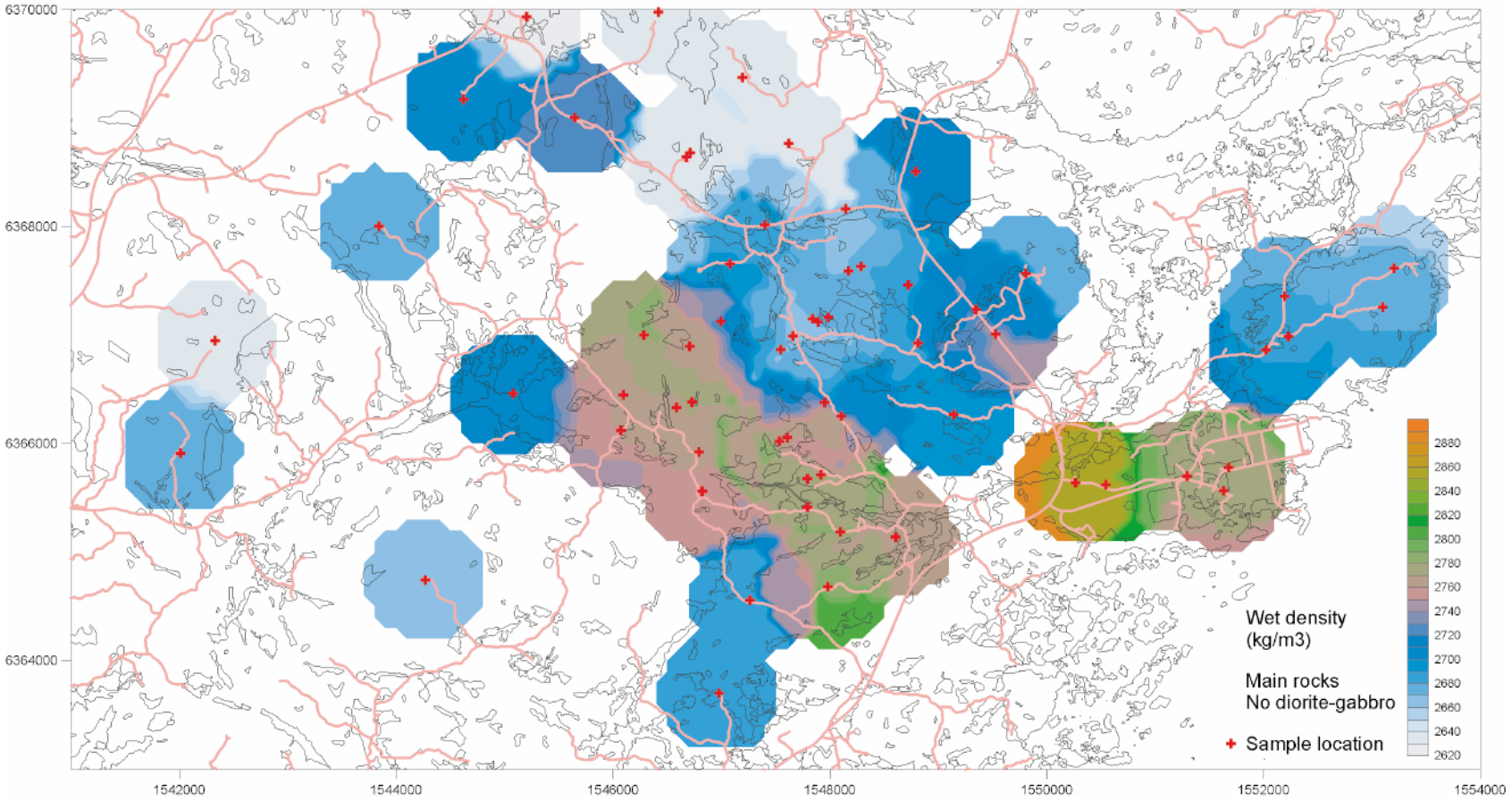

Figure 4-4. *Contour plot of wet densities of main rock types (fine-grained granite dykes and diorite-gabbro rocks excluded) in the area of Oskarshamn site investigation. The red crosses denote sample locations. From GSD-terrängkartan ©Lantmäteriet Gävle 2001, permission M2001/5268 Swedish Nuclear Fuel & Waste Management Co 2004-11-09.*

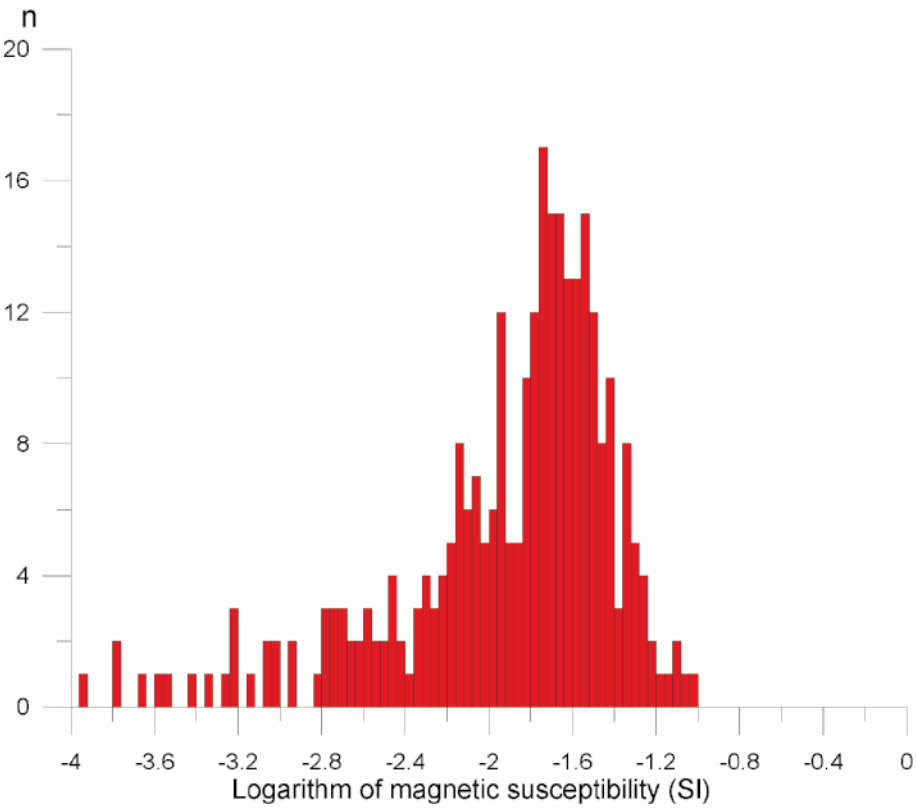

Figure 4-5. *Histogram of the mean susceptibility of all individual specimens.*

The magnetic susceptibility approximately varies between 0.0001 SI and 0.100 SI (Figure 4-5). The distribution is tri-modal with one cluster at 0.0025 SI, a larger at 0.0080 SI and the largest at 0.0251 SI. A majority of the specimen susceptibilities cluster in the range of c 0.01 SI to 0.1 SI, which indicates that the induced magnetization of a majority of the sampled rocks is dominated by ferromagnetic minerals, most likely magnetite. Natural remanent magnetization (NRM) intensities are fairly high, averaging at c 250 mA/m, and Q-values lay in the range of Q = 0.08 to Q = 6.23, with an average of $Q_{average}$ = 0.52 (Figure 4-6). This indicates that magnetite governs the remanent magnetization of a majority of the samples. The fairly well defined grouping of the data in Figure 4-6 indicates that the magnetic mineralogy is proportionately equivalent for most rock types. Two outstanding outliers are the medium to coarse grained red granite samples at locations PSM002111 and PSM003766 with Q = 4.50 and Q = 2.30 respectively. These rocks have low susceptibility, which could indicate a different magnetic mineralogy, possibly influenced by hematite, compared to the rocks at the other sample locations. The rock at the sample location PSM002091 (fine-grained dioritoid) that differed significantly from its group in the density susceptibility rock classification diagram (Figure 4-1) has a Q-value within the same range as the other rocks in that group.

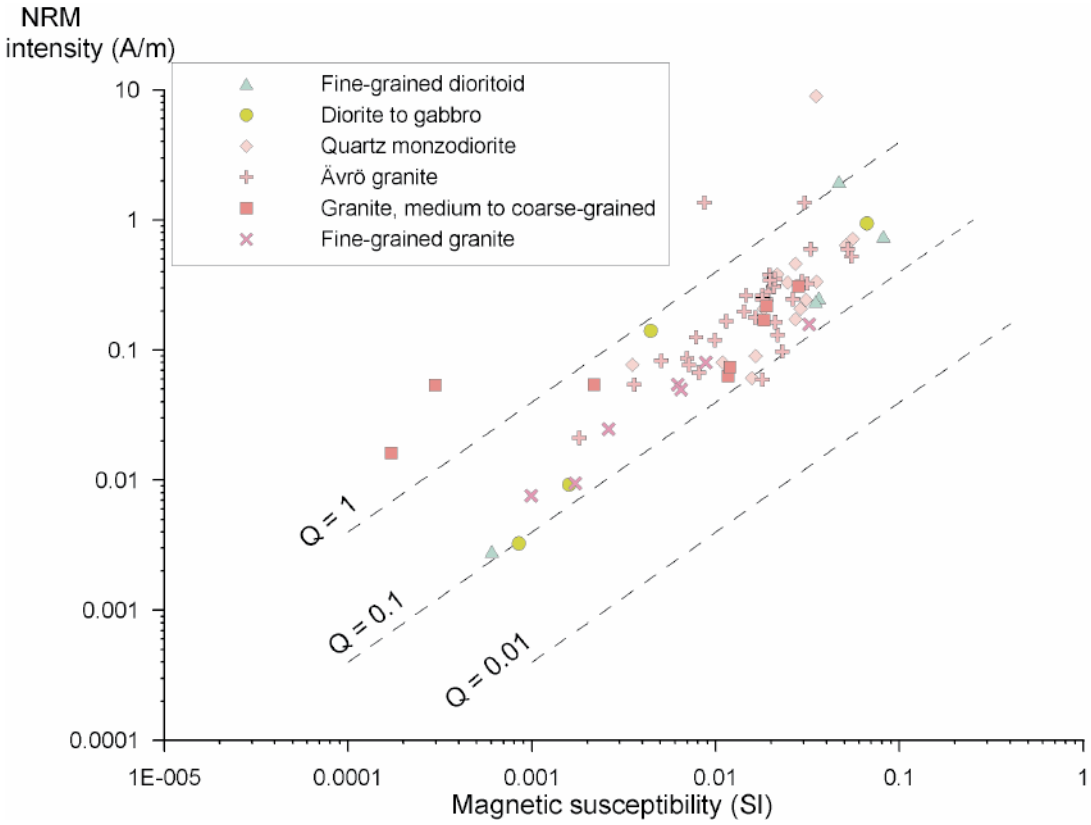

Figure 4-6. *Natural remanent magnetization (NRM) intensity versus magnetic susceptibility.*

The directions of the NRM (Natural Remanent Magnetization) scatter in declination and vary from moderate to steep inclinations (Figure 4-7). The mean direction of decl = 336° and incl = 78° is fairly close to the direction of the present earth magnetic field. Four samples have negative inclination which means that the remanence vector points upwards; these are all Ävrö granite rocks from the locations PSM005988, PSM002104, PSM002123 and PSM002124. The Q-values of these rock samples are Q = 3.81 (PSM005988), Q = 0.36 (PSM002104), Q = 0.08 (PSM002123) and Q = 0.15 (PSM002124). The upward direction of the remanence vector counteracts the induction part of the total magnetic field (measured in the aeromagnetic helicopter measurements) and if large parts of the bedrock in this area carries upward directed remanence directions, there is risk of distorted anomaly patterns in the aeromagnetic data, which may cause misinterpretations of the area of distribution of rock units and falsely interpreted locations of rock contacts. The Q-value of PSM005988 is high, and if this Q-value is representative for a large part of the surrounding rocks, the magnetic anomaly pattern in this part of the Laxemar area could be significantly distorted.

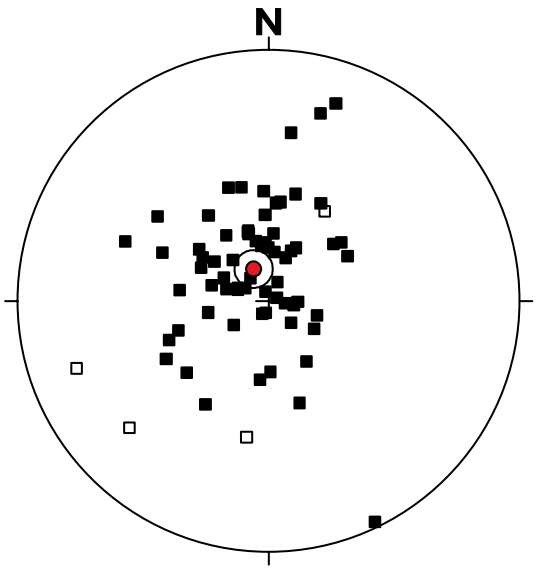

Figure 4-7. *Equal area projection plot showing natural remanent magnetization (NRM) directions of the rocks within the Oskarshamn site investigation area. Open symbols denote negative inclination of the remanence vector. The red symbol shows the mean NRM direction and the circle is the 95% cone of confidence of the mean.*

4.2 In situ measurements of magnetic susceptibility

The results of the in situ susceptibility determinations are presented in the two Figures 4-8 and 4-9 where Figure 4-8 shows rock types of mainly felsic composition and Figure 4-9 of mainly mafic composition.

In Figure 4-8 the Ävrö granite shows a roughly tri-modal distribution in magnetic susceptibility. The most magnetic samples have a frequency peak in the interval –1.75 to –1.5 in the histogram which equals approximately 0.01800 to 0.03200 SI-units. The middle frequency peak is around –3.675 (eq approx 0.00020 SI units).

The quartz monzodiorite shows a frequency distribution in recorded magnetic susceptibilities which very much resembles the one of the Ävrö granite, though the character is more bi-modal as the lowest peak is smeared out. The frequency peak in the high susceptibility range is located in the same position for both rock types. One difference is however that susceptibilities above approx 0.03000 SI units are absent in the Ävrö granite while they occur in the quartz monzodiorite. However, in spite of the differences pointed out here, it would be difficult to separate the two units provided the magnetic susceptibility would be the only discriminator.

The Granite, medium- to coarse-grained has a roughly bi-modal distribution in magnetic susceptibility with a high susceptibility frequency peak around –2.125 (approx eq 0.00750 SI units). The lower susceptibility frequency peak approximately equals a susceptibility of c 0.00010 to 0.00020 SI units.

The fine-grained granite has a very broad and flat distribution in the frequency diagram where values are found to vary typically between approx 0.00020 to 0.02100 SI units. Also some very low susceptibilities have been recorded in this rock type.

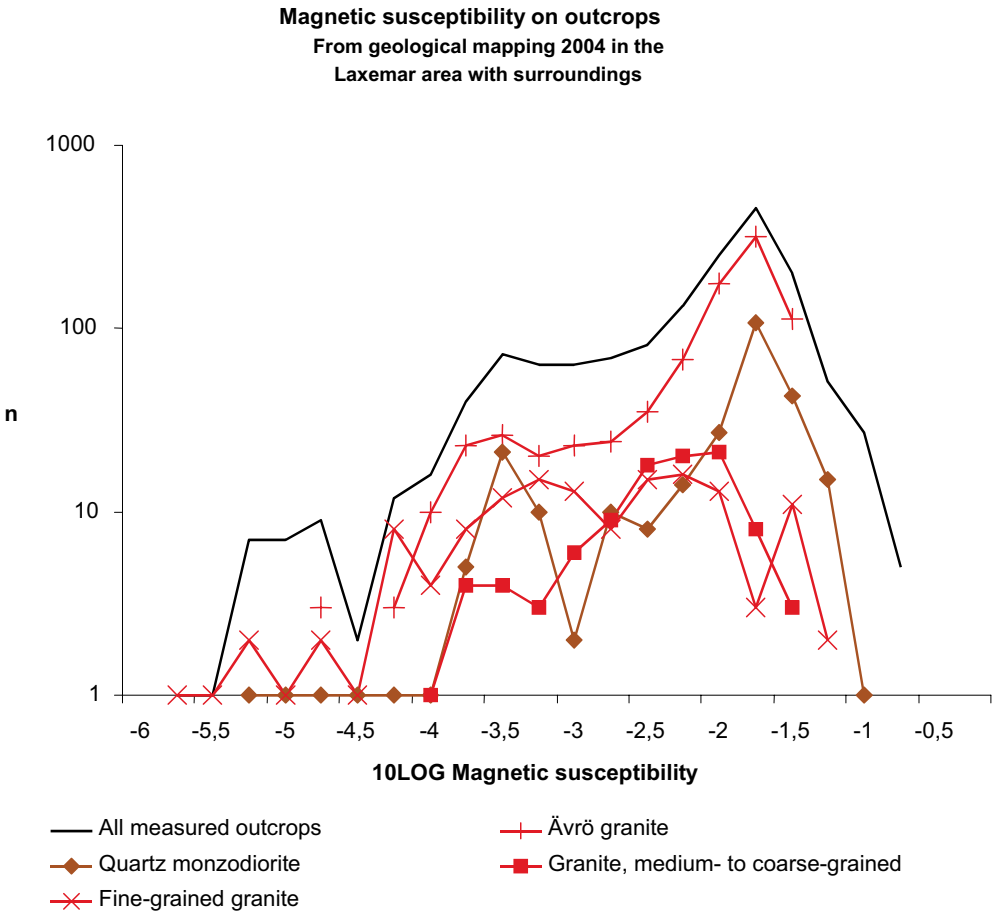

Figure 4-8. *The magnetic susceptibility on outcrops from the activity "Geological mapping 2004 in the Laxemar area with surroundings". Rock types of felsic composition are presented.*

In order to preserve the clearness of the illustration the rock type pegmatite is not shown in Figure 4-8. Furthermore the number of localities measured where pegmatite occurs are only six. The measurements carried out indicate that the magnetic susceptibility varies between approx 0.00030 to 0.00140 SI-units.

In Figure 4-9 the diorite to gabbro shows a roughly tri-modal distribution in magnetic susceptibility. The most magnetic samples have a frequency peak in the interval of approx 0.03200 to 0.05600 SI units in the histogram. The middle frequency peak is around in-between approx 0.00060 to 0.00180 SI units. Obviously some studied units have very low magnetic susceptibilities they are however scarce. Statistically this rock type appears to have the highest frequency of very high magnetic susceptibilities recorded. It explains almost the entire "bulge" observed at the high end of the curve for the frequency distribution of all samples.

Fine-grained dioritoid is a rock type with a frequency distribution with some similarity with the distribution in quartz monzodiorite. The high magnetic frequency peak is however less pronounced in the former unit. Furthermore the number of locations measured is quite low (41). Most of the magnetic susceptibilities are found in the interval of approx 0.00020 to 0.02200 SI units.

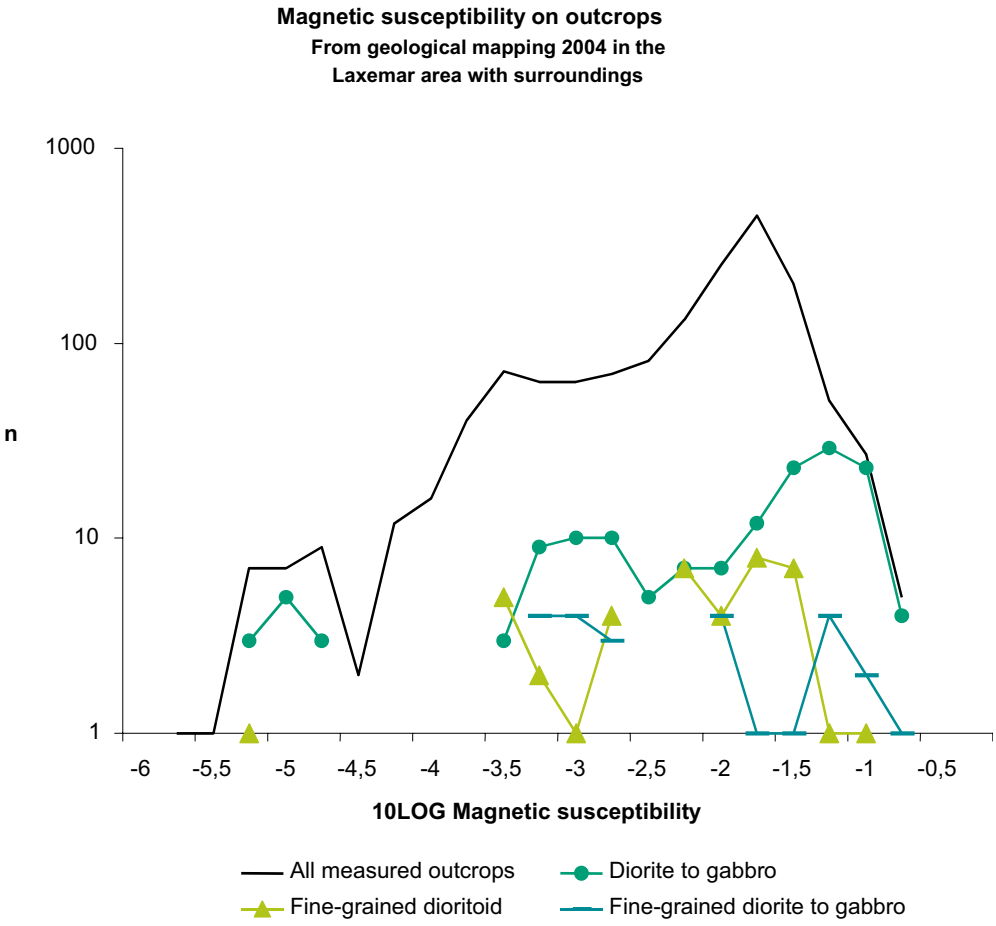

Figure 4-9. *The magnetic susceptibility on outcrops from the activity "Geological mapping 2004 in the Laxemar area with surroundings". Rock types of mafic composition are presented.*

The rock type fine-grained diorite to gabbro appears to be heterogeneous. The heterogeneity manifests itself through a very scattered frequency distribution. Partly the low number of localities measured could explain this, but difficulties in the coding of the rock could also be a contributing factor.

The distribution of localities where the magnetic susceptibility has been measured on outcrops during the bedrock mapping activity of 2004 in the Laxemar area is shown in Figure 4-10. The majority of the localities are situated in the Laxemar area where the coverage is quite dense. Outside the Laxemar area observations of the magnetic susceptibilities are scarce and scattered.

In Figure 4-10 it is possible to study the spatial variations of the average of the magnetic susceptibility for the most common rock type of every outcrop measured. As seen the magnetic susceptibilities as measured on outcrops reflect most of the major anomalies in the map of the magnetic total field in Figure 4-11. It can thus be concluded that the sources to the major magnetic anomalies are identified.

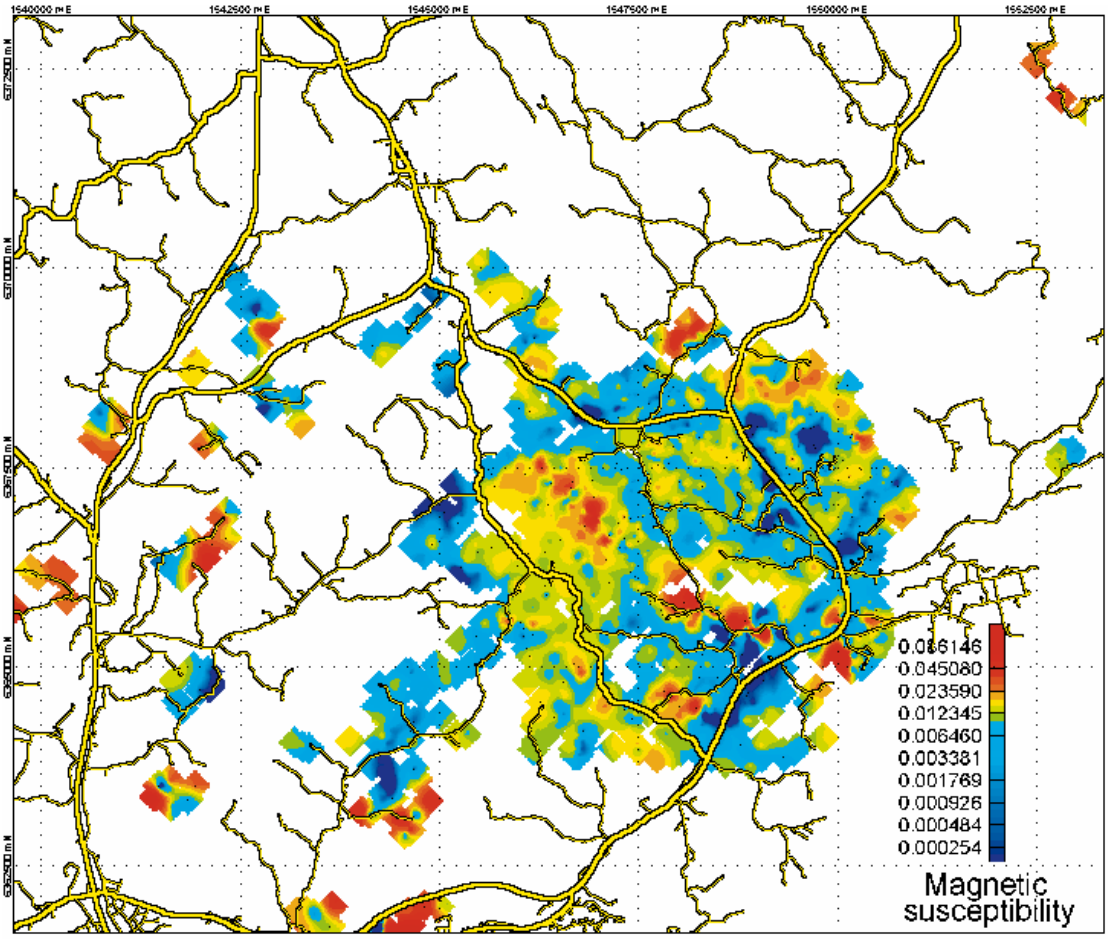

Figure 4-10. *Average of the magnetic susceptibility on outcrops for the most frequent rock type in every outcrop. The spatial variations in the magnetic susceptibility reflect the character of the magnetic total field as recorded in helicopter-borne geophysics (see Figure 4-11). From GSD-terrängkartan ©Lantmäteriet Gävle 2001, permission M2001/5268 Swedish Nuclear Fuel & Waste Management Co 2004-11-09.*

In the comments on the magnetic susceptibility frequency distribution of different rock types above, it was pointed out that the highest magnetic susceptibilities encountered were found in the diorite to gabbro unit. In the Laxemar area a band with high magnetic total field has been observed in the airborne surveys. The anomaly complex is striking NW to SE and is easily observed in the map of the magnetic total field from the helicopter-borne survey. This anomaly is also observed in Figure 4-10 in the same position and the results from the bedrock mapping indicate that rocks belonging to the diorite to gabbro unit commonly occur here. There is no doubt that the majority of the contribution to the anomaly recorded emanates from these mafic rocks.

Above the distribution of the magnetic susceptibilities has been described of the most common rock types of the Laxemar area. The frequency distributions are often bi- or tri-modal where one of the peaks is found at very low values. These low susceptibility values are often connected to the lineaments identified /14/. In Figures 4-11 the low magnetic anomalies indicate the presence of the Äspö shear zone and a parallel zone further west, passing near Mederhult, also are reflected as low magnetic susceptibilities measured on outcrops. This means that magnetite has been partly transformed into other minerals due to oxidation processes in these tectonic zones.

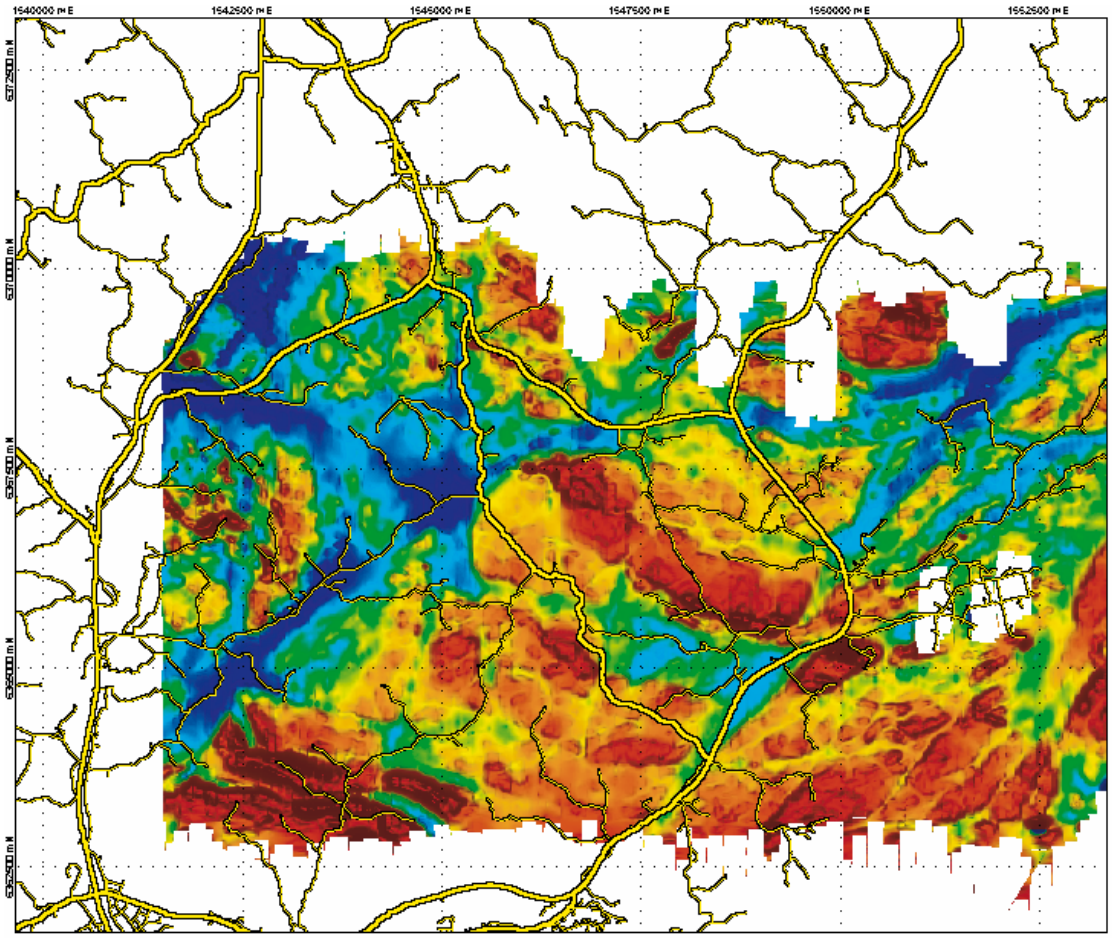

Figure 4-11. *The magnetic total field as recorded in helicopter-borne geophysics. Many of the major anomaly features recognized are reflected in the map over the magnetic susceptibility in Figure 4-10. From GSD-terrängkartan ©Lantmäteriet Gävle 2001, permission M2001/5268 Swedish Nuclear Fuel & Waste Management Co 2004-11-09.*

4.3 Anisotropy of magnetic susceptibility (AMS)

Based on the data shown in chapters 4.1 and 4.2, it is likely to assume that magnetite governs the magnetic properties of a majority of the rocks in the Simpevarp area. This implies that the anisotropy of magnetic susceptibility is primarily governed by the grain shape and orientation of the magnetite grains. The AMS-ellipsoids show a continuous variation in shapes from strongly prolate ("cigar-shape") to strongly oblate ("disc-shape") and degrees of anisotropy are below 1.4 for most samples (Figure 4-12a). There is no correlation between the degree of anisotropy and the magnetic susceptibility (Figure 4-12b), which indicates that the degree of magnetic anisotropy is independent of the concentration of magnetite and that this parameter may indicate variations in the degree of strain. The degree of anisotropy of unaltered magnetite is approximately P = 1.2 /9/, so the data in Figure 4-12 indicates that parts of the investigated rock have suffered from weak plastic deformation.

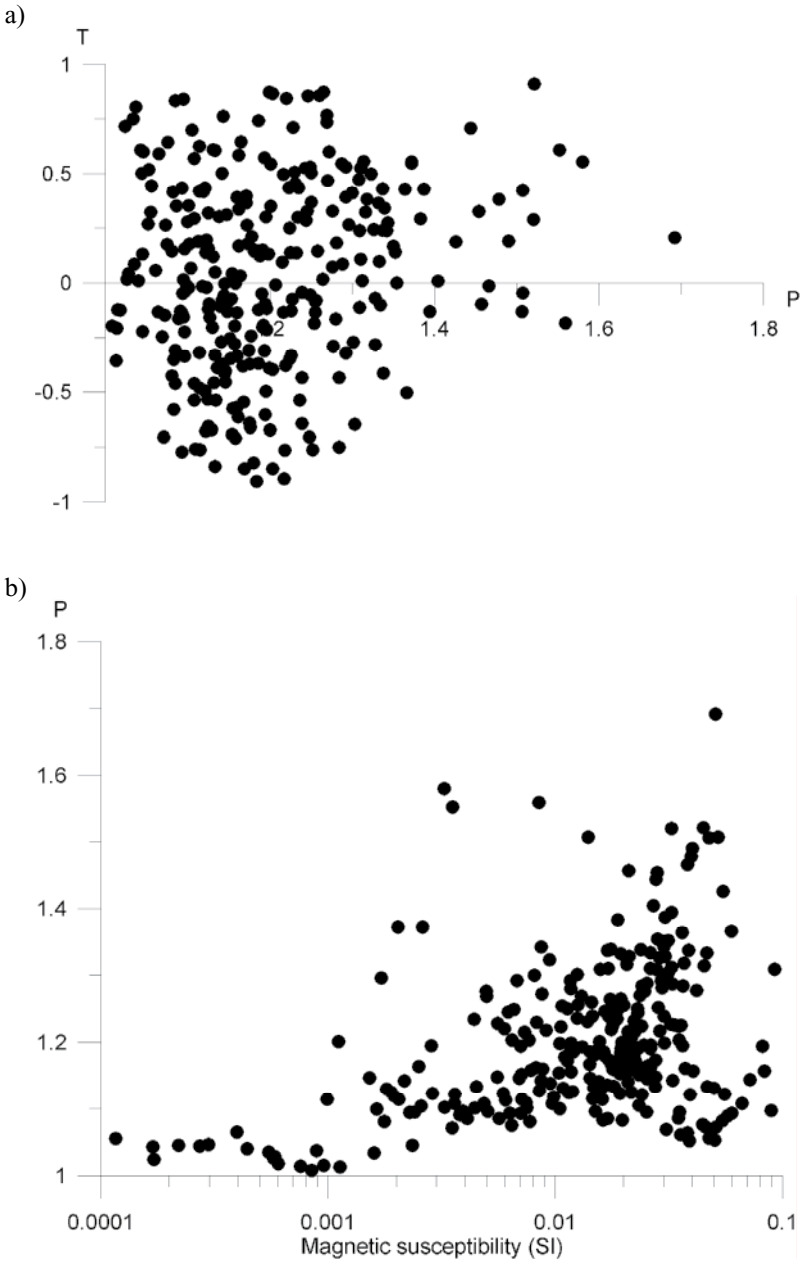

Figure 4-12. *Anisotropy of magnetic susceptibility parameters for individual specimens from all sampling locations, a) Shape parameter (T) versus degree of anisotropy (P) and b) Degree of anisotropy (P) versus mean magnetic susceptibility.*

The degree of anisotropy taken as a mean value at each site (vector addition) is mainly moderate to low for a majority of the rocks (Figure 4-13). This indicates that a majority of the rocks within the site investigation area are primary and unaffected by any major deformation. However, at 8 locations the degree of anisotropy exceeds P > 1.3 and at two locations, PSM002098 and PSM002113, the anisotropy degree exceeds P > 1.4. The rocks at these 8 sampling locations may have been affected by plastic deformation, e.g. related to local shear zones.

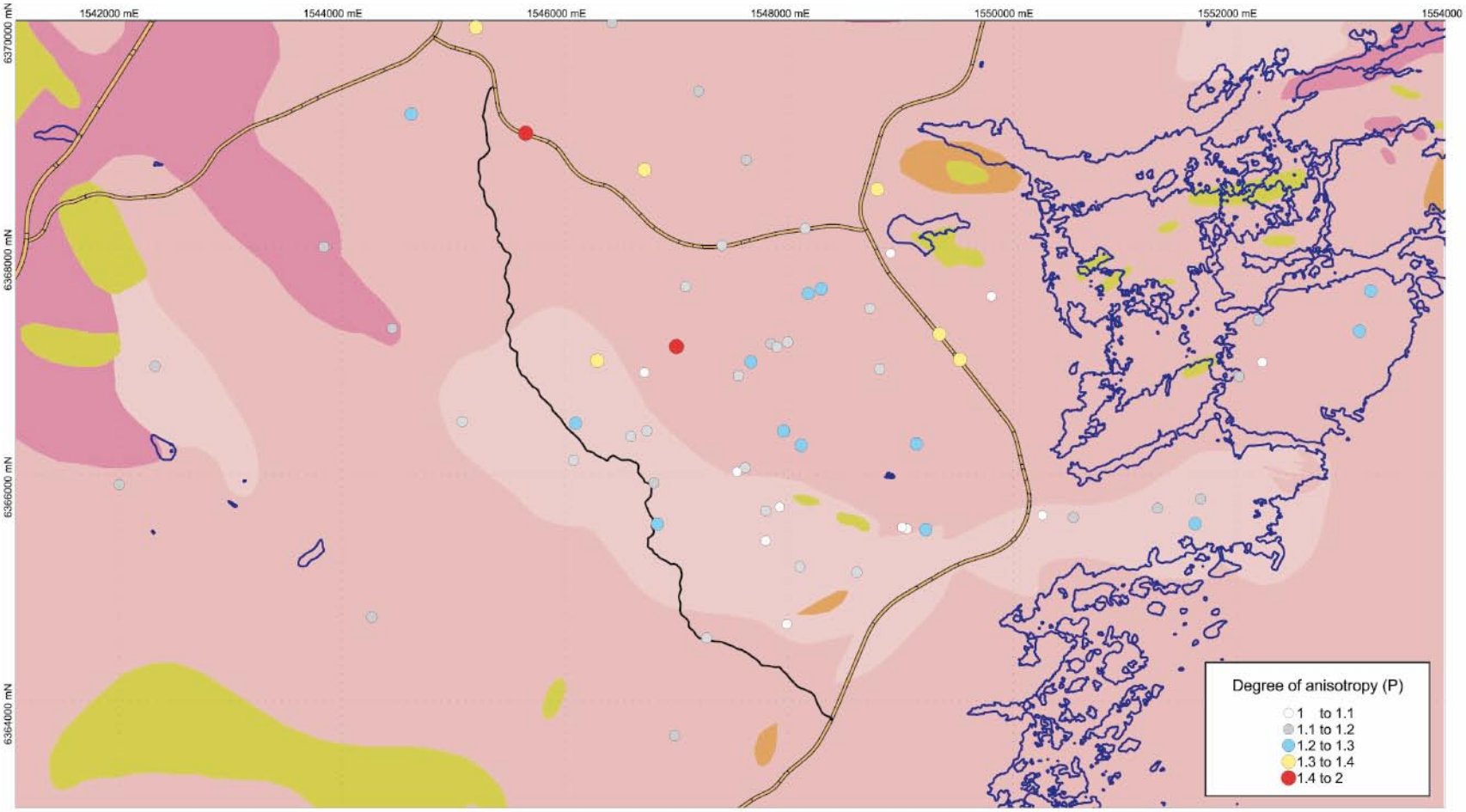

Figure 4-13. *Geographical distribution of the degree of anisotropy (mean values) for the main rocks in the Simpevarp area. The same rock type legend as in Figure 4-3. From GSD-terrängkartan ©Lantmäteriet Gävle 2001, permission M2001/5268 Swedish Nuclear Fuel & Waste Management Co 2004-11-09.*

The AMS principal axis orientations clearly show a consistent pattern in spite of the fact that a vast majority of the sampled rocks appear to be of primary origin and lack visible tectonic fabrics. The poles to the foliation (Kmin) form a girdle distribution, which indicates a folded geometry. By calculating the pole of the best fitting plane to the distribution of foliation poles, the orientation of the indicated fold axis is estimated at c Decl = 290° and Incl = 21° (Figure 4-14 lower plot).

The magnetic lineations (Kmax, maximum strain) cluster (with a scatter) in the north-west direction with mainly moderate to sub horizontal dips (Figure 4-14 upper plot). The mean direction of Kmax (large blue square in Figure 4-14) is sub-parallel to the fold axis estimated from the poles to the foliations, thus indicating that the regional maximum strain is sub-parallel to the estimated fold axis. The fine-grained granite dykes (triangle symbols in Figure 4-14) all show westward strike directions of the magnetic foliation planes. Three of them have sub-vertically dipping foliation planes and also sub-vertically dipping lineations, which marks these dykes as possible outliers in the general structural pattern of the area.

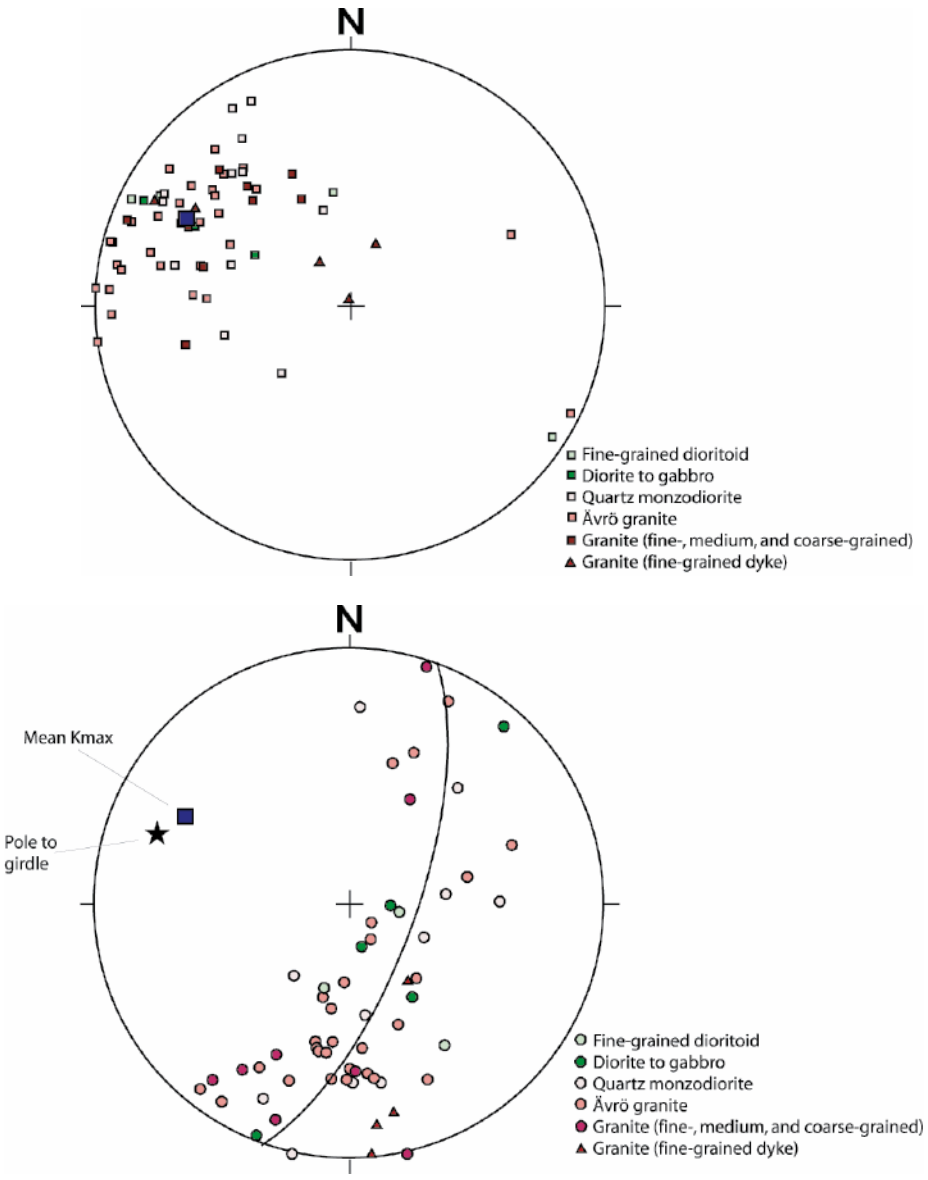

Figure 4-14. *Equal area projection plots of maximum (lineation) and minimum (poles to foliation) site mean anisotropy axes for the rocks in the Simpevarp site investigation area.*

In Figure 4-15 the geographical distribution of the orientation and dip of the magnetic foliation planes is shown. In general, the strikes of the foliation planes follow the east-west to east-southeast – west-northwest orientation of the major lithological boundaries. Together with the generally low degrees of anisotropy, this probably indicates that most rocks carry a primary magnetic fabric related to the stress field that prevailed during the emplacement of the rocks. However, the girdle distribution in Figure 4-14 shows that the structural pattern is more complex than this, but there is no indication of regional folding in the geographical distribution of the foliation planes in Figure 4-15. The two sampling locations that are situated closest to the so-called Äspö shear zone (PSM002091 and PSM002117), both carry a magnetic foliation that is parallel to the ENE-WSW orientation of the shear zone, but their degree of anisotropy is only moderate to low. The similar orientation of the deformation zone and the magnetic foliations indicates that these rocks have been affected by the deformation. It is therefore possible that the AMS data display two (or more) generations of structural fabrics, one primary related to the emplacement of the rocks giving rise to east-southeast – west-northwest orientations, and one secondary related to weak deformation giving rise to N-S to NE-SW directed orientations. The distribution of poles in Figure 4-14 indicates that both orientation directions (WNW and SW strike) occur for all rock types except fine-, medium- and coarse-grained granites. The granite rocks show mainly W to WNW trending orientations.

A contour plot of the dip of the foliation planes is displayed in Figure 4-16a. The contour lines have been interpolated by taking the mean value of values within a search radius of 600 meters. The plot shows that the investigated area roughly can be divided into three structural regions; a southern region dominated by moderate to steep dips, a central region dominated by shallow to moderate dips and a northern region dominated by steeply dipping foliation planes.

The geographical distribution of the magnetic lineation (maximum strain) directions shows consistent north-westward orientations at the Simpevarp peninsula and mainly north-westward (but partly westward) orientations in the central and western part of the investigated area (Figure 4-17). Dips are generally moderate to shallow. At the Ävrö island the lineations show consistent westward orientations with dips varying from 0° to 43°. Note that for many site locations where the foliation planes show scattered orientation directions, the lineations are consistently sub-parallel and have NW trending orientation.

A contour plot of the dip of the lineations (Figure 4-16b) roughly supports a division of the investigated area into three structural regions. The contour lines have been interpolated by taking the mean value of values within a search radius of 600 metres.

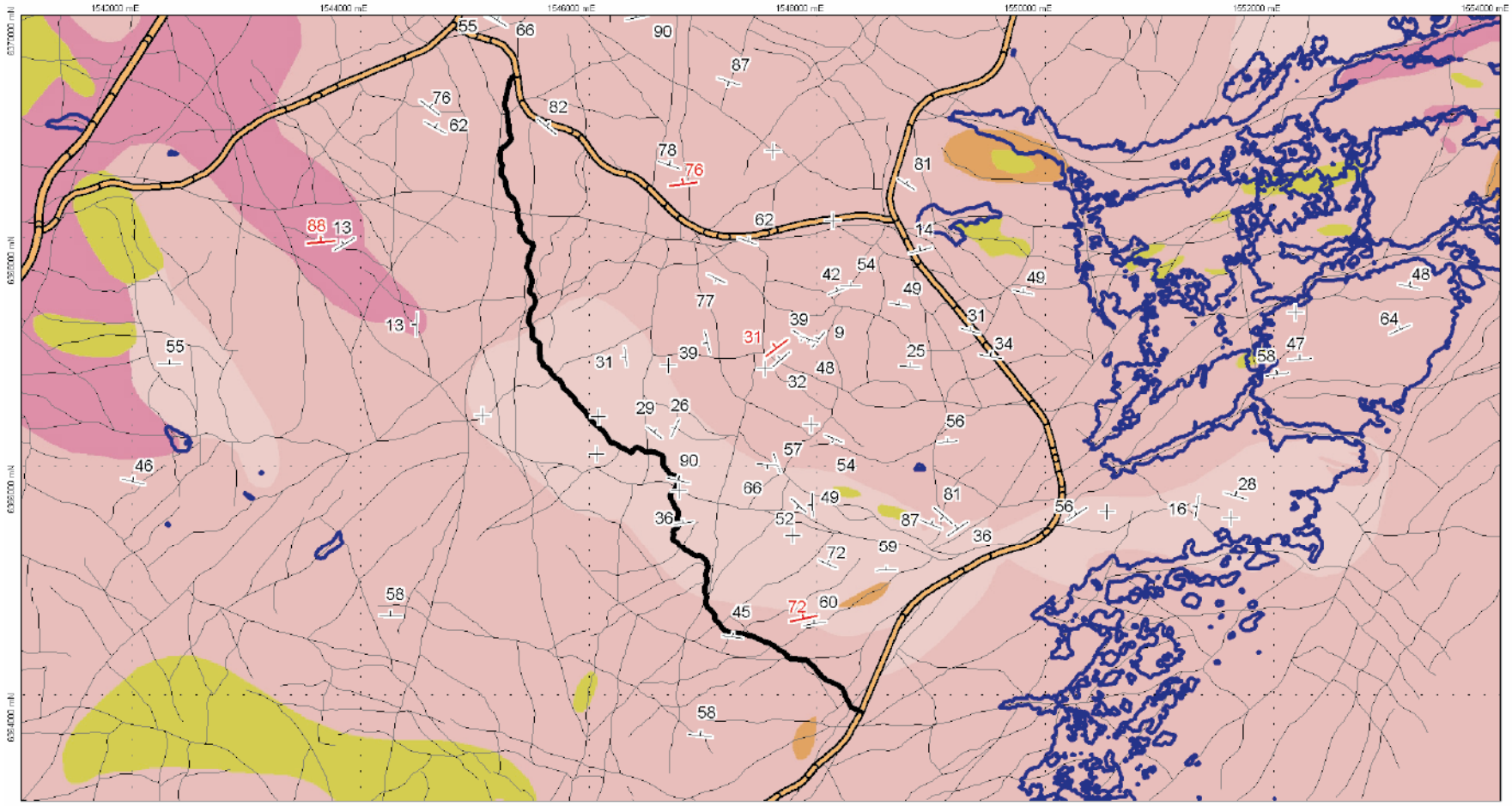

Figure 4-15. *Strike and dip of magnetic foliation planes (mean values) in the Simpevarp site investigation area. Black symbols denote main rocks and red symbols denote fine-grained granite dykes. The crosses denote sampling location where no mean direction could be established. The thin black lines show lineaments from /14/. The same rock type legend as in Figure 4-3. From GSD-terrängkartan ©Lantmäteriet Gävle 2001, permission M2001/5268 Swedish Nuclear Fuel & Waste Management Co 2004-11-09.*

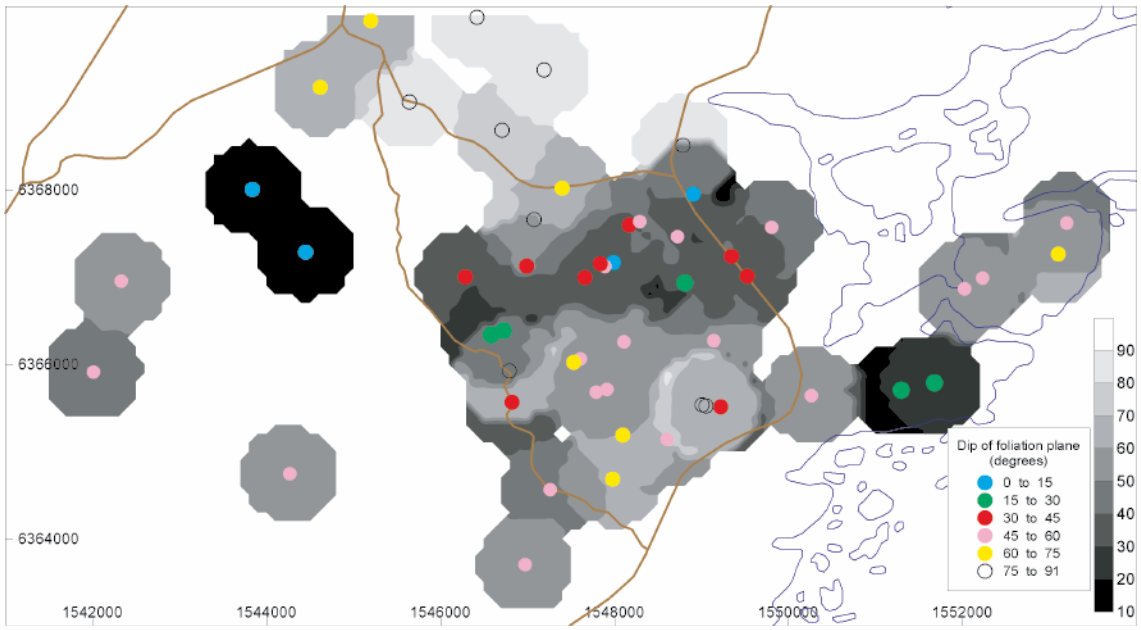

a)

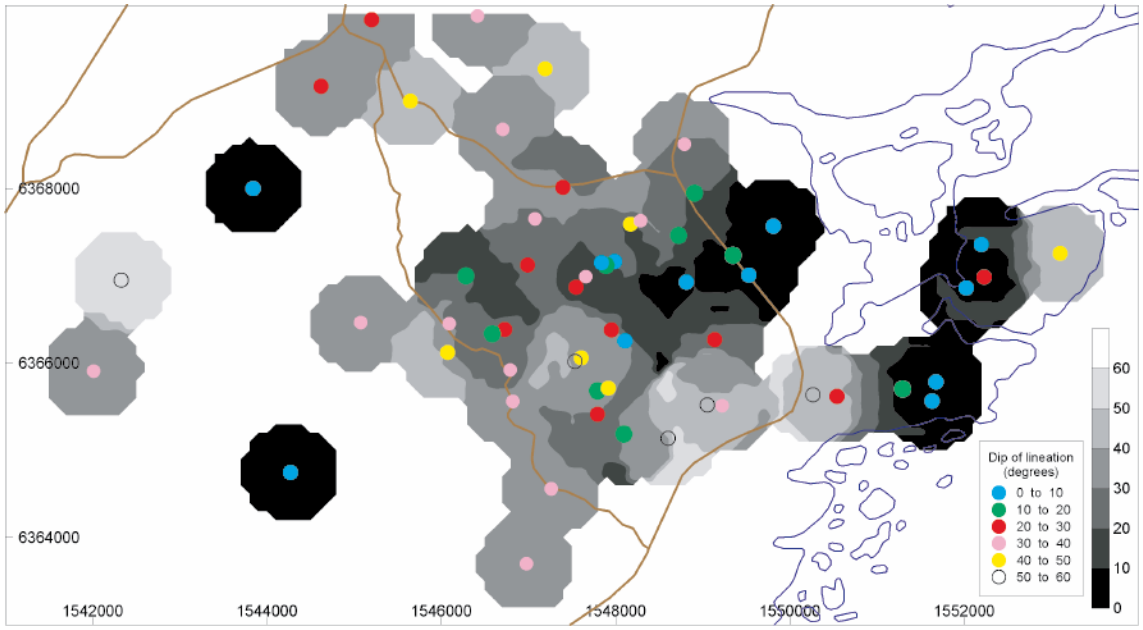

b)

Figure 4-16. *a) Contour plot of the dip of the magnetic foliation planes (symbols denote sampling position and dip of foliation in intervals of 15°). b) Contour plot of the dip of the magnetic lineations (symbols denote sampling position and dip of foliation in intervals of 10°). From GSD-terrängkartan ©Lantmäteriet Gävle 2001, permission M2001/5268 Swedish Nuclear Fuel & Waste Management Co 2004-11-09.*

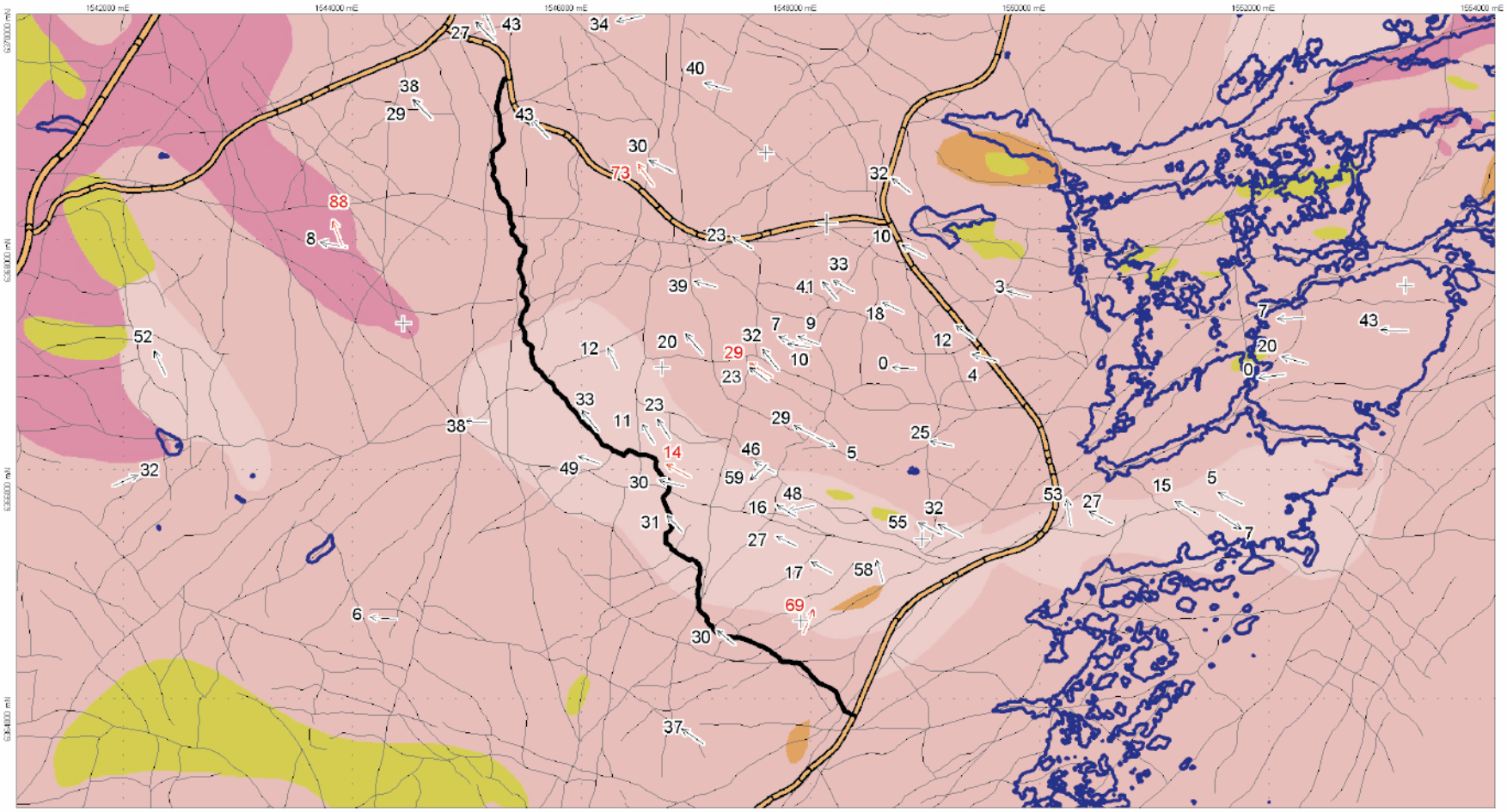

Figure 4-17. *Orientation and dip of magnetic lineations (mean values) in the Simpevarp site investigation area. Black symbols denote main rocks and red symbols denote fine-grained granite dykes. The crosses denote sampling location where no mean direction could be established. The thin black lines show lineaments from /14/. The same rock type legend as in Figure 4-3. From GSD-terrängkartan ©Lantmäteriet Gävle 2001, permission M2001/5268 Swedish Nuclear Fuel & Waste Management Co 2004-11-09.*

4.4 Electric resistivity, induced polarization and porosity

4.4.1 Porosity

The distribution of measured porosities can be seen in the histograms in Figure 4-18. The range of porosities between 0.1 and 1.0% is fairly normal for crystalline rocks of Proterozoic age. Although the porosity ranges of the rock types overlap and the number of samples is small, some differences can be noted. The more mafic rock types (fine grained dioritoid and diorite to gabbro) have low porosities with median values of 0.29 and 0.28% respectively. The highest median porosity is found for Ävrö granite (0.63%).

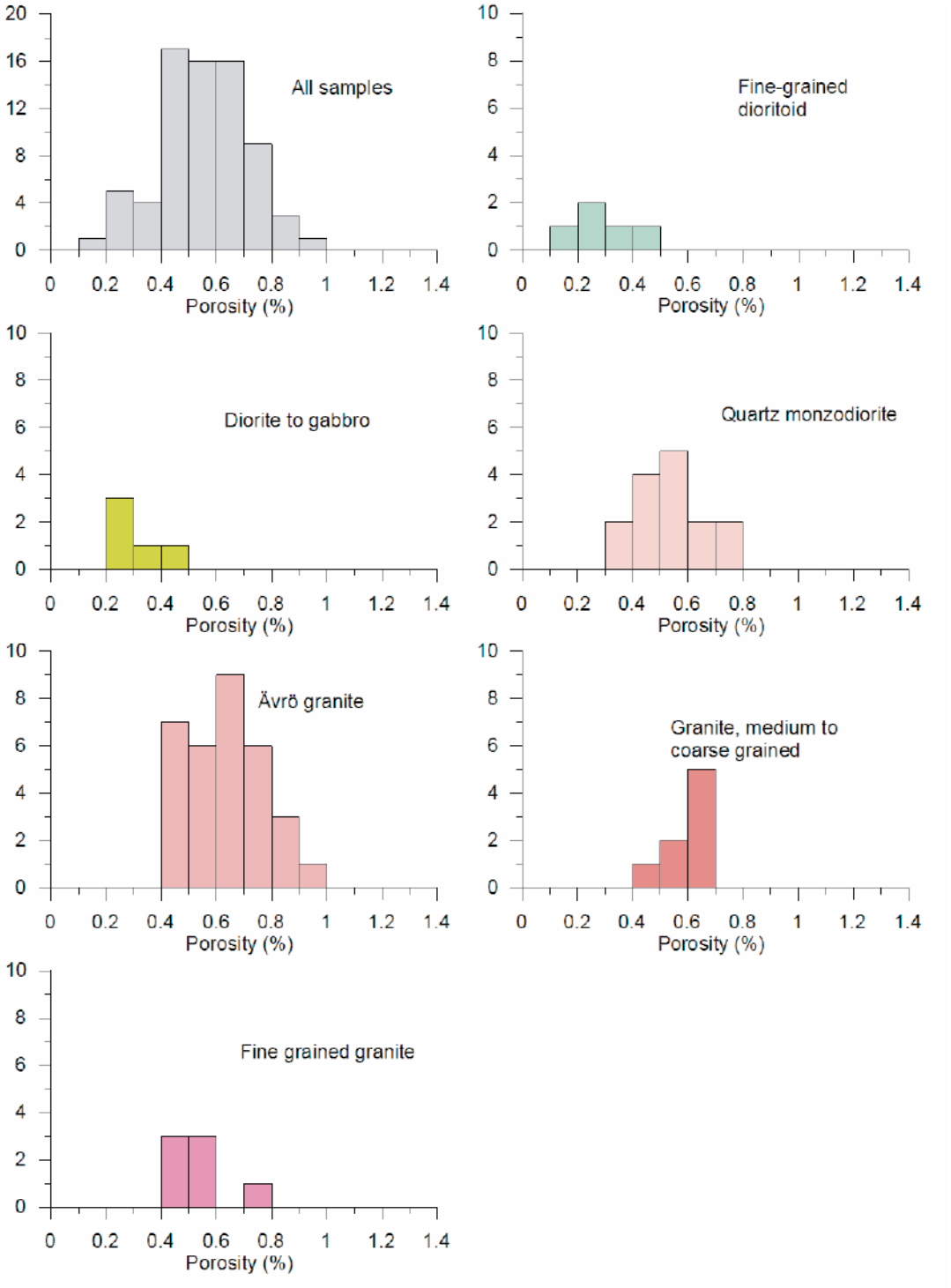

Figure 4-18. *Histograms showing distribution of measured porosities for the rock types.*

A map showing the porosity as countour lines is shown in Figure 4-19. The contour lines have been found by taking the median porosity value within a search radius of 800 metres. The lines have also been slightly smoothed. Low porosities are indicated for the Simpevarp peninsula but this might be a lithological effect since all samples from this area are of fine-grained dioritoid. The highest porosity values are found for the central part of the sampled area. Most samples from this area are Ävrö granite.

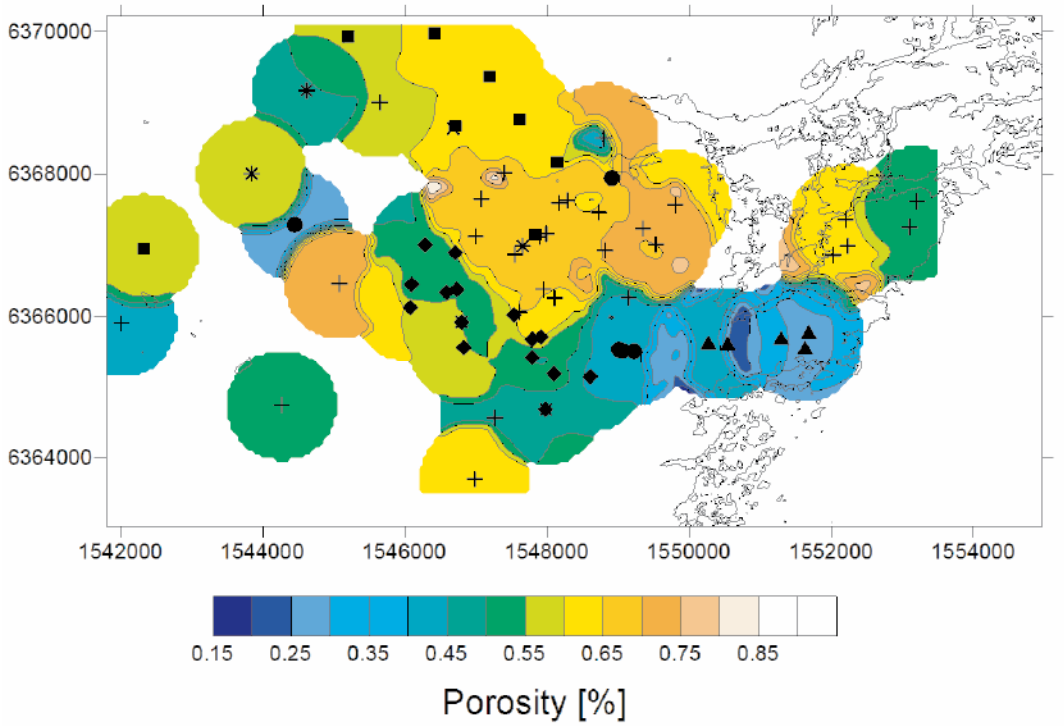

Figure 4-19. *Map showing the measured porosity of samples. The symbols indicate the sampling locations and the symbol type indicates the sampled rock type according to the legend in e.g. Figure 4-20. Note that more than one rock type has been sampled at some sites. The contour lines have been interpolated by taking the median value within a search radius of 800 metres. From GSD-terrängkartan ©Lantmäteriet Gävle 2001, permission M2001/5268 Swedish Nuclear Fuel & Waste Management Co 2004-11-09.*

4.4.2 Electric resistivity and induced polarization properties

The spatial dependence of electrical properties and the properties of different rock types have been analyzed.

The IP effect as a function of resistivity in fresh water can be seen in Figure 4-20. With a few exceptions the samples have resistivities from 6,000 to 30,000 Ωm and IP-values from 3 to 20 mrad. Both ranges can be considered to be quite normal for non-mineralised crystalline rocks. No correlation can be seen between the two parameters.

The ranges of resistivity and IP values overlap for the different rock types. Still, some differences can be seen although conclusions are difficult to draw due to the rather small number of samples for some of the rock types. High resistivities have mainly been

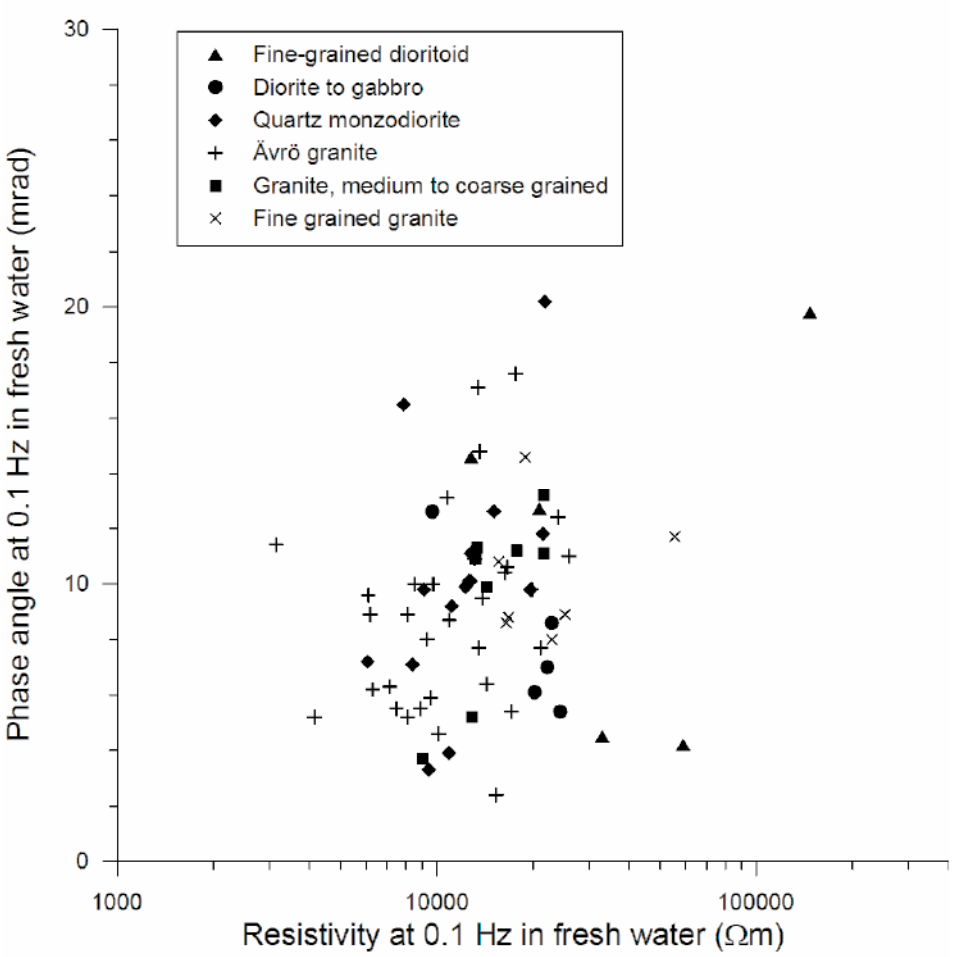

Figure 4-20. *Resistivity and IP-effect (phase angle) for samples soaked in tap water.*

measured on samples of fine-grained dioritoid and diorite to gabbro. This is probably due to the generally lower porosities of these rock types compared to the different granite types. The fine to medium grained granite has higher resistivity than the other granite types. Slightly higher IP values have been measured on the fine-grained dioritoid samples than for the other rock types.

Maps showing the resistivity and IP values of the samples are presented in Figures 4-21 and 4-22. Contour lines have been interpolated by finding the median values within a search radius of 800 metres. The contours have also been slightly smoothed. Petrophysical data ideally should not be interpolated in this way but it was done in order to make patterns in the data recognisable.

The samples from an area in the central part of the map seem to have slightly lower resistivity than the rest of the samples. The area roughly coincides with the high porosity area in the contour map of porosities in Figure 4-19. High resistivity values are seen for the Simpevarp peninsula, which corresponds to a low porosity area in Figure 4-19.

The IP data hardly show any significant spatial pattern (Figure 4-22). The fine grained dioritoid samples from the Simpevarp peninsula causes a positive phase angle anomaly.

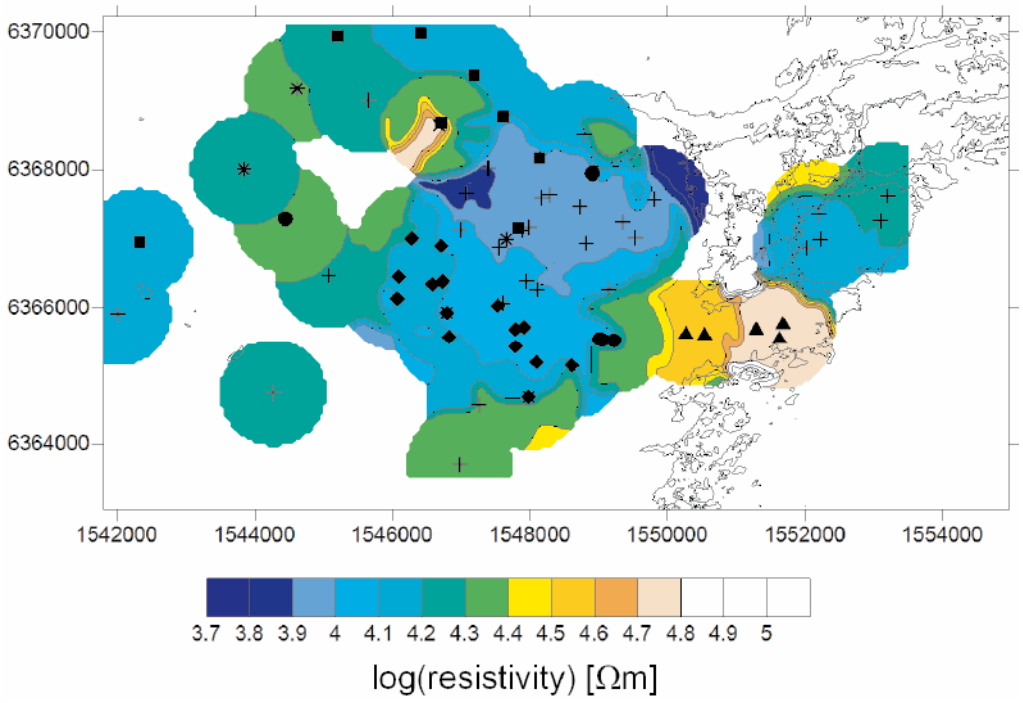

Figure 4-21. *Map showing the resistivity of samples measured in fresh water. The symbols indicate the sampling locations and the symbol type indicated the sampled rock type according to the legend in e.g. Figure 4-20. Note that more than one rock type has been sampled at some sites. The contour lines have been interpolated by taking the median value within a search radius of 800 metres. From GSD-terrängkartan ©Lantmäteriet Gävle 2001, permission M2001/5268 Swedish Nuclear Fuel & Waste Management Co 2004-11-09.*

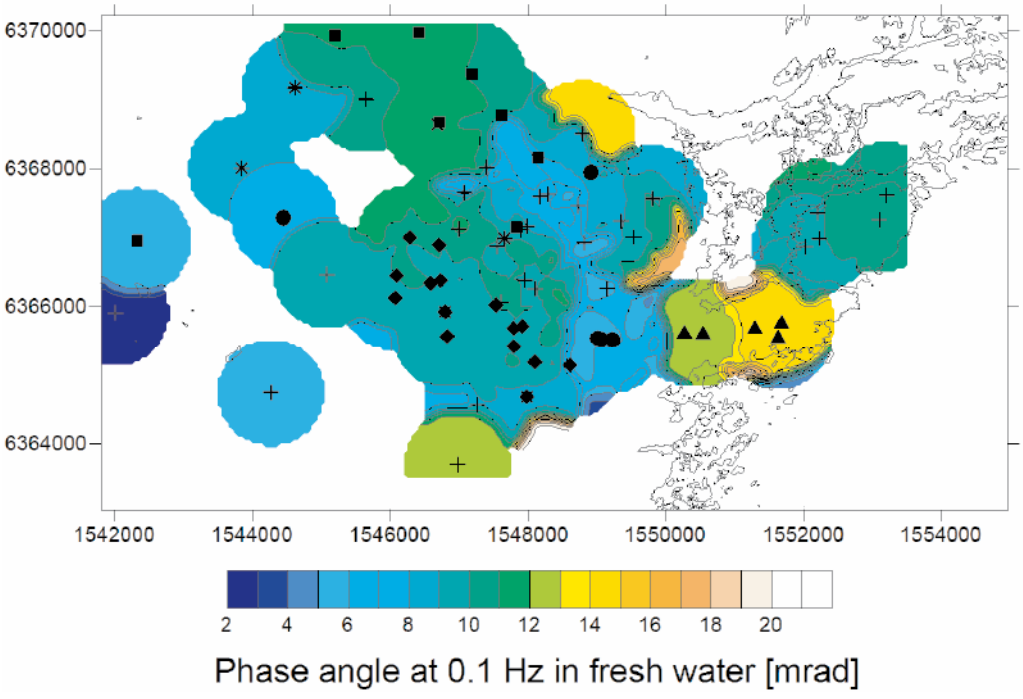

Figure 4-22. *Map showing the IP-effect (phase angle at 0.1 Hz) of samples measured in fresh water. The symbols indicate the sampling locations and the symbol type indicates the sampled rock type according to the legend in e.g. Figure 4-20. Note that more than one rock type has been sampled at some sites. The contour lines have been interpolated by taking the median value within a search radius of 800 metres. From GSD-terrängkartan ©Lantmäteriet Gävle 2001, permission M2001/5268 Swedish Nuclear Fuel & Waste Management Co 2004-11-09.*

The measured resistivity in saline water (2.5% NaCl by weight) as a function of porosity is plotted in Figure 4-23. A negative correlation might be expected since high porosity should correspond to low resistivity and vice versa. This relationship can be modelled with Archie's law according to the discussion in section 3.4. However, such a correlation is rather poor. There are some possible reasons for this. Firstly, the porosity has been measured on all drill cores from a site assembled to one sample in order to get a high accuracy, whereas the resistivity has been measured on one drill core only. This procedure will introduce some scatter in the plot in Figure 4-23. However, it can hardly entirely explain the poor correlation. A second reason is that samples have different surface conductivity properties, even if they belong to the same rock group. Surface conductivity should have less influence in saline water compared to fresh water but some effect might still exist. Samples where the porosity to a relatively large degree consists of thin membranes will have a lower resistivity than a sample with the same porosity but wider pore spaces. A third reason for the poor correlation in Figure 4-23 is that the samples might be anisotropic. It has only been possible to measure the resistivity in one direction for each sample. The porosity is a simple scalar and this means that the position of a sample in the plot in Figure 4-23 to some degree might be dependent on the drill core orientation relative rock foliation/lineation. A final reason might be that different samples have different types of pore space geometry. A sample where the pore space contains constrictions, vugs, dead-ends and crooked paths will have a higher resistivity than a sample with the same porosity but with fairly straight paths with constant cross-sectional area. Such a property is modelled by the exponent *m* in Archie's law. For crystalline rocks, high values for m are expected for altered rocks where e.g. quartz grains have been dissolved.

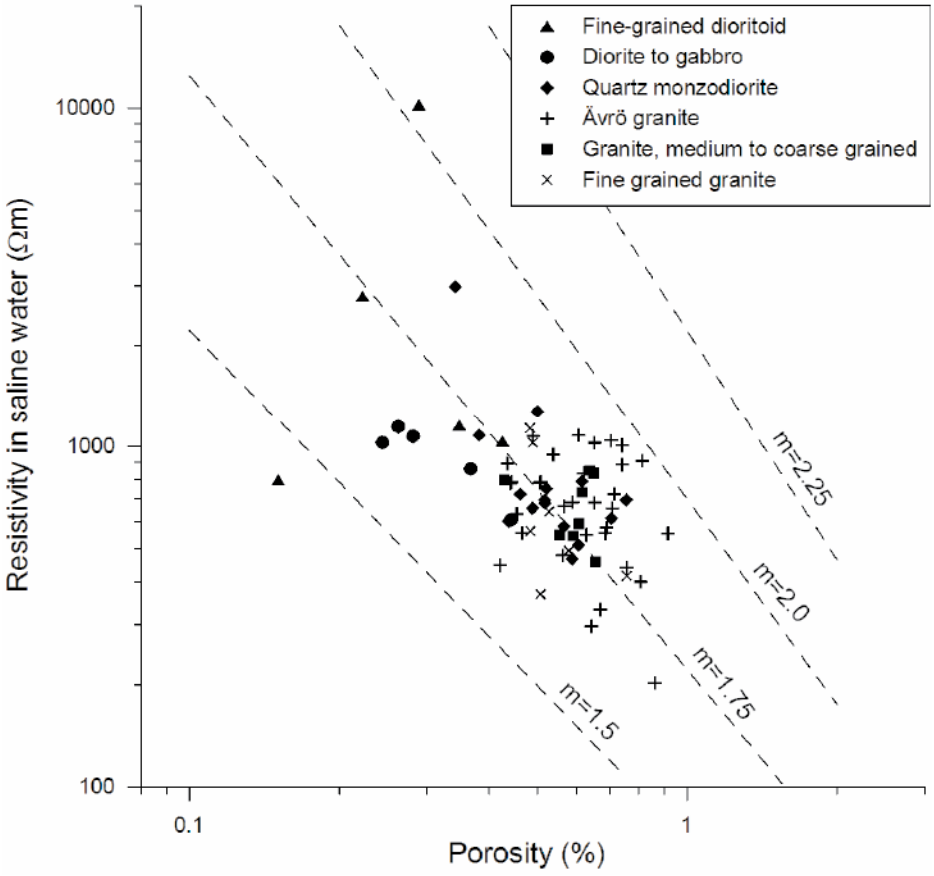

Figure 4-23. *Measured resistivity as a function of porosity for samples soaked in saline water. The four dashed lines represent the resistivity according to Archie's law calculated for a = 4 and* σ_w *= 3.57 S/m. The samples then show different apparent m-values which might correspond to different of pore-space geometry characteristics.*

Lines according to Archie's law for *a*=4 and different values for m can be seen in Figure 4-23. Apparent m-values can be calculated for all samples based on the above assumptions:

$$m_a = \frac{\ln\left(\frac{\sigma_s}{a_s \cdot \sigma_{ws}}\right)}{\ln \phi}$$

where σ_s and σ_{ws} are the electric conductivities of the sample and saline water respectively, a_s is the surface conductivity correction factor for saline water in Archie's law and φ is the porosity.

The resistivity measured in fresh water as a function of porosity can be seen in Figure 4-24. The correlation between porosity and resistivity is rather poor also for this case and no reliable fit to Archie's law can be made. However, if apparent *m*-values from saline water measurements are used, it is possible to calculate apparent a-values according to:

$$a_a = \frac{\sigma_f \cdot \sigma_{ws}}{\sigma_{wf} \cdot \sigma_s} \cdot a_s$$

where σ_f and σ_{wf} are the electric conductivities of the sample and fresh water respectively. Note that no porosity data are required to calculate apparent a-values. The calculations rely upon an assumption of the a-value for saline water. However, even if this value is wrongly estimated, the ratio of a-values for fresh and saline water will be the same.

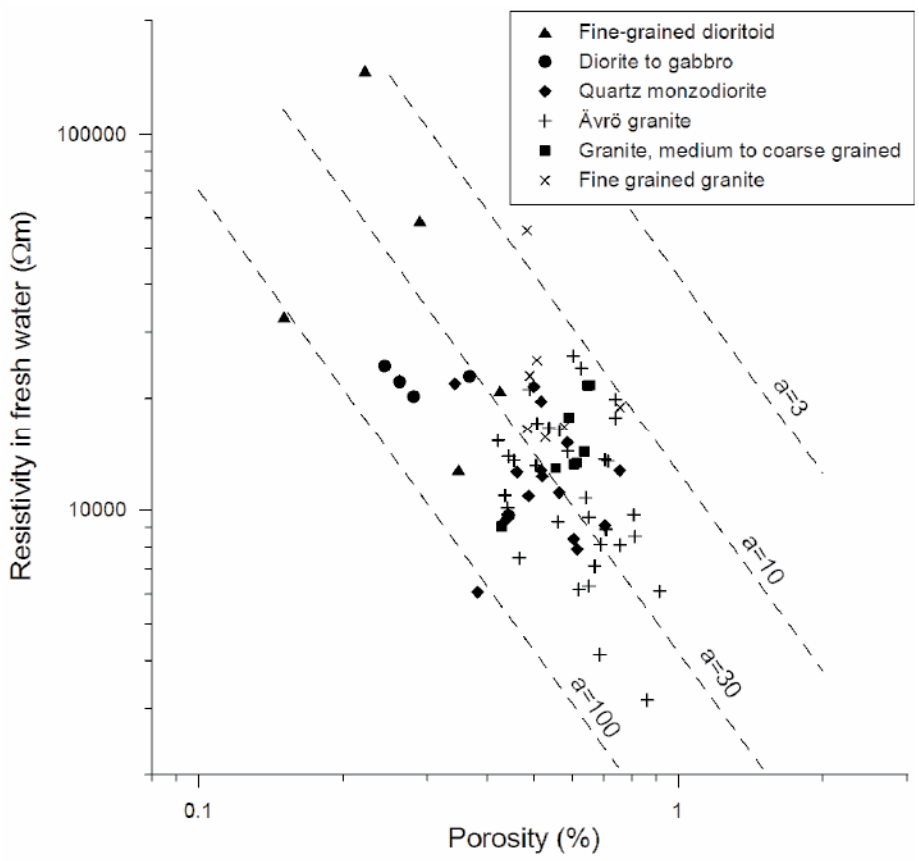

Figure 4-24. *Measured resistivity as a function of porosity for samples soaked in fresh water. The four dashed lines represent the resistivity according to Archie's law calculated for m = 1.75 and σ_w = 0.025 S/m. Apparent a-values equal to one would then correspond to no surface conductivity.*

High apparent a-values are expected for samples where the pore space to a large degree consists of thin membranes. This is expected for samples containing chlorite, fine-grained mica and clay minerals. Apparent m- and a-values are plotted for all samples in Figure 4-25. The apparent m-values range from c 1.6 to 2.0 for most samples. This can be regarded as fairly normal values. Sampling of altered rocks from KSH02 /15/ gave apparent a-values of up to 2.4. Values of around 2.0 might still indicate a minor alteration of the rock. Most samples have apparent a-values exceeding 10. This means that surface conductivity is the dominating electrical conduction mechanism in fresh water. Some of the samples have apparent a-values exceeding 40. This might indicate some kind of alteration of the rock that has resulted in formation of e.g. chlorite, sericite or clay minerals. High apparent a-values were found for the strongly altered rocks from KSH02 /15/. High apparent a-values were also found for samples from KFM01A, KFM02A and KFM03A in Forsmark where sericite-altered plagioclase and chlorite was found in microscopic investigations /16/. Low apparent a-values are found for fine grained granite.

Maps showing the distribution of apparent m- and a-values can be seen in Figure 4-26 and 4-27 respectively. The highest apparent m-values are found in the northern and central part of the study area. The highest apparent a-values are found in the eastern part of the Simpevarp peninsula. Slightly elevated values are also seen in the central part of the area.

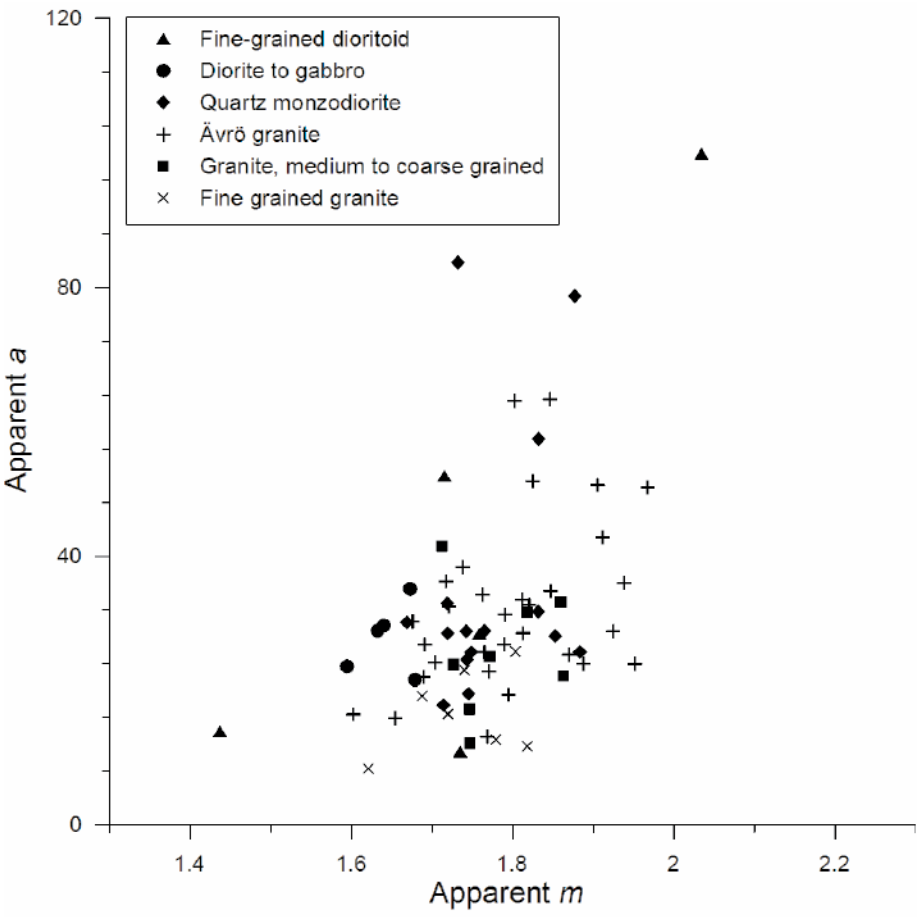

Figure 4-25. *Apparent m- and a-values in Archie's law.*

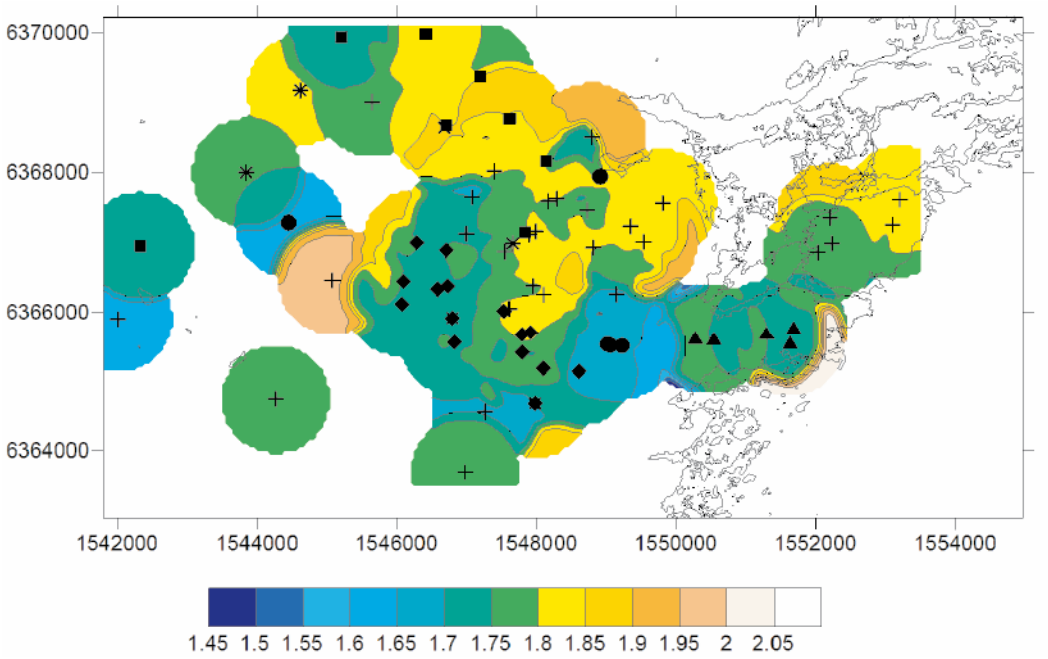

Figure 4-26. *Map showing apparent m-values in Archie's law. The symbols indicate the sampling locations and the symbol type indicates the sampled rock type according to the legend in e.g. Figure 4-25. Note that more than one rock type has been sampled at some sites. The contour lines have been interpolated by taking the median value within a search radius of 800 metres. From GSD-terrängkartan ©Lantmäteriet Gävle 2001, permission M2001/5268 Swedish Nuclear Fuel & Waste Management Co 2004-11-09.*

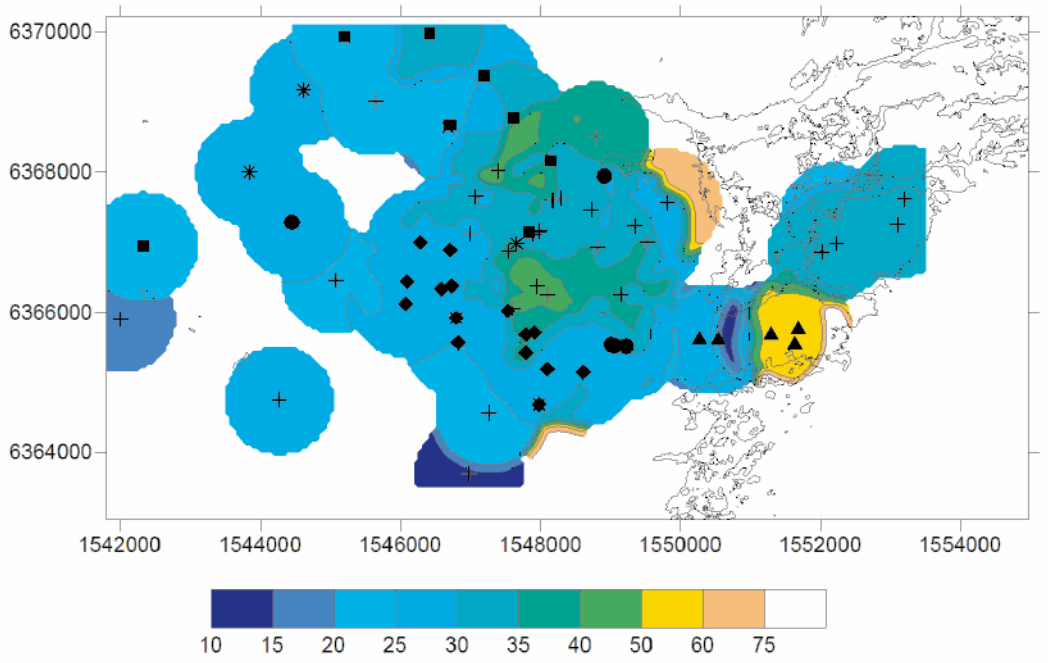

Figure 4-27. *Map showing apparent a-values in Archie's law. The symbols indicate the sampling locations and the symbol type indicates the sampled rock type according to the legend in e.g. Figure 4-25. Note that more than one rock type has been sampled at some sites. The contour lines have been interpolated by taking the median value within a search radius of 800 metres. From GSD-terrängkartan ©Lantmäteriet Gävle 2001, permission M2001/5268 Swedish Nuclear Fuel & Waste Management Co 2004-11-09.*

The relation between IP measured in fresh and saline water can be seen in Figure 4-28. Most samples have low IP in saline water indicating that the IP in fresh water is mainly due to membrane polarisation. The samples with significant IP effect in saline water have quite high magnetic susceptibility indicating that magnetite might be a major cause of that IP. However, not all samples with high magnetic susceptibility show this effect. The most magnetic fine-grained dioritoid and gabbro to diorite samples have rather low IP in saline water.

The IP-effect has been plotted for two different frequencies in Figure 4-29. Stronger IP in the higher frequency compared to the lower frequency indicate IP with a short time constant. Most samples plot slightly above the straight line indicating slightly higher IP for the higher frequency. This means that all samples have a short or moderate time constant.

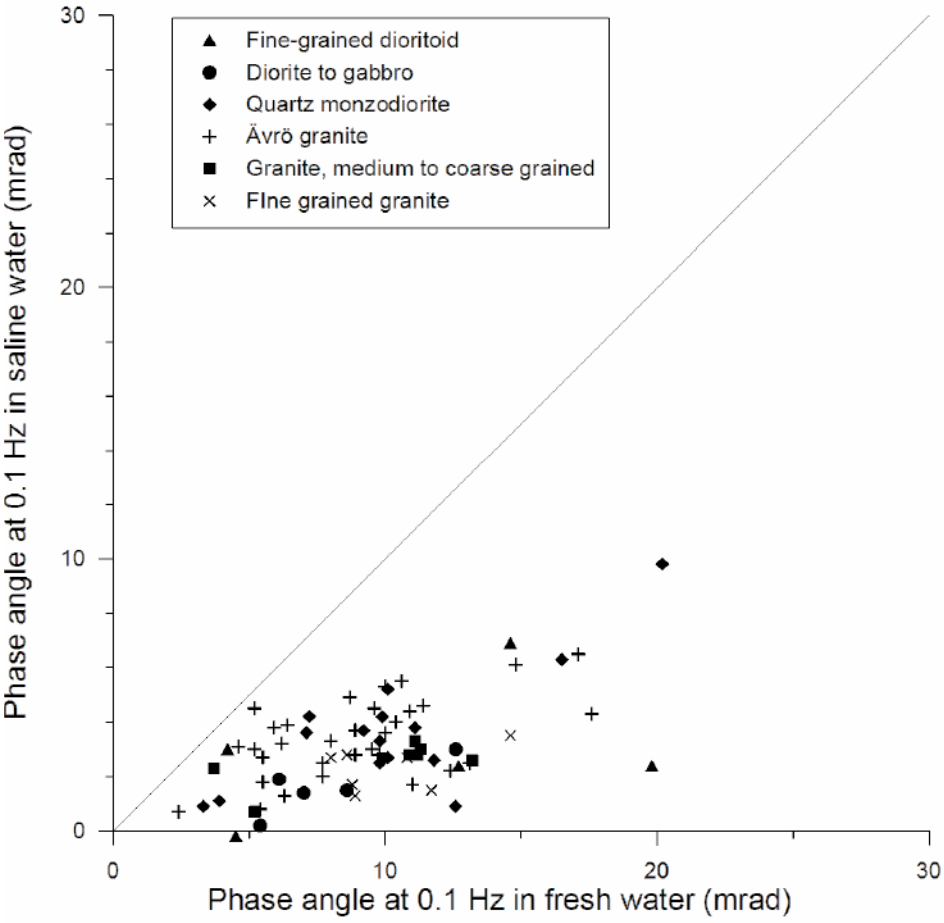

Figure 4-28. *IP-effect measured with the samples soaked in fresh and saline water. The straight line indicates equal IP for the two cases. Most samples show low IP in saline water indicating that membrane polarisation is the dominating IP effect in fresh water. With a few exceptions, the samples with significant IP in saline water have high magnetic susceptibility indicating that magnetite is a major cause to this IP-effect.*

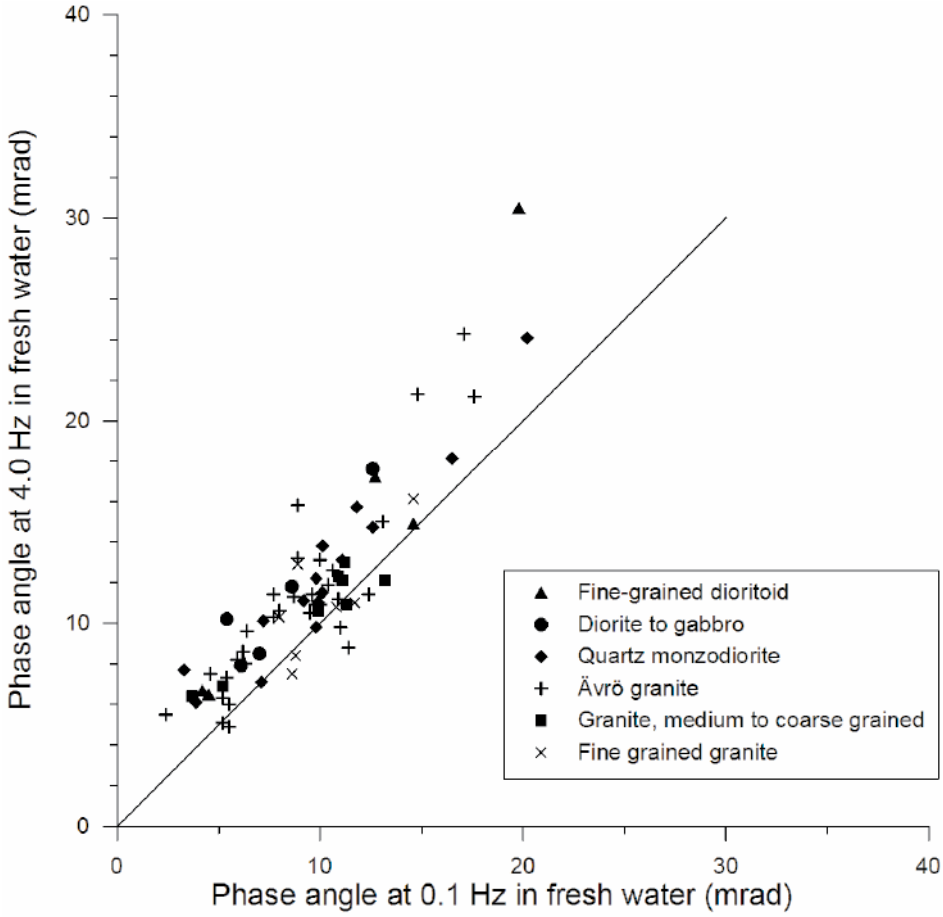

Figure 4-29. *IP-effect as phase angle for two frequencies. Samples that plot above the straight line are expected to have short time constants.*

Since several complicated processes cause the polarisation it is not possible to describe the frequency or time dependence of IP with any analytical function. It is however common to model the complex resistivity of a rock material with the empirical Cole-Cole model:

$$\rho(\omega) = \rho_0\left[1 - m\left(1 - \frac{1}{1 + (i\omega\tau)^c}\right)\right]$$

where

ρ_0 = resistivity at zero frequency (Ωm)

ω = angular frequency (rad/s)

m = chargeability

τ = time constant (s)

c = shape factor

$i = \sqrt{-1}$

The complex resistivity is thus described by ρ_0, m, τ and c. High chargeability is expected for rocks containing significant amounts of conductive minerals but also for rocks with clay alteration or considerable membrane pore space. The frequency at which the IP effect is strongest is related to the time constant. IP caused by conductive minerals or clay will in

general give IP with long time constants whereas membrane polarisation will cause IP with short time constants that might be just of the order of milliseconds. The time constant is also texture dependent, where coarse-grained rocks in general will cause IP with longer time constants than fine grained rocks.

Cole-Cole parameters have been calculated for two of the samples to give an idea of what values to expect from typical rocks of the study area. The results are shown in Table 4-2. It should be remembered that fits to the Cole-Cole model not are accurate for very short and very long time constants due to the limited frequency range of the measurements. The sample PSM006003 is of quartz monzodiorite. Compared to the other samples in the study, it has fairly high IP with a long time constant. The sample PSM007844 is classified as Ävrö granite. It also has fairly high IP but the time constant is more typical for the majority of samples in the study. Cole-Cole parameters have been estimated for measurements in both fresh and saline water, indicated by the value for water resistivity (ρ_w) in Table 4-2.

Table 4-2. Estimated Cole-Cole parameters for some selected samples with different electrical properties. Note that the estimates are very rough for samples with time constants shorter than 5 ms or longer than 1.7 s.

Sample	ρ_0 (Ωm)	τ (s)	m	C	ρ_w(Ωm)
PSM006003	12,727	0.096	0.098	0.257	33
PSM006003	760	0.0059	0.052	0.250	0.28
PSM007844	9,868	0.0061	0.126	0.327	33
PSM007844	404	0.0035	0.042	0.286	0.28

Both samples have low chargeability values, especially in saline water. Time constants are very short although longer for PSM006003, at least in fresh water. The modelling results can be seen in Figures 4-30 and 4-31. The fits are fairly good and within the measurements errors. The accuracy of the fits are however not very good due to the low phase angle values that are not very large in comparison to the accuracy of the measurements. The frequencies 0.1, 0.6 and 4.0 Hz are the base frequencies of the measurement equipment and the other frequencies are harmonics or averaged harmonics of those base frequencies.

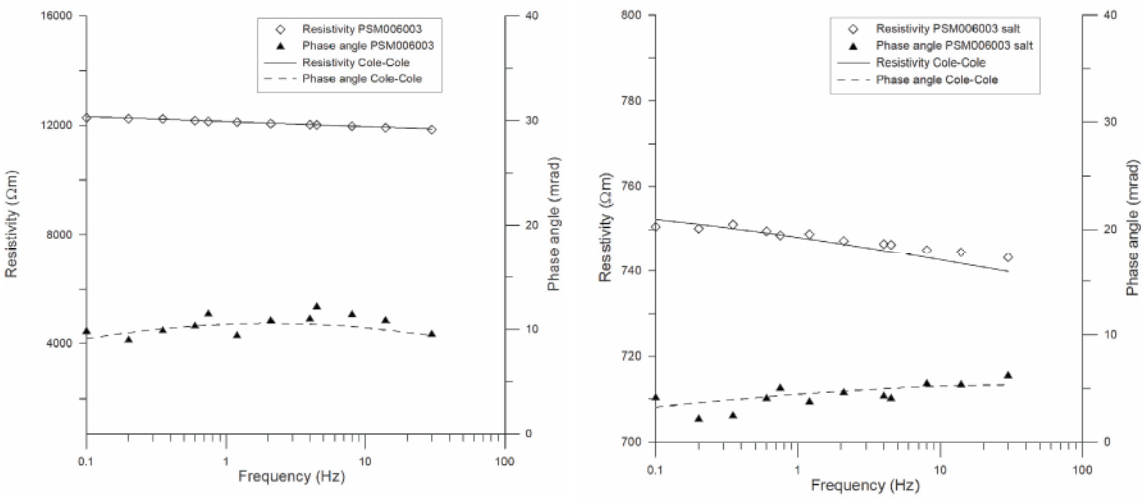

Figure 4-30. *Complex resistivity for the sample PSM006003. Measurement data are shown with symbols and fitted Cole-Cole model with lines.*

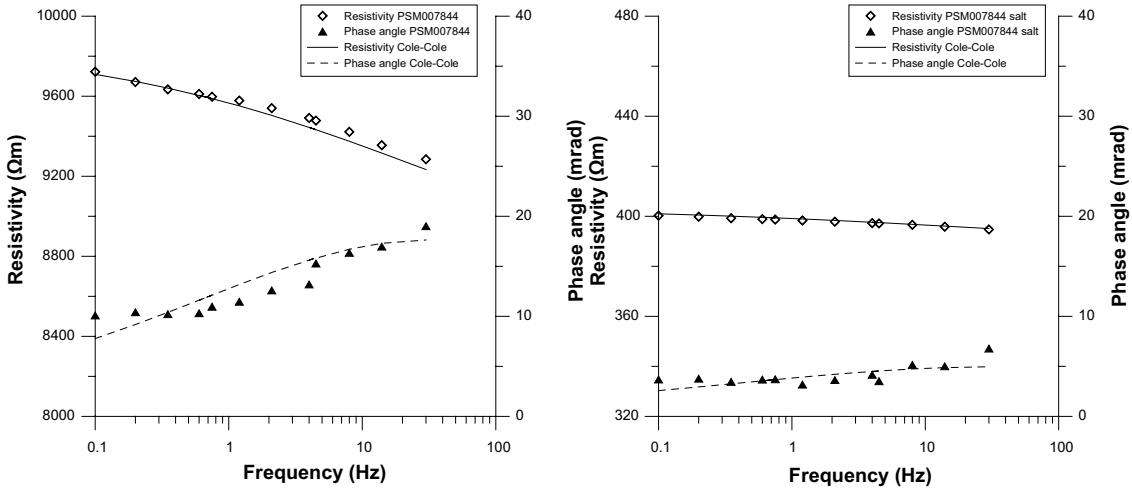

Figure 4-31. *Complex resistivity for the sample PSM007844. Measurement data are shown with symbols and fitted Cole-Cole model with lines.*

4.5 In situ gamma-ray spectrometry

In total 171 individual localities have been investigated with gamma ray spectrometry between 2002 and 2004. Furthermore 26 locations were investigated within a special study of the radiation characteristics of fine-grained granites /12/. The spatial coverage of all measurements, except for the special study of fine-grained granites, is presented in Figure 4-32. Inside the bedrock mapping area of 2004 the coverage is sufficient to provide a reliable description of the gamma ray characteristics of the most common rocks. As seen on the map there are remote clusters of measurements also outside the mapped area. Many of these localities were measured in 2002 and 2003 during the follow-up of airborne survey data, but some where investigated in 2004.

In Table 4-3 average values and corresponding standard deviations of potassium, uranium and thorium content are presented for the main rock types present in the Laxemar area with surroundings. In the table the results from the special study of fine-grained granite dykes have been treated separately.

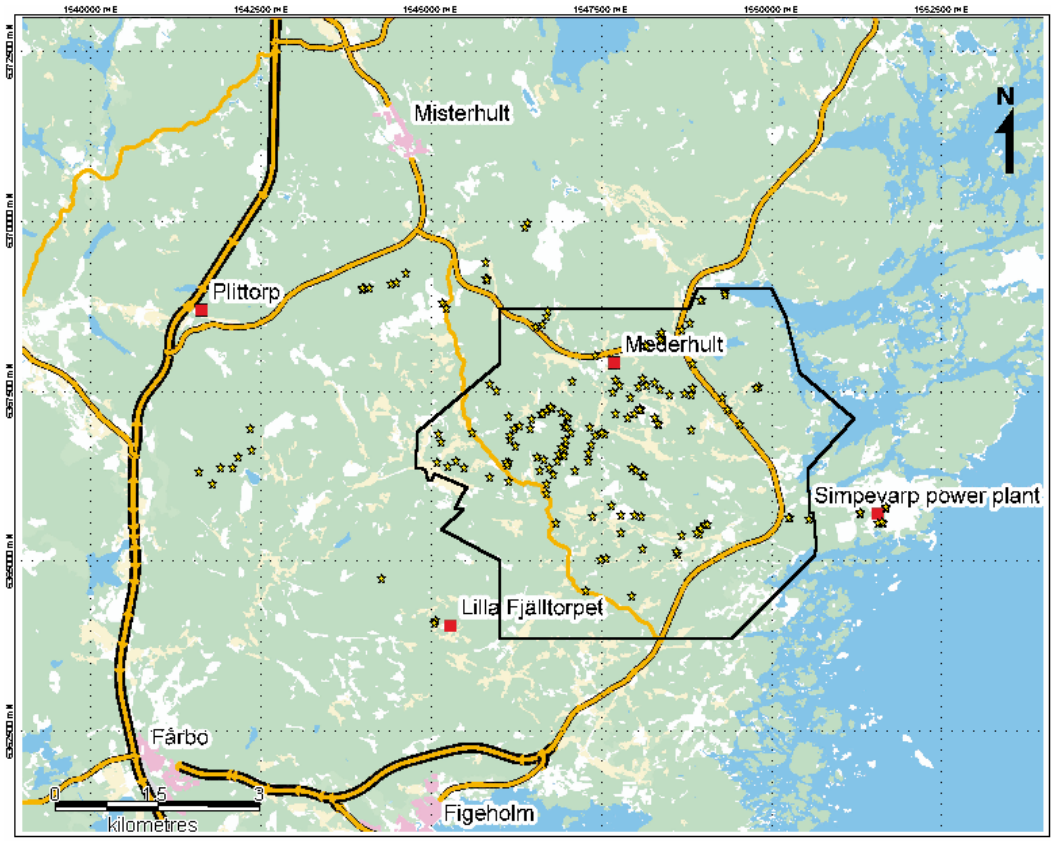

Figure 4-32. *Distribution of the 171 localities studied with gamma ray spectrometry during the period 2002 to 2004. Localities from the special study of fine-granite dykes /12/ are not included. The black frame marks the principal area covered by the bedrock mapping during 2004 /4/. From GSD-terrängkartan ©Lantmäteriet Gävle 2001, permission M2001/5268 Swedish Nuclear Fuel & Waste Management Co 2004-11-09.*

Table 4-3. Rock types measured with gamma ray spectrometry. L=number of localities measured for each rock type. The shaded rows contain data from the previous investigation of fine-grained granite dykes /12/. The names of the rock types, with exception of the special study of fine-grained granite dykes, follow the updated nomenclature (number code).

Rock type and code (lithostratigraphic)	L	Potassium (%)	eUranium (ppm)	eThorium (ppm)
Fine-grained dioritoid (Metavolcanite, volcanite) 501030	14	3.1 ± 0.3	3.7 ± 1.6	12.5 ± 5.8
Diorite to gabbro 501033	18	1.4 ± 0.5	1.4 ± 0.8	4.0 ± 2.7
Quartz monzodiorite 501036	38	3.0 ± 0.3	3.2 ± 0.8	9.9 ± 1.8
Quartz monzodiorite to granodiorite (Äspö Island)	5	3.3 ± 0.4	4.8 ± 2.7	11.2 ± 2.4
Ävrö granite 501044	79	3.3 ± 0.4	3.8 ± 1.5	11.9 ± 4.3
Ävrö granite (Ävrö Island)	7	3.6 ± 0.2	4.9 ± 0.8	16.6 ± 6.6
Granite, medium- to coarse-grained 501058	13	4.0 ± 0.5	4.3 ± 1.4	15.4 ± 5.0
Pegmatite 501061	1	2.7	6.8	11.4
Pegmatite	3	5.2 ± 0.4	9.8 ± 7.4	23.2 ± 8.7

Rock type and code (lithostratigraphic)	L	Potassium (%)	eUranium (ppm)	eThorium (ppm)
Fine-grained diorite to gabbro 505102	1	1.5	0.7	3
Fine-grained granite 511058	7	4.5 ± 0.5	7.7 ± 2.5	30.2 ± 10.5
Granite, fine- to medium-grained (red dyke)	11	5.6 ± 0.4	6.1 ± 2.3	48.9 ± 20.9

The results from the gamma ray spectrometry surveys are presented in a Th-K plot in Figure 4-33 as the average values for the most common rock types from the area.

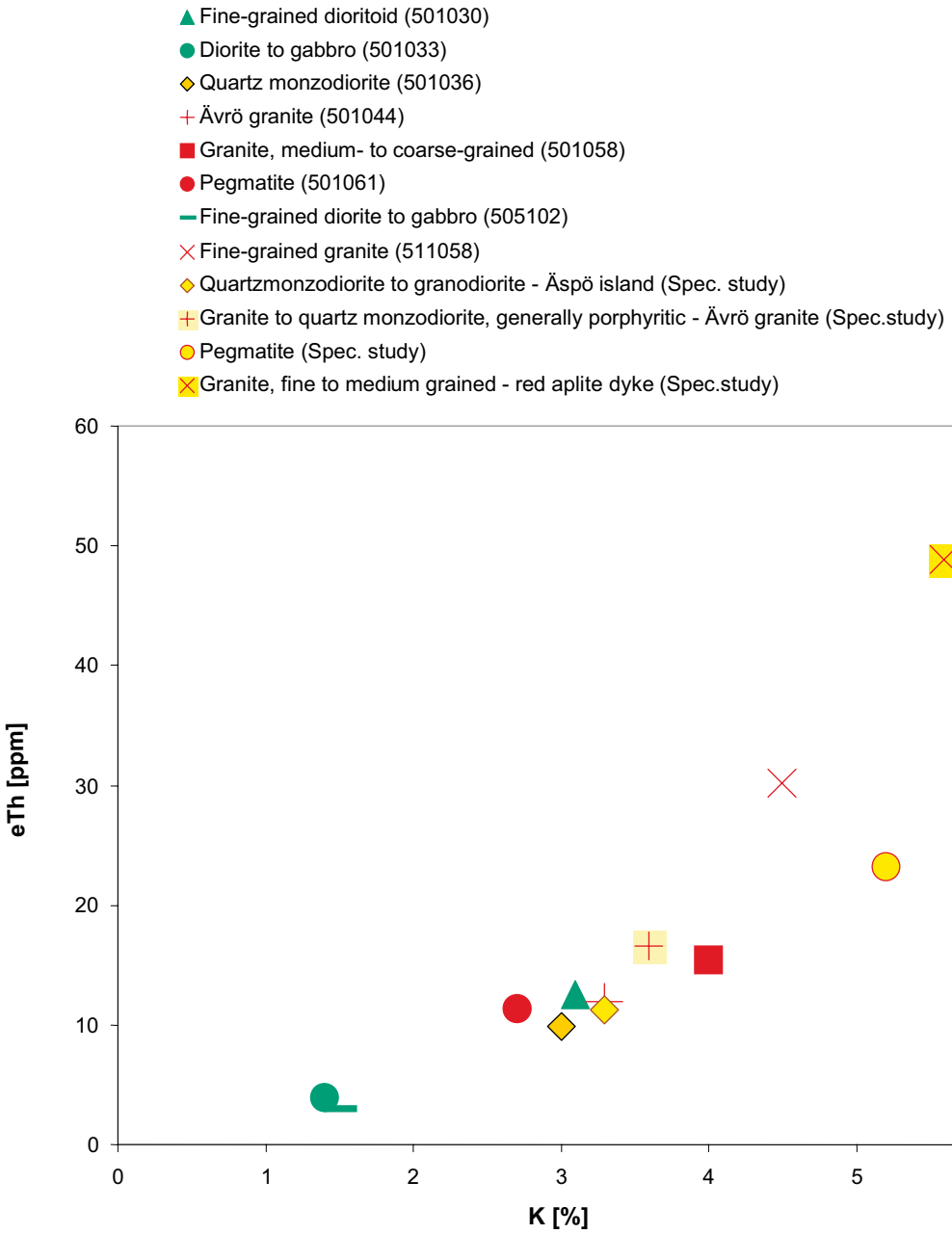

Figure 4-33. *Averages of the equivalent content of thorium (Th) and potassium (K) for the rock types investigated by gamma ray spectrometry. Data from the special study on fine-grained granite dykes /12/ are separated with yellow background colour and their names are not entirely conformal with the updated vocabulary.*

As expected the mafic rocks such as diorite to gabbro and fine-grained diorite to gabbro have the lowest contents of potassium and thorium.

The two most common rock types in the Laxemar area, the quartz monzodiorite and the Ävrö granite, have been compared. The latter has a higher content of potassium and thorium together with a higher standard deviation in uranium and thorium content. This fact is illustrated more explicitly in Figure 4-34. In connection to this observation it is important to point out that already the name of the rock type Ävrö granite indicates that the allowed heterogeneity is quite liberal. By studying the IUGS (International Union of Geological Sciences) classification of Igneous Rocks /17/ it becomes obvious that the span, within which the content of quartz, alkali feldspar and plagioclase can vary, is wider in the Ävrö granite as compared to the quartz monzodiorite. It could thus be expected that these variations in composition for respective rock type, also should be reflected in the standard deviations of the petrophysical properties for the two types. The variations in content of potassium, uranium and thorium may thus indicate compositional varieties within one rock type. One example is demonstrated further below in this section and in section 5.8.

The radiation character of the fine-grained dioritoid resembles the one of the quartz monzodiorite.

The highest content of thorium is found in the fine-grained granite. The uranium and potassium contents are also quite high. The pegmatites appear to partly resemble the red fine-grained granites though one of the measured localities has very low content of potassium and thorium.

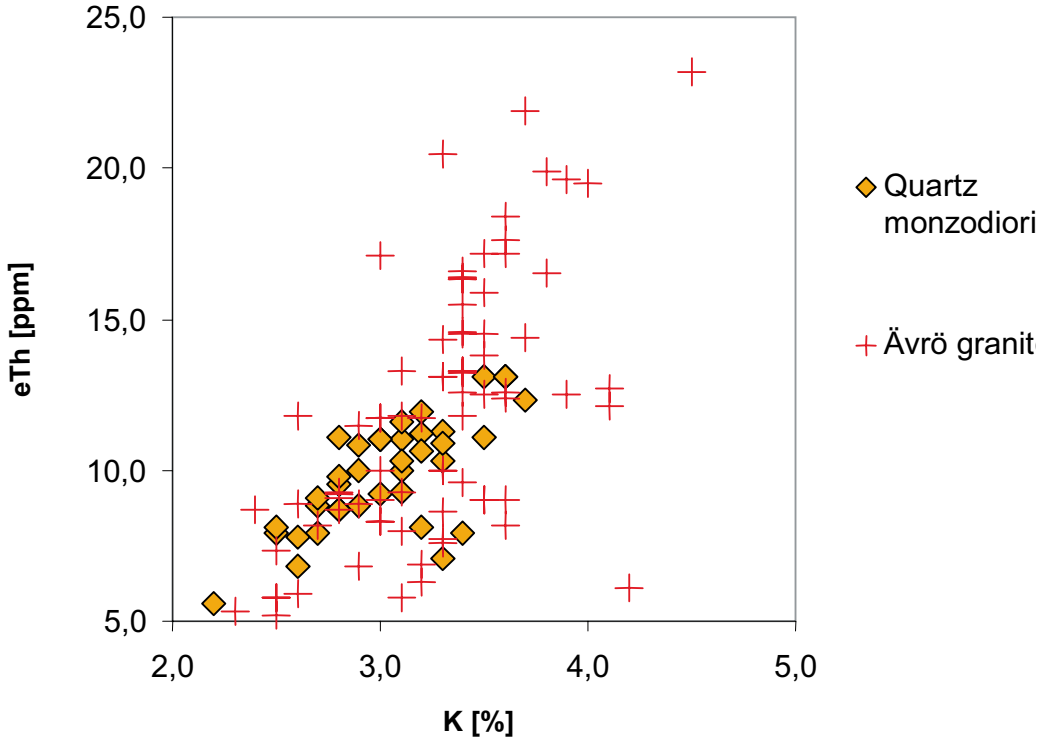

Figure 4-34. *Equivalent content of thorium (Th) and potassium (K) from gamma ray spectrometry in individual localities where the rock types quartz monzodiorite and Ävrö granite occur.*

It is worthwhile to compare the outcome of the gamma ray spectrometry made on ground with the pattern received from the helicopter borne survey over the same area. In Figure 4-35 a ternary plot of the normalised three components (K, U and Th) from the ground survey is compared with a similar plot of low-pass filtered normalised data from the helicopter borne gamma ray survey. The similarities are obvious and the heterogeneity of the Ävrö granite in the Laxemar area with a central comparatively Th-rich area and a relatively thorium- and uran-depleted southern rim stands in clear contrast to the more homogeneous quartz monzodiorite bordering the Ävrö granite at south.

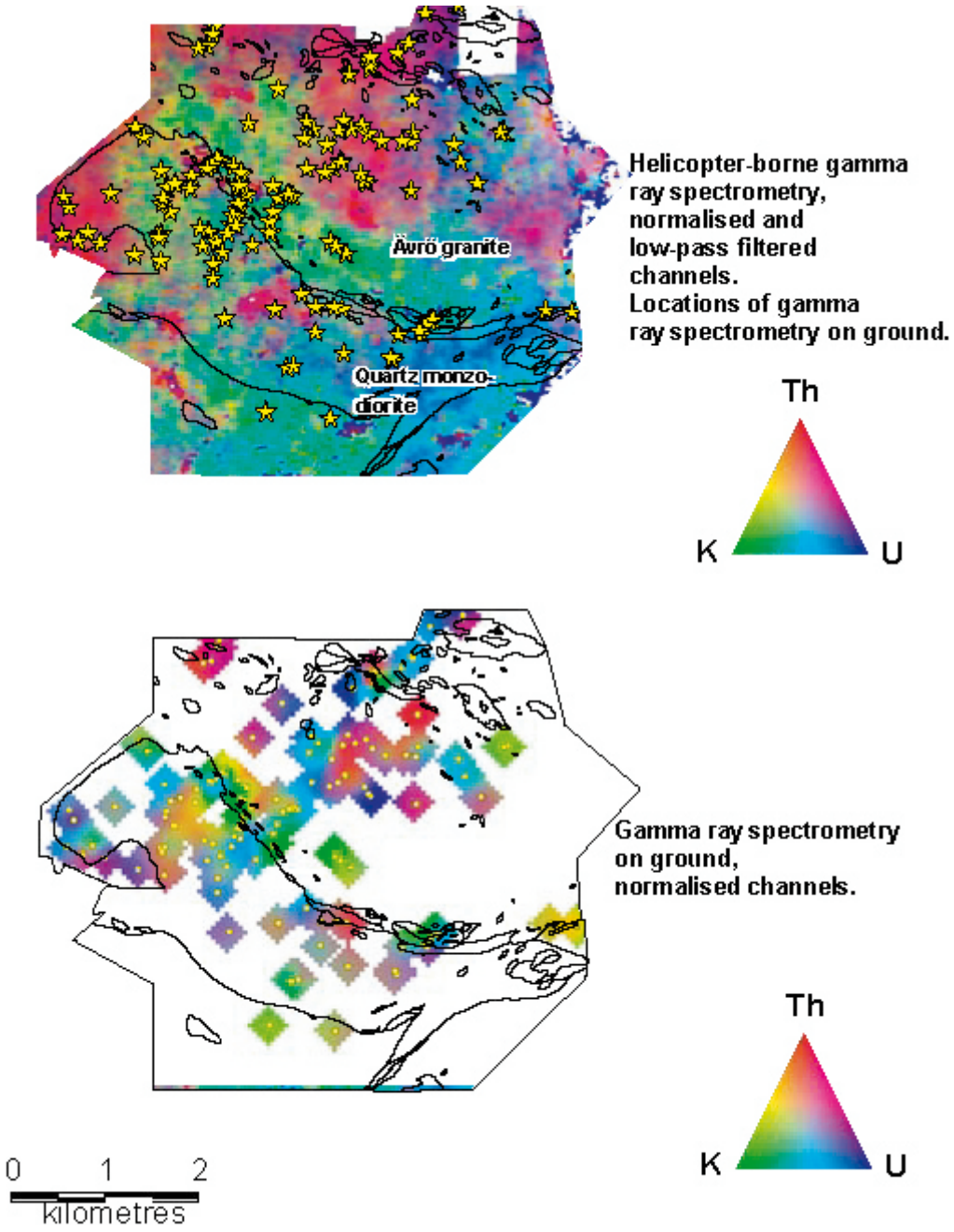

Figure 4-35. *Gamma ray spectrometry from helicopter and on ground, presented as normalised components in ternary maps, where green is potassium, red is thorium and blue uranium. The data from the helicopter borne gamma ray spectrometry survey are low-pass filtered. In the background is found the borders between different rock types from the preliminary geological map of Laxemar /4/.*

The differences in the content of potassium, uranium and thorium as deduced from gamma ray spectrometry on outcrops have been described above. It is indicated that gamma ray spectrometry may add useful information for the characterisation of the bedrock and for distinguishing between different rock types. Furthermore, spectrometry data may reflect a compositional variation within rock types which together with chemical, mineralogical and petrophysical information may lead to a further subdivision of the rock types in different compositional varieties.

4.6 Nonconformities

For revision no. 1 of this report a change in some of the ID-codes has been performed. In the earlier report ID-codes in the interval PSM 006055–PSM006095 have been changed to the corresponding ID-codes in the interval PSM007836–PSM007876.

5 Comparison of some geophysical anomaly complexes, geological bedrock mapping and petrophysical data

In the Simpevarp and Laxemar areas with surroundings, gravity, and airborne geophysics with both with fixed-wing and helicopter-borne systems, have resulted in maps showing the variations of a number of physical parameters. These parameters are density, electrical conductivity, magnetic susceptibility and content of radioactive elements where their variations among others could indicate compositional changes in the ground reflecting the quaternary and bedrock geology. To identify the sources behind the variations it is necessary to connect the anomaly complexes to observations made on ground. The latter could come from geological mapping and measurements of petrophysical properties on outcrops and in boreholes.

Previous work with petrophysics was carried out in connection to the extensive investigations at Äspö, for an example see /18/, and in near relation to the interpretation of the fixed-wing geophysical survey of 1986 /19/. As identities and co-ordinates of the surface samples have not been found, it is however difficult or even impossible, to relate some of these earlier data to the rock type nomenclature used today. Hence a new era in petrophysical studies was commenced in 2002. Several localities have been sampled since, and measured, in order to get a database of petrophysical properties of the common rock types in the area. Furthermore, within these latest studies, the number of petrophysical parameters investigated was also increased compared to the earlier studies.

In this chapter some comments will be made on the relation between results from the helicopter borne survey of 2002, the geological bedrock mapping of 2004 and the petrophysical investigations carried out from 2002 until today. At this stage of the site investigations it is believed necessary to address the major anomaly complexes only.

In Section 4.2 above the correspondence between the measurements of magnetic susceptibilities on outcrops and the map of the magnetic total field as recorded from helicopter was compared in general. It was shown that the main pattern recognised in the susceptibility data from outcrops reflected the picture of the magnetic total field quite well. The conclusion is that most of the anomaly sources behind variations in the magnetic total field are at least partly outcropping. A similar conclusion is possible to make from the comparison of gamma ray spectrometry data gathered in measurements on ground and from air, se Section 4.5.

Below, some major anomaly complexes are commented in detail as they show the connection between variations in bedrock and quaternary geology and petrophysical parameters.

5.1 Highly magnetized rock volumes traversing the central part of the Laxemar area

In the central part of the Laxemar area there is a pronounced maximum in the magnetic total field traversing with a strike apparently northwest-southeast. This maximum is located at the contact between the Ävrö granite to the northeast and the quartz monzodiorite to the southwest (Figure 5-1). Numerous bodies belonging to the rock type diorite to gabbro occur along the contact, and the highest magnetic susceptibilities are detected within these bodies (Figure 5-1). In this anomalous area however, also some of the outcrops of quartz monzodiorite show high magnetic susceptibilities, but usually at levels slightly below the diorite to gabbro. There appear to be a spatial correlation between the occurrence of diorite to gabbro bodies and areas where the quartz monzodiorite is enriched in magnetite. The main sources to the high magnetic anomalies traversing the Laxemar area are consequently the scattered bodies of diorite to gabbro. However, the conditions for formation of magnetite appear to have been favourable, either along the contact between Ävrö granite and the quartz monzodiorite or near the diorite to gabbros. As a consequence elevated content of magnetite can also be found in parts of the quartz monzodiorite.

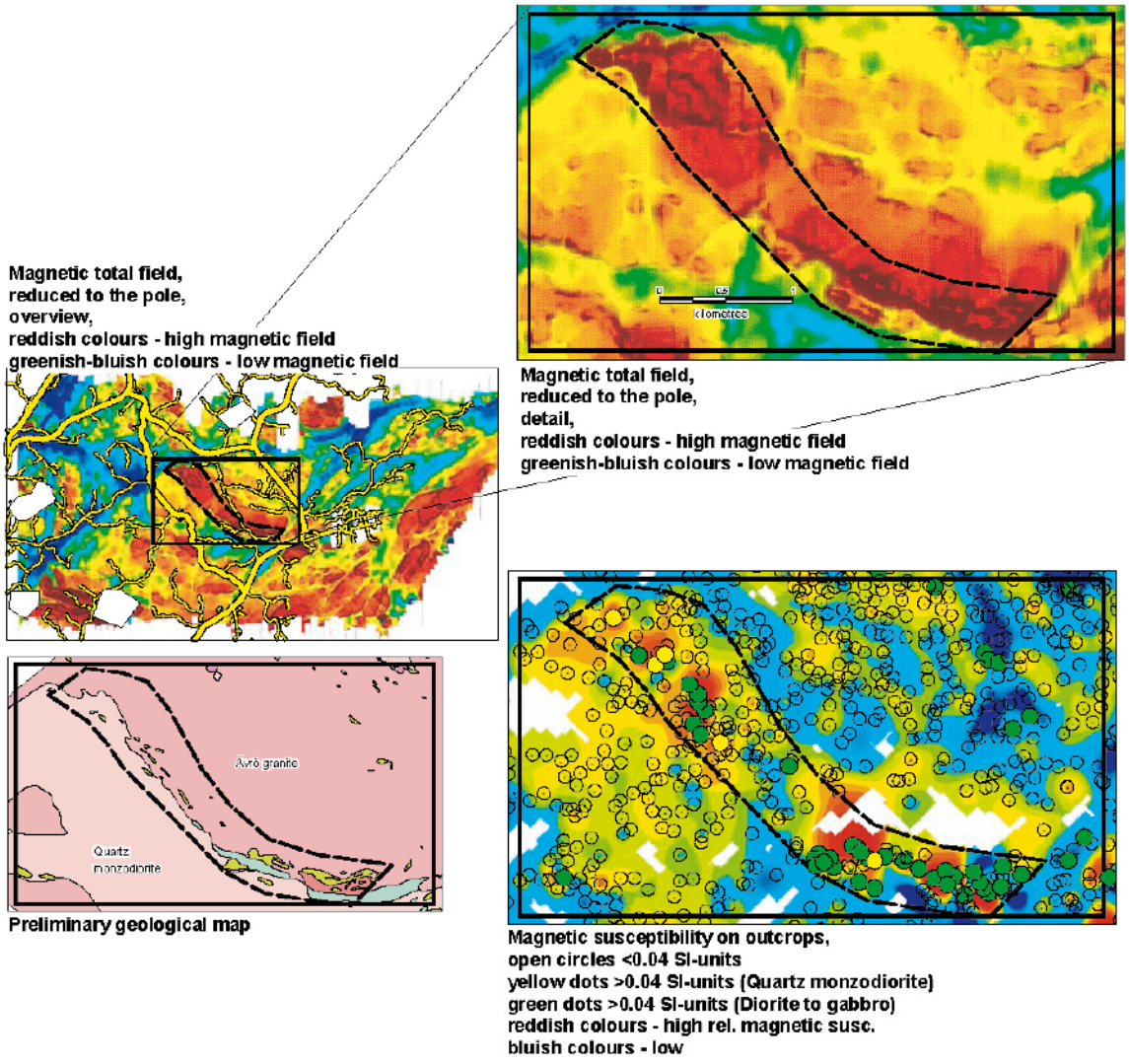

Figure 5-1. *Area with high magnetisation traversing the central part of the Laxemar area. The main sources to the high magnetic anomalies are the bodies of diorite to gabbro near the contact between Ävrö granite and quartz monzodiorite.*

5.2 Rock volumes of quartz monzodiorite with low magnetization in the south-eastern part of the Laxemar area

In the south-eastern part of the Laxemar area an unexpected low relative magnetization is dominant. This area is located within the borders of an apparently homogenous unit of quartz monzodiorite (Figure 5-2). The magnetization is however significantly reduced as compared to volumes of the same rock type further north-west. As seen in Figure 5-2 various localities have quite low magnetic susceptibilities, or below 0.00500 SI-units. These localities constitute the lower part in the histogram of the magnetic susceptibilities of this rock type (see Figure 4-8 in Section 4.2 above).

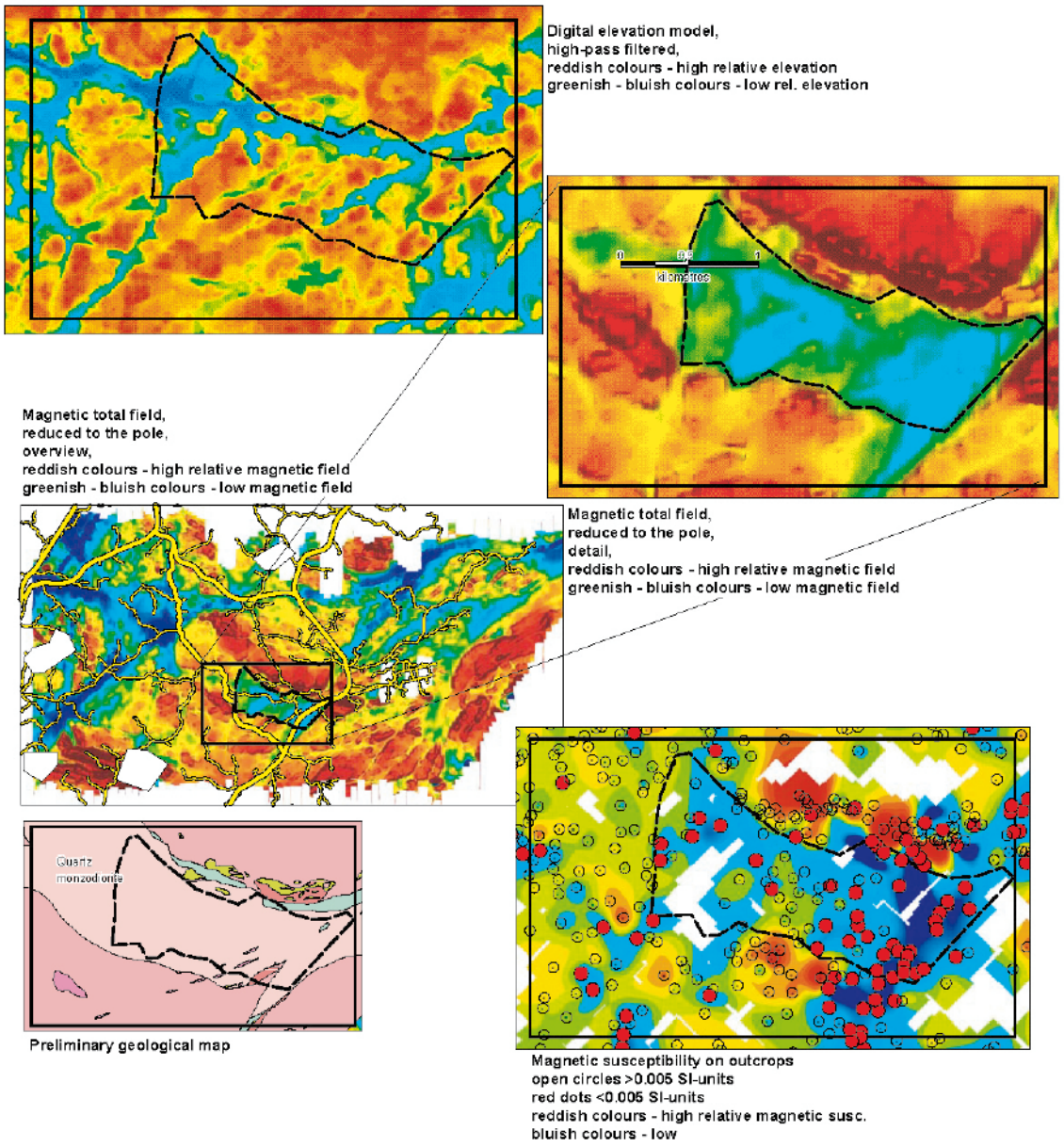

Figure 5-2. *Area with low magnetization at the south-eastern part of the Laxemar area. The main source to the low magnetization is probably increased fracturing due to a brittle component in the tectonics.*

The Äspö shear zone is located at the eastern border of the low magnetic area. Within the sheared zone the magnetic susceptibility is radically reduced due to oxidation of magnetite. West of the Äspö shear zone the digital elevation model indicates increased fracturing of brittle character. In Figure 5-2 numerous linear features trending ENE-WSW are observed in the digital elevation model. In the helicopter borne EM survey the data quality in this area is reduced due to a nearby power line, but still they indicate a slightly increased electric conductivity in the bedrock. The reduction in magnetic susceptibility in this area outside the Äspö shear zone could thus be interpreted to emanate from a general increased fracturing of the rocks.

5.3 A pronounced high magnetic anomaly east of main road Fårbo – Simpevarp

There is a pronounced magnetic total field anomaly with high intensity east of the main road between Fårbo and the Simpevarp Nuclear Power plant (Figure 5-3). The source to the main portion of the anomaly seems to be the rock unit diorite to gabbro found at the northern part of the anomaly. Here are also the magnetic susceptibilities in outcrops the highest (Figure 5-3). Though the magnetic anomaly is pronounced, it is likely that the major part of the source is not outcropping. The first vertical derivative of the reduced-to-the-pole magnetic total field has been calculated. With a colour scale enhancing the highest values only, the map of the derivative indicates that the most near-surface part could be interpreted to form a fold (Figure 5-3). Probably the outcropping parts of the diorite to gabbro constitute scattered minor bodies that could be found along the horizon with the highest vertical derivative values. The plunge of the apparently folded body could be towards east.

As the preliminary version of the geological bedrock map presented in the figure shows the major rock type units only, there appears to be a mismatch between the geological and the geophysical information. This is however only apparent as the final version of the geological bedrock map will also include minor rock type inclusions and consequently the folded shape will then be visible.

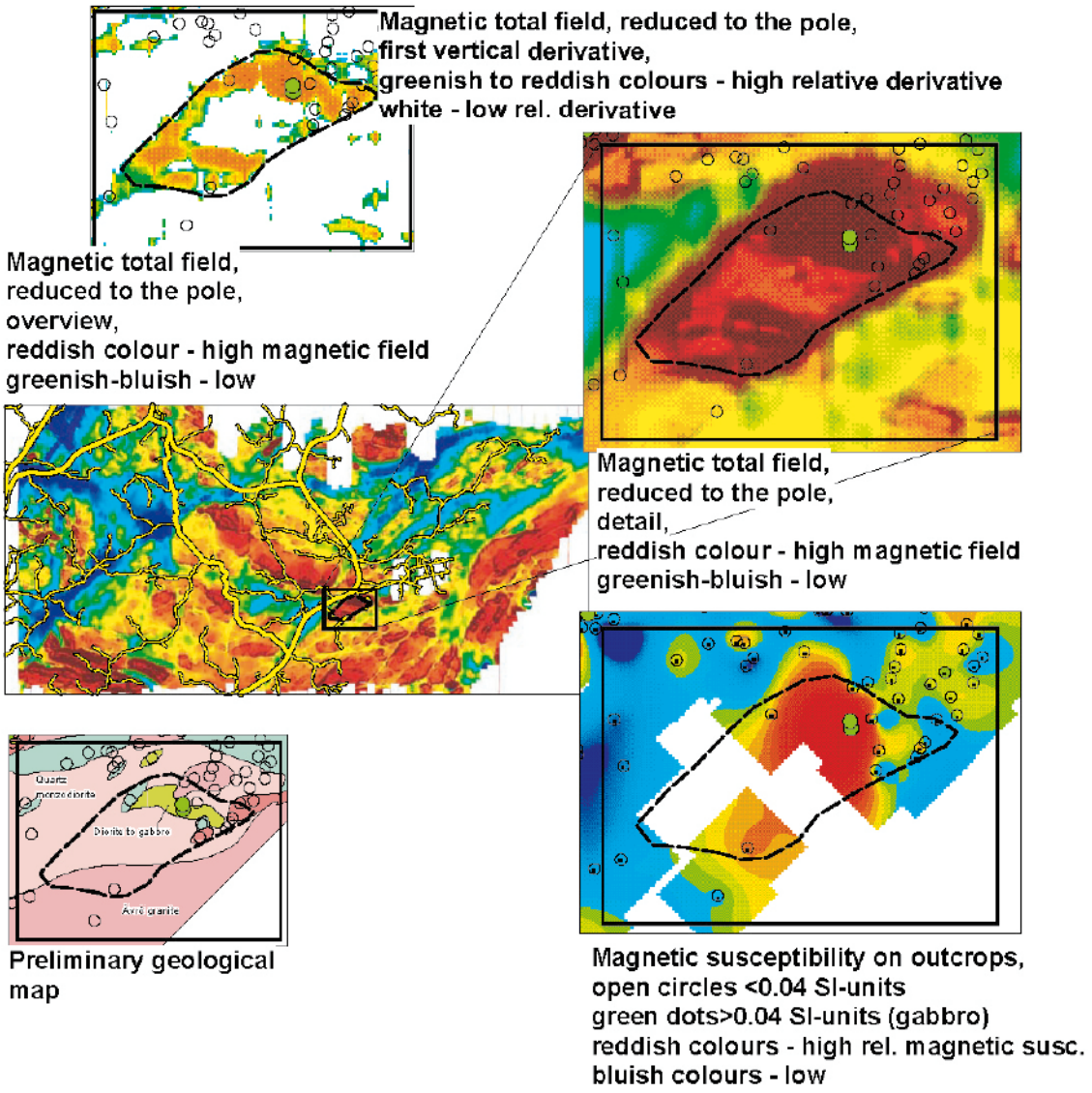

Figure 5-3. *Area with high magnetisation at the south-eastern part of the Laxemar area, east of the main road between Fårbo and the Simpevarp nuclear power plant. The main source to the anomaly is the diorite to gabbro.*

5.4 Banded magnetic anomaly complex associated to a diorite to gabbro north-east of Fårbo

Approximately two kilometres north-east of Fårbo there is an area where a diorite to gabbro ("Släthultsgabbron") with a banded magnetic pattern is outcropping (Figure 5-4). On a map of the first vertical derivative three parallel bands with high magnetization are visible. The highest recorded magnetic susceptibilities are found on these magnetic bands. Geological mapping has been carried out in two smaller areas, one at the eastern part of the anomaly complex and one at the western part (Figure 5-4). The geological mapping and the associated measurements of the magnetic susceptibility indicate that the rock type diorite to gabbro could be outcropping in most of the banded area. The content of magnetite is thus distributed in a banded manner in the body.

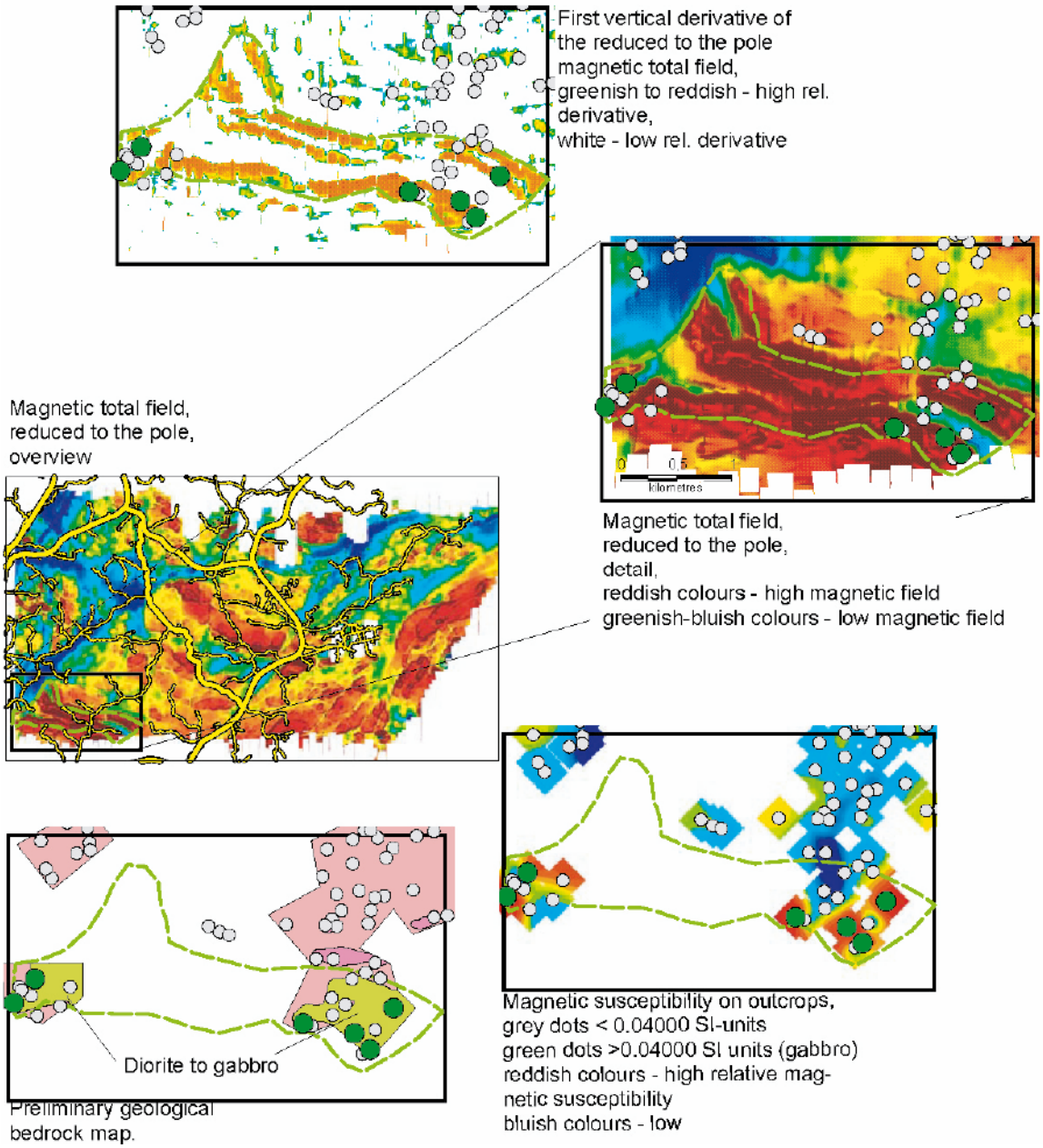

Figure 5-4. *Area with a banded pattern in the magnetization approximately 2 km north-east of Fårbo. The main source to the anomaly is a diorite to gabbro with high and low magnetization in bands.*

5.5 High magnetic anomaly associated with diorite to gabbro north-east of Mederhult

North-east of Mederhult a sharp maximum is observed in the magnetic total field (Figure 5-5). The geological mapping in the area reports the rock type diorite to gabbro and the corresponding measurements of magnetic susceptibility show high values (above 0.04000 SI units) at three locations. In Figure 5-5 there appears to be a slight displacement of the observed high magnetic susceptibilities in relation to the anomaly in the helicopter borne survey. This is probably only apparent as the geological observations, and hence the susceptibility determinations, were carried out over fairly large outcrops although a point represents them. The rock type diorite to gabbro is thus the source to the high magnetic anomaly in the area.

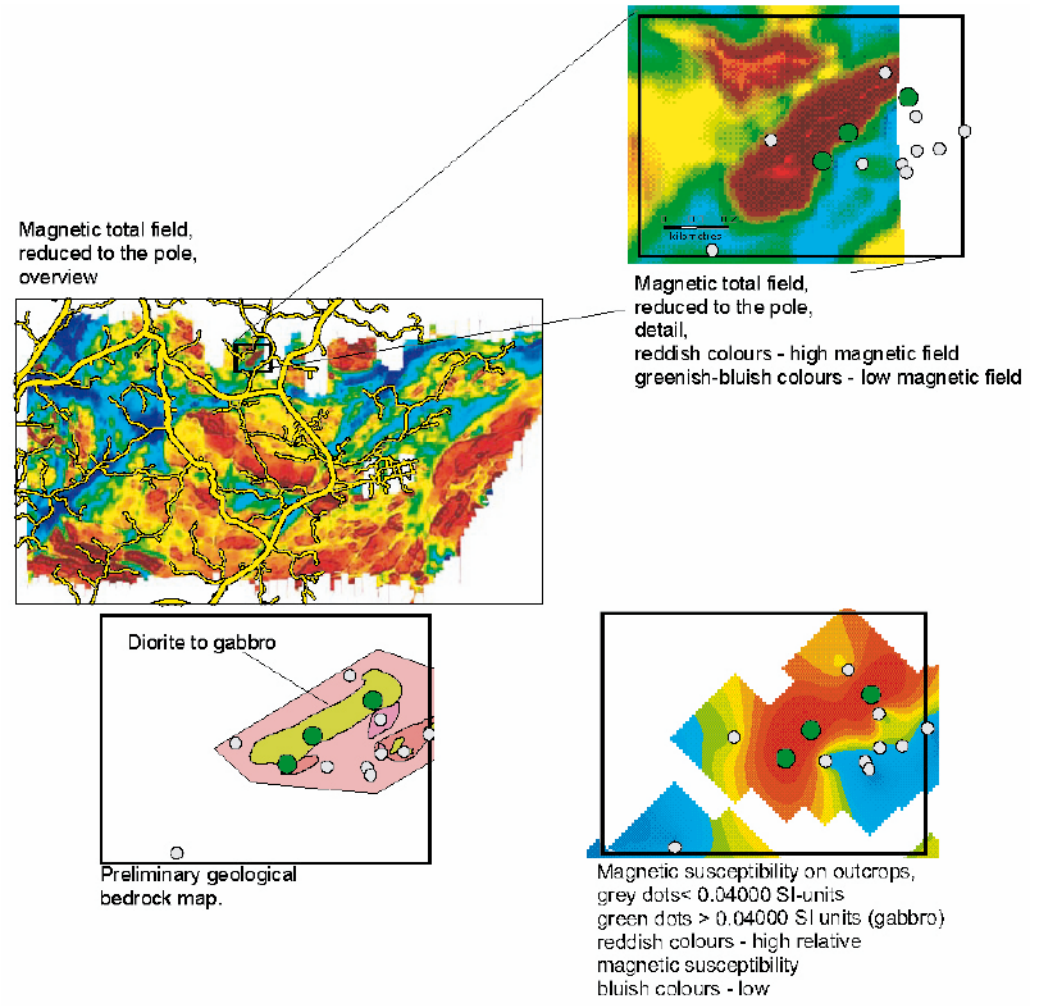

Figure 5-5. *Area with a high magnetic anomaly north of Mederhult. The source to the anomaly is a diorite to gabbro.*

5.6 Area with scattered high magnetic anomalies and low gamma ray radiation with low potassium associated with diorite to gabbro north of Fårbo

East of the road between Västervik and Oskarshamn, a few kilometres north of Fårbo, there is an anomaly complex of scattered high magnetic anomalies with a corresponding deviation from the normal character of the gamma ray radiation in the area (Figure 5-6). In data from gamma ray spectrometry it is possible to see a slightly lower intensity in the radiation and a change from a potassium-enriched surrounding to a depletion of potassium in relation to uranium and thorium. Field checks show that the rock type diorite to gabbro is found in many of the outcrops and as the magnetic susceptibilities in the rock type often are high and the gamma radiation levels in ground spectrometry are low on the same rock type, the source is identified.

This anomaly complex could be the tectonically displaced continuation of the diorite to gabbro complex described in section 5.2.4 above.

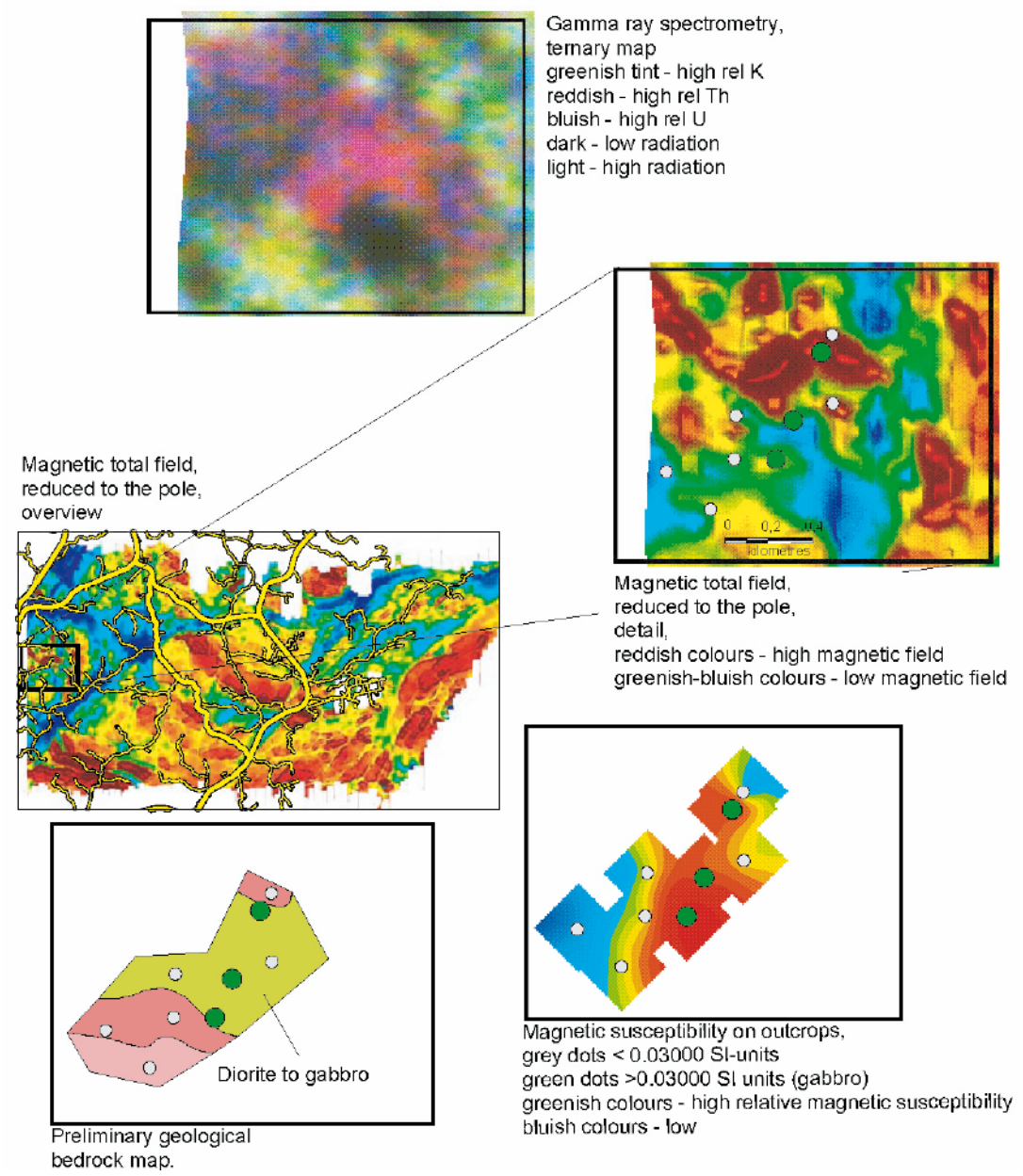

Figure 5-6. *Scattered high magnetic anomalies and low gamma ray radiation with low potassium associated with diorite to gabbro approximately 5 km north of Fårbo. The main source to the anomaly complex is the diorite to gabbro.*

5.7 Low magnetic area associated with a lineament north of Fårbo

A few kilometres north of Fårbo a low magnetic linear feature is easily recognized on the map of the magnetic total field (Figure 5-7). This linear feature has been identified in several types of data and is presented as a linked lineament (ZSM0011A0) of regional character in an earlier work /14/.

Geological mapping was carried out in a small area partly over the pronounced low magnetic feature. At four locations the magnetic susceptibility was below 0.00100 SI units. At the same location numerous signs where noted of tectonics in brittle and ductile mode in connection to the geological bedrock mapping /4/. At all four locations micro-cracks, epidote, and quartz are noted, in some localities also phrenite and severe oxidation. Altogether this demonstrates that the anomaly cause is the tectonic overprint on the Ävrö granite. The helicopter borne EM measurements also indicate bedrock with anomalously low resistivity more or less coinciding with the low magnetic rocks in this area.

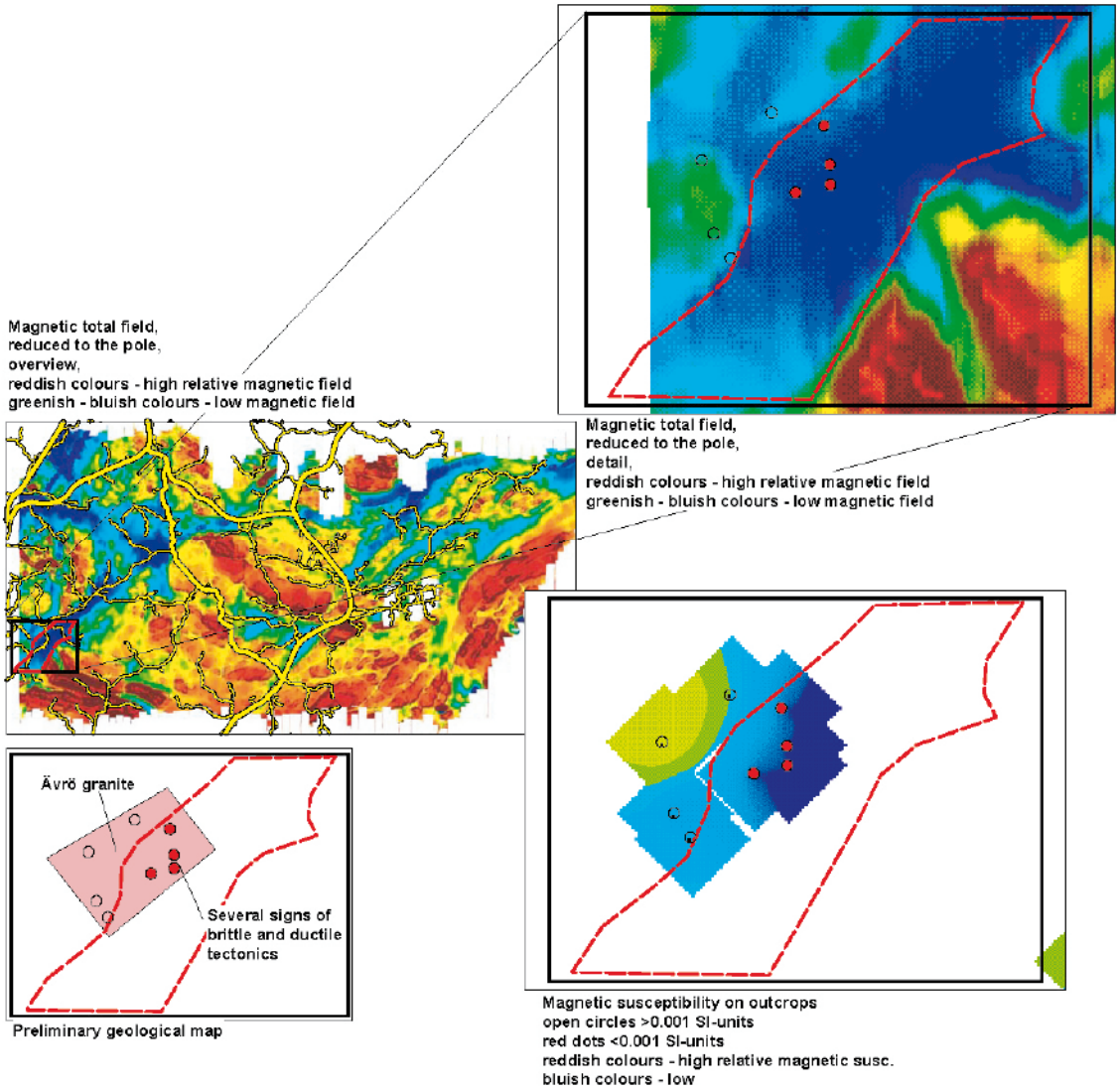

Figure 5-7. *Area with low magnetization north of Fårbo. The magnetic low is associated with a linked lineament of regional character /14/. In outcrops on the lineament low magnetic susceptibilities were measured and several signs noted of tectonic overprint on the rock /4/.*

5.8 Comparison of helicopter borne gamma ray spectrometry and the preliminary version of the geological bedrock map in terms of anomalies within uniform rock types.

In Figure 5-8 a comparison is made between the preliminary geological map of the Laxemar area /4/ and the gamma ray spectrometry data from the helicopter-borne survey carried out in 2002 /20 and 21/. There is a good correlation between the preliminary geological map and the outcome of the gamma ray spectrometry data, however some discrepancies are also observed.

The ternary map of the normalised low-pass filtered gamma ray spectrometry response from the area shows some unexpected deviations within the two main rock types; these anomalies may have different sources that will be explained below.

Gamma ray spectrometry is a geophysical method sensitive to variations in the content of potassium, uranium and thorium at the surface. It is thus affected by the overburden. In areas with thick overburden, and especially where the overburden is alluvial, the signature from the local bedrock is almost completely hidden. Such an example is marked in Figure 5-8 with **1** where the farmland in the valley is interpreted to be the cause to the gamma ray spectrum anomaly. But there are other gamma radiation anomalies that are not possible to explain with influence from overburden. One example is found in the northern central part of the geologically mapped area, where Ävrö granite dominates. Here the thorium level rises (marked with **2** in the figure). During fieldwork with gamma ray spectrometry, outcrops of rocks with granitic compositions appeared to be more frequently observed in this area as compared to elsewhere within the Ävrö granite. By comparing the distribution of density in rock samples from this area, with surrounding areas of the same rock type, slightly lower densities are also indicated. The conclusion could be that the anomaly reflects a slight change in the composition of the Ävrö granite within area 2 as compared to its surroundings.

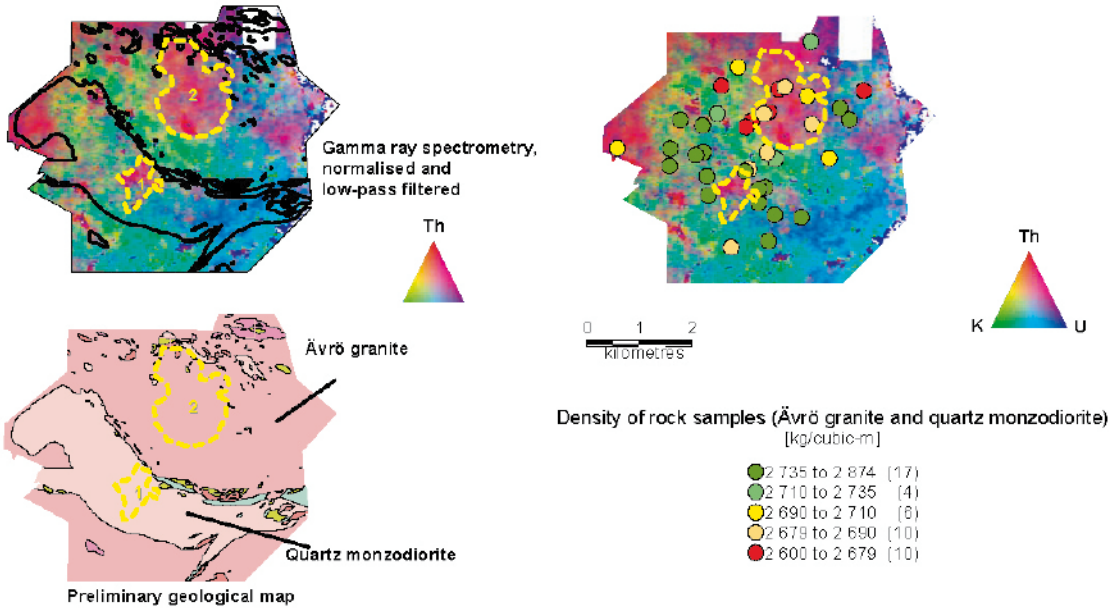

Figure 5-8. *Comparison of the preliminary version of the bedrock geological map of the Laxemar area an, the helicopter-borne gamma ray spectrometry data. Within the rock type quartz monzo-diorite a significant anomaly in the spectrometric map is recognised* ***1.*** *It is probably caused by farmland in the valley obscuring the response from the bedrock. Within the other main rock type Ävrö granite an area with a significant increase of the relative content of thorium as compared to its surroundings is observed* ***2.*** *The anomaly probably reflects a change in the bulk composition of the rock as compared to the surrounding areas within the same rock type.*

6 Discussion of the results

A summary of the petrophysical properties of the rocks in the Simpevarp area, as concluded from this work, is presented in Table 6-1 below. The number of sample locations per rock type is in most cases sufficient to confidently describe the properties; the exceptions are the rock types pegmatite and fine-grained diorite to gabbro, where only very few locations have been surveyed with spectrometry.

The susceptibility – density rock classification indicates that a majority of the rocks have mineral compositions corresponding to a continuous variation from low-density granites (leucocratic granite) to tonalite rock. The result from this "petrophysical rock classification" generally conforms well to the geological rock classification (keeping in mind that the rock type curves in the susceptibility – density diagram differ from the actual rock types in the area). The magnetic susceptibility is fairly high for a majority of the investigated rock samples and the magnetic mineralogy of these rocks is most likely dominated by magnetite. The measurements on samples show that granite (fine, medium and coarse grained) have a lower mean susceptibility and lower density than the other main rock types. The lower density is most likely related to a relatively lower content of dark minerals in these granite rocks (Table 6-1). However, from the in situ susceptibility measurements it is evident that the distribution of the susceptibility is complex and that a majority of the rock types include volumes of low as well as high magnetization. The highest magnetic susceptibilities are found in the rock type diorite to gabbro, which explains most of the very high magnetic anomalies recorded in the geophysical airborne and helicopter-borne surveys. In some areas there appear to be a spatial correlation between occurrences of these bodies of diorite to gabbro, and rock volumes of quartz monzodiorite with extra-ordinary high magnetic susceptibilities. In the frequency diagrams of the magnetic susceptibility for different rock types some very low values are encountered. Comparisons made with earlier identified lineaments and observations of tectonic features in outcrops show a clear correlation between these low susceptibilities and ductile and brittle deformation. The magnetite has thus been partly transformed into other minerals due to oxidation processes in these tectonic zones.

Q-values are generally low indicating that the magnetic remanence plays a subordinate role when interpreting magnetic field measurements. However, the negative inclination of the remanence vector reported at four sampling locations is important, especially at the location PSM005988 where the Q-value is high (Q = 3.81) and the NRM vector has a negative inclination (points upwards), which calls for further investigations.

The structural fabric of the rocks in the area, as indicated by the AMS data, is dominated by c west to west-northwest-striking foliation planes, with mainly moderate to steep dips. The poles to the foliations form a girdle distribution indicating a rotated or folded geometry. However, there is no indication of folding when viewing the spatial distribution of the foliation planes, and the orientations that deviate from the main pattern are distributed irregularly over the area. Since a majority of the foliation planes are oriented parallel to the major rock boundaries, and the degrees of anisotropy are generally low, it seems likely that the west to west-northwest striking foliations indicate a primary structural fabric related to the stress field that prevailed during the emplacements of these rocks. The deviating south to south-westerly foliation strikes are possibly related to a secondary deformation and could therefore be related to ductile shear zones. There is, for example, a clear spatial and orientation relation between the c NE-SW oriented Äspö shear zone and the NE-SW strike directions of the foliations of the two closest situated sampling locations.

The amount of the dip of the foliation planes show a spatial variation which indicates that the investigated area roughly can be divided into three structural sub-areas: a southern sub-area (around St. Laxemar and Ström) dominated by moderate to steep dips, a central sub-area (south of the road through Mederhult) dominated by shallow to moderate dips and a northern sub-area (north of the road through Mederhult) dominated by steeply dipping foliation planes. The vast majority of the magnetic lineations show west-northwest orientation and moderate to sub-horizontal dips. The orientation of the lineation is independent of the strike direction of the magnetic foliation, and the lineation data clearly indicate that there is one dominating regional maximum strain direction with c NW directed orientation.

Porosities of the investigated rocks are low, in general below 1%. The highest porosities within this range are found for samples in the central Laxemar area. The electric resistivity lay in the range of 8,000 Ωm to 30,000 Ωm (fresh water, 0.1 Hz) and the induced polarization is below 20 mrad (fresh water, 0.1 Hz) for a majority of the samples. The data indicate "normal" properties for non-mineralized primary and unaltered crystalline basement-rocks, typical for the Swedish bedrock. The porosity and resistivity data have been combined in order to analyze the pore space geometry of the samples. The empirical Archie's law has been used as a base for this work. All samples fall within the normal range for the exponent m in Archie's law that can be used as an indicator of the amount of complexity of the pore space. Slightly elevated values, an indication of minor alteration, is found for some samples, most of them from the central and northern part of the investigated area. Surface conductivity, indicating presence of e.g. chlorite or sericite, is high for samples of fine-grained dioritoid from the Simpevarp peninsula. Slightly elevated values are also found for some samples of Ävrö granite in the Laxemar area. The fine-grained granite has less surface conductivity than the other rock types.

Gamma ray spectrometry from air and on ground show that the highest contents of potassium and thorium are found in fine-grained granite. This has been observed also in an earlier work /12/ where also a few measurements on the rock type pegmatite showed high relative content of potassium, uranium and thorium. In general mafic rock types like diorite to gabbro and fine-grained diorite to gabbro have the lowest content of potassium, uranium and thorium. Gamma ray spectrometry indicates that the rock type Ävrö granite is quite heterogeneous as compared to the other major rock type of the area, quartz monzodiorite. The content of thorium generally increases in areas where the Ävrö granite appears to be more granitic in composition. Such an area is found in the central part of the Laxemar area.

As the geological mapping has now covered the entire Laxemar area and also parts of its surroundings it is now possible to relate different types of geophysical anomaly complexes to the observed geology to a greater extent than was previously possible. It is now clear that most of the anomaly complexes, observed in the airborne and helicopter-borne surveys, are reflected in the observed petrophysical parameters on ground. Most of the sources to the major anomalies are hence outcropping and it is possible to relate them to variations in bedrock geology, both regarding rock type and tectonics. The investigations of petrophysical parameters carried out within this activity indicate that the geophysical anomaly maps and petrophysical parameters may add useful information for the characterisation of the bedrock in terms of tectonics and for distinguishing between different rock types. Furthermore the geophysical data may reflect a compositional variation within rock types which together with chemical and mineralogical information may lead to further subdivision of rock types in different compositional varieties.

Table 6-1. Petrophysical parameters of rock types in the Simpevarp area. The rock type names follow the updated nomenclature with exception for the shaded rows where data from the special study of fine-grained granite dykes /12/ are presented.

Rock type and corresponding lithostrati-graphic code	Wet density (kg/m^3) (number of locations)	Magnetic susceptibility (Log 10^{-5} SI) (number of locations)	Q-value (dimension less) (number of locations)	Electric resistivity, fresh water 0.1 Hz (Log Ωm) (number of locations)	Induced polarization, fresh water 0.1 Hz (mrad) (number of locations)	Porosity (%) (number of locations)	K (%) (number of locations)	e U (ppm) (number of locations)	e Th (ppm) (number of locations)
Diorite to gabbro (501033)	2967 ± 33 (5)	3.117 ± 0.797 (5)	0.35 ± 0.32 (4)	4.28 ± 0.16 (5)	7.9 ± 2.9 (5)	0.32 ± 0.08 (5)	1.4 ± 0.5 (18)	1.4 ± 0.8 (18)	4.0 ± 2.7 (18)
Fine-grained dioritoid (501030)	2803 ± 52 (5)	3.220 ± 0.839 (5)	0.35 ± 0.40 (5)	4.58 ± 0.41 (5)	11.2 ± 6.7 (5)	0.29 ± 0.11 (5)	3.1 ± 0.3 (14)	3.7 ± 1.6 (14)	12.5 ± 5.8 (14)
Quartz monzodiorite (501036)	2779 ± 36 (15)	3.373 ± 0.233 (15)	0.67 ± 1.54 (15)	4.08 ± 0.16 (15)	10.2 ± 4.3 (15)	0.53 ± 0.11 (15)	3.0 ± 0.3 (38)	3.2 ± 0.8 (38)	9.9 ± 1.8 (38)
Ävrö granite (501044)	2690 ± 24 (32)	3.221 ± 0.247 (32)	0.44 ± 0.64 (32)	4.04 ± 0.21 (32)	9.0 ± 3.5 (32)	0.63 ± 0.13 (32)	3.3 ± 0.4 (79)	3.8 ± 1.5 (79)	11.9 ± 4.3 (79)
Granite, medium- to coarse-grained (501058)	2647 ± 17 (8)	2.940 ± 0.388 (8)	1.06 ± 1.56 (8)	4.17 ± 0.13 (8)	9.6 ± 3.3 (8)	0.59 ± 0.07 (8)	4.0 ± 0.5 (13)	4.3 ± 1.4 (13)	15.4 ± 5.0 (13)
Pegmatite (501058)	No data	No data	No data	No data	No data	No data	2.7 (1)	6.8 (1)	11.4 (1)
Fine-grained diorite to gabbro (505102)	No data	No data	No data	No data	No data	No data	1.5 (1)	0.7 (1)	3 (1)
Fine-grained granite (511058)	2625 ± 12 (7)	2.681 ± 0.262 (7)	0.21 ± 0.05 (7)	4.35 ± 0.19 (7)	10.2 ± 2.3 (7)	0.55 ± 0.10 (7)	4.5 ± 0.5 (7)	7.7 ± 2.5 (7)	30.2 ± 10.5 (7)
Granite, dyke, fine-grained	No data	No data	No data	No data	No data	No data	5.6 ± 0.4 (11)	6.1 ± 2.3 (11)	48.9 ± 20.9 (11)
Quartz monzodiorite to granodiorite (Äspö diorite)	No data	No data	No data	No data	No data	No data	3.3 ± 0.4 (5)	4.8 ± 2.7 (5)	11.2 ± 2.4 (5)
Ävrö granite	No data	No data	No data	No data	No data	No data	3.6 ± 0.2 (7)	4.9 ± 0.8 (7)	16.6 ± 6.6 (7)
Pegmatite	No data	No data	No data	No data	No data	No data	5.2 ± 0.4 (3)	9.8 ± 7.4 (3)	23.2 ± 8.7 (3)

7 Data delivery

The delivered data have been inserted in the database (SICADA) of SKB. The SICADA reference to the present activity are field note no 380 and no 537 respectively.

References

/1/ **Mattsson H, Thunehed H, 2003.** Measurements of petrophysical parameters on rock sample during autumn 2002. SKB P-03-19. Svensk Kärnbränslehantering AB.

/2/ **Mattsson H, Thunehed H, Triumf C-A, 2003.** Compilation of petrophysical data from rock samples and in situ gamma-ray spectrometry measurements. SKB P-03-97. Svensk Kärnbränslehantering AB.

/3/ **Wahlgren C-H, Persson L, Danielsson P, Berglund J, Triumf C-A, Mattsson H, Thunehed H, 2002.** Geologiskt underlag för val av prioriterad plats inom området väster om Simpevarp. Delrapport 1–4. SKB P-03-06.

/4/ **Nilsson K P, Bergman T, Eliasson T, 2004.** Bedrock mapping 2004 – Laxemar subarea and regional model area. Outcrop data and description of rock types. SKB P-04-221. Svensk Kärnbränslehantering AB.

/5/ **Henkel H, 1991.** Petrophysical properties (density and magnetization) of rock from the northern part of the Baltic Shield. Tectonophysics 192, 1–19.

/6/ **Collinson D W, 1983.** Methods in rock magnetism and paleomagnetism, Chapman and Hall, London, United Kingdom. 503 pp.

/7/ **Parasnis D S, 1997.** Principles of applied geophysics. Chapman and Hall, London, 429 pp.

/8/ **Puranen R, 1989.** Susceptibilities, iron and magnetite content of precambrian rocks in Finland. Geological survey of Finland, Report of investigations 90, 45 pp.

/9/ **Tarling D, Hrouda H, 1993.** The magnetic anisotropy of rocks. Chapman & Hall, New York.

/10/ **Archie G E, 1942.** The electrical resistivity log as an aid in determining some reservoir characteristics: Trans. Am. Inst. Min, Metallurg, Petr.Eng, 146, 54–62.

/11/ **Keller G V, Frischknecht F C, 1966.** Electrical methods in geophysical prospecting. Pergamon Press.

/12/ **Mattsson H, Triumf C-A, Wahlgren C-H, 2002.** Prediktering av förekomst av finkorniga granitgångar i Simpevarpsområdet. SKB P-02-05. Svensk Kärnbränslehantering AB.

/13/ **Bergman T, Johansson R, Lindén A H, Lindgren J, Rudmark L, Wahlgren C-H, Isaksson H, Lindroos H, 1998.** Förstudie Oskarshamn – Jordarter, bergarter och deformationszoner. SKB R-98-56. Svensk Kärnbränslehantering AB.

/14/ **Triumf C-A, 2004.** Oskarshamn site investigation. Joint interpretation of lineaments. SKB P-04-49. Svensk Kärnbränslehantering AB.

/15/ **Mattsson H, Thunehed H, 2004.** Interpretation of geophysical borehole data and compilation of petrophysical data from KSH02 (80–1000 m) and KAV01. SKP P-04-77. Svensk Kärnbränslehantering AB.

/16/ **Mattsson H, Thunehed H, Isaksson H, 2004.** Interpretation of petrophysical data from the cored boreholes KFM01A, KFM02A, KFM03A and KFM03B. SKB P-04-107. Svensk Kärnbränslehantering AB.

/17/ **Le Maitre R W, 2002.** Igneous Rocks: A Classification and Glossary of Terms. Recommendations of the International Union of Geological Sciences Subcommission on the Systematics of Igneous Rocks. 2nd Edition.

/18/ **Nisca D H, 1988.** Geophysical laboratory measurements on core samples from KLX01, Laxemar and KAS02, Äspö. SKB Progress report 25-88-06.

/19/ **Nisca D, 1987.** Aerogeophysical interpretation bedrock and tectonic analysis. SKB HRL Progress Report 25-87-04. Svensk Kärnbränslehantering AB.

/20/ **Rönning H J S, Kihle O, Mogaard J O, Walker P, 2003.** Simpevarp site investigation. Helicopter borne geophysics at Simpevarp, Oskarshamn, Sweden. SKB P-03-25. Svensk Kärnbränslehantering AB.

/21/ **Triumf C-A, Thunehed H, Kero L, Persson L, 2003.** Oskarshamn site investigation. Interpretation of airborne geophysical survey data. Helicopterborne survey data of gamma ray spectrometry, magnetics and EM from 2002 and fixed wing airborne survey data of the VLF-field from 1986. SKB P-03-100. Svensk Kärnbränslehantering AB.

/22/ **Shives R B K, Ford K L, Charbonneau B W, 1995.** Applications of Gamma ray spectrometry, magnetic and VLF-EM surveys. Workshop Manual, Geological Survey of Canada. Open File Dossier Public 3061.